Treball de Fi de Màster

Màster universitari en Enginyeria Tèrmica

Analysis of the thermal behaviour of bioclimatic facades by means of 1D unsteady simulations of the heat transfer phenomena involved

REPORT

Autor: Lincoln Josue Arellano Ortega
Director: Carlos David Pérez Segarra

Semester: Spring 2023

ETSEIB

Escola Tècnica Superior
d'Enginyeria Industrial de Barcelona

UPC

To my parents,
Angel and Lizeth
and to my brothers,
Esteban, Adrian and Elian

Abstract

The problems facing the world today make energy saving a very popular topic lately. Saving energy is not only related to reducing air and water pollution but also conserving natural sources, which in turn creates a better environment for people around the world. Using energy more efficiently is also a way to save energy, and this is one of the fastest and most cost-effective solutions to save money and help reduce emissions. This issue is undoubtedly of interest to the thermal field since it is constantly involved in the air conditioning of closed spaces. To contribute to energy savings in this type of application, it is essential to study the enclosing elements of a building such as the floor, roof and facade. It is mainly intended that these elements serve to capture and accumulate energy in the best way. That is why during the development of humanity some ideas have been proposed that contribute to this, one of them is the historical element to capture and accumulate energy: the Trombe wall. Consequently, this study focuses on the development of numerical models that, without having to be complex or require a lot of calculation time, allow simulating the energy transfer in different types of facades. These models are one-dimensional and transitory that are based on the Finite Volume Methodology and that are implemented through in-house numerical codes in the high-level programming language C++. Therefore, this study proposes five different cases, each of them with interesting variations to consider that could contribute to energy efficiency. The results obtained show that the implementation of a passive solar-heating system such as the Trombe wall helps to increase the temperatures inside an enclosure without the need to consume energy, which would reduce individual bills and stabilize the prices of the electricity.

Resumen

Los problemas que enfrenta el mundo hoy en día hacen que el ahorro de energía sea un tema muy popular últimamente. El ahorro de energía no solo está relacionado con la reducción de la contaminación del aire y el agua, sino también con la conservación de las fuentes naturales, lo que a su vez crea un mejor medio ambiente para las personas en todo el mundo. Usar la energía de manera más eficiente también es una forma de ahorrar energía, y esta es una de las formas más rápidas y rentables de ahorrar dinero y ayudar a reducir las emisiones. Este tema es sin duda de interés para el campo térmico ya que está constantemente involucrado en la climatización de espacios cerrados. Para contribuir al ahorro energético en este tipo de aplicaciones, es fundamental estudiar los elementos de cerramiento de un edificio como son el suelo, la cubierta y la fachada. Se pretende principalmente que estos elementos sirvan para captar y acumular energía de la mejor manera. Es por ello que durante el desarrollo de la humanidad se han propuesto algunas ideas que contribuyen a ello, una de ellas es el elemento histórico para captar y acumular energía: el muro Trombe. En consecuencia, este estudio se centra en el desarrollo de modelos numéricos que, sin tener que ser complejos ni requerir mucho tiempo de cálculo, permitan simular la transferencia de energía en diferentes tipos de fachadas. Estos modelos son unidimensionales y transitorios que se basan en la Metodología de Volumen Finito y que se implementan mediante códigos numéricos propios en el lenguaje de programación de alto nivel C++. Por lo tanto, este estudio propone cinco casos diferentes, cada uno de ellos con variaciones interesantes a considerar que podrían contribuir a la eficiencia energética. Los resultados obtenidos muestran que la implementación de un sistema de calefacción solar pasiva como la pared Trombe ayuda a aumentar las temperaturas en el interior de un recinto sin necesidad de consumir energía, lo que reduciría las facturas individuales y estabilizaría los precios de la electricidad.

Resum

Els problemes que enfronta el món avui fan que l'estalvi d'energia sigui un tema molt popular darrerament. L'estalvi d'energia no només està relacionat amb la reducció de la contaminació de l'aire i l'aigua, sinó també amb la conservació de les fonts naturals, cosa que alhora crea un medi ambient millor per a les persones a tot el món. Utilitzar l'energia de manera més eficient també és una forma d'estalviar energia, i aquesta és una de les formes més ràpides i rendibles d'estalviar diners i ajudar a reduir les emissions. Aquest tema és sens dubte d'interès per al camp tèrmic, ja que està constantment involucrat en la climatització d'espais tancats. Per contribuir a l'estalvi energètic en aquest tipus d'aplicacions, és fonamental estudiar els elements de tancament d'un edifici com son el terra, la coberta i la façana. Es pretén principalment que aquests elements serveixin per captar i acumular energia de la millor manera. És per això que durant el desenvolupament de la humanitat s'han proposat algunes idees que hi contribueixen, una és l'element històric per captar i acumular energia: el mur Trombe. En conseqüència, aquest estudi se centra en el desenvolupament de models numèrics que, sense haver de ser complexos ni requerir molt de temps de càlcul, permetin simular la transferència d'energia en diferents tipus de façanes. Aquests models són unidimensionals i transitoris que es basen en la metodologia de volum finit i que s'implementen mitjançant codis numèrics propis en el llenguatge de programació d'alt nivell C++. Per tant, aquest estudi planteja cinc casos diferents, cadascun amb variacions interessants a considerar que podrien contribuir a l'eficiència energètica. Els resultats obtinguts mostren que la implementació d'un sistema de calefacció solar passiva com la paret Trombe ajuda a augmentar les temperatures a l'interior d'un recinte sense necessitat de consumir energia, cosa que reduiria les factures individuals i estabilitzaria els preus de l'electricitat.

Contents

List of Figures

List of Tables

.

1 Introduction

1.1 Motivation of the project

In the field of thermal energy engineering, there are many important areas, such as heat and mass transfer and fluid dynamics, numerical methods in thermal engineering, and the design of thermal systems. Many of these areas are present in our daily lives, as well as in industries. It is important to mention that all the various process from which raw material becomes a final product must undergo heat and mass transfer in one way or another. This can be at a household level, such as cooking, or at an industrial level, such as extracting valuable components from a carrier substance. Heat transfer commonly refers to the transfer of thermal energy from a region of higher temperature to that of a lower one. This process occurs in nature by three means: conduction, convection and radiation. This highlights the need to know about these processes, so that we can understand what exactly is going on around us.

Going into a little more detail in the application of this project, at the domestic level, it is essential to mention that things like the optimal thickness of insulation in the walls and ceilings of the houses is determined again on the basis of a heat transfer analysis. This topic is currently of great interest in the thermal field since saving energy or using it more efficiently contributes significantly to society. For this, the enclosing elements of a building such as roof or facades must be studied. Unfortunately, there are certain limitations in the current tools that allow studying this phenomenon, since complex equations must be solved and this is often associated with high computational costs. Therefore, the thermal field has a great interest in developing numerical models that, with little calculation time, allow simulating a certain situation without having to solve complex equations.

1.2 Scope of the project

The scope of this study is summarized as follows:

- State of the art on the evolution of the Trombe wall and numerical simulation in the field of fluid dynamics and heat and mass transfer.
- Introduction to the techniques of the Finite Volume Method as well as the numerical background required for solving Partial Differential Equations.
- Development of an in-house numerical code in C++ environment to solve the one-dimensional transient heat conduction equation. This code will be verified through reference situations proposed by the Heat and Mass Transfer Technological Center (CTTC) and using analytical solutions when applicable.
- Study and discussion of different case studies proposed with topics of interest in the thermal field.

1.3 Requirements of the project

The requirements to conduct this project effectively are outlined below:

- The project must be completed in one quadrimester.
- The report must follow the guidelines indicated by the UPC.
- The codes must be non-commercial and self-developed type.
- The codes must be written in C++ language and can be post-processed in another environment such as Matlab in order to convert the numerical data into graphs.
- The codes must be tested using reference cases found in the literature to verify if they are accurate enough and detect errors in time.
- The code must be executed in conventional computers.

1.4 Objectives of the project

The general objective of this thesis is formulated as:

"To develop numerical models in order to analyze the thermal behavior of bio-climatic facades by means of unsteady simulations of the heat transfer phenomena involved."

In order to fulfill this aim, the following specific objectives play an important role:

- To understand the phenomena of heat and mass transfer and the three types of heat transfer: conduction, convection and radiation.
- To consolidate the basic mathematical formulations of fluid dynamics and heat and mass transfer phenomena.
- To become familiar with empirical formulations obtained from previous simulations when evaluating some parameters such as the heat transfer coefficients for natural convection.
- To develop methodologies for solving a wide variety of practical engineering problems using real meteorological data.
- To apply different computational techniques for the numerical solution of this phenomenon.
- To get hands-on programming experience in MATLAB and C++ environment.
- To develop in-house numerical codes in order to study the thermal behaviour of different cases of technological interest.
- To apply code verification and validation techniques of numerical solutions of mathematical formulations.

1.5 Project planning

The development of this project follows the planning detailed below. This planning consists of the 17 weeks in a four-month period and is divided into four phases.

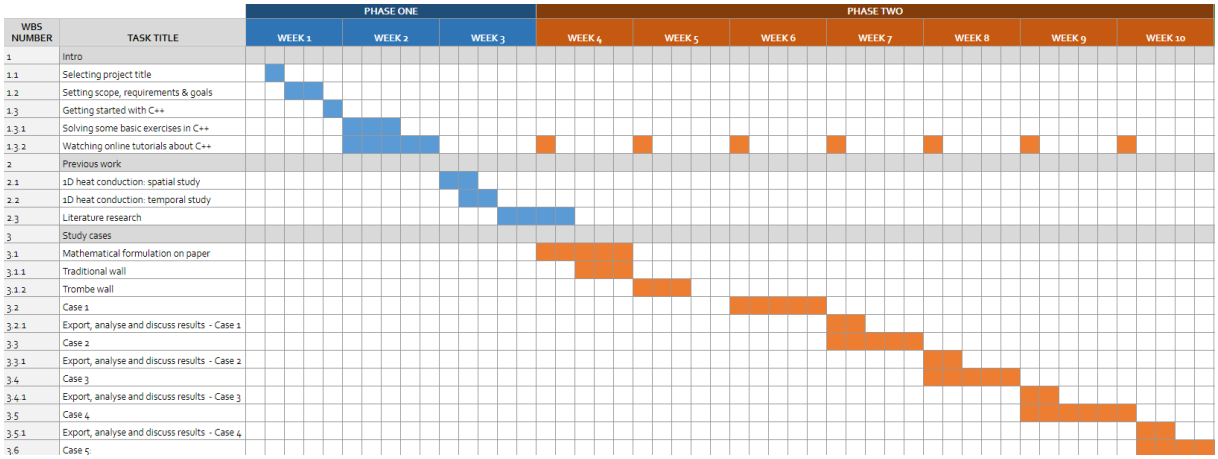

Figure 1: *Gantt diagram of the project – Phase 1 and 2*

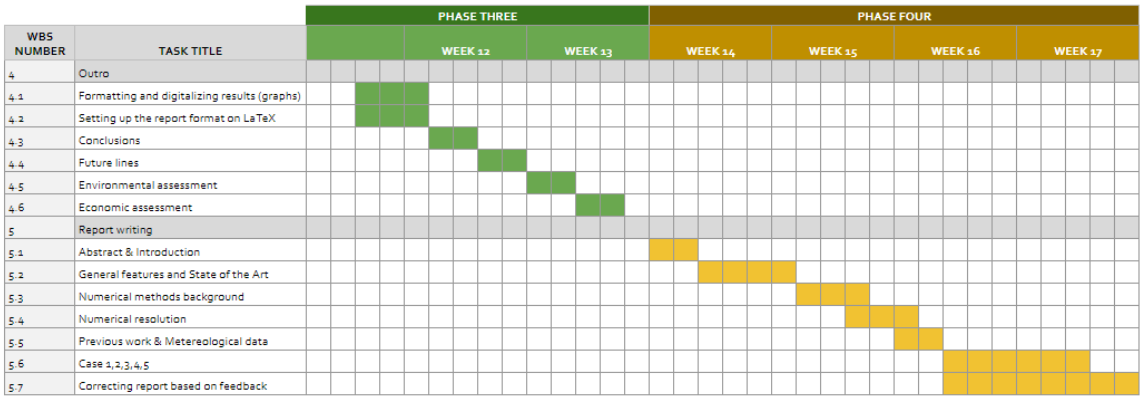

Figure 2: *Gantt diagram of the project – Phase 3 and 4*

2 General features and state-of-the-art

2.1 Evolution of the Trombe wall

The *Trombe wall* is a huge sun-facing wall that is usually painted a dark color to absorb thermal energy. This type of wall is covered with external glazing with an insulating air-gap between the glass and wall. This technology aims to achieve energy efficiency in buildings with passive heating [1]. This is achieved by absorbing solar radiation during sunny hours and then releasing this energy as heat inside the living space at night. The idea of this Trombe wall system goes back a lot further. It is said in the literature that it was first developed by the American Edward Morse in 1881 who designed an 'air heater' that shares similar characteristics – glazed box with a dark absorber, air space and two set of vent at top and bottom [2, 3].

It is reported that around the 1920s, the ideas of solar heating took place in Europe. In many European countries, innovative solutions were being developed to take advantage of the sun [4]. Despite this interest, the evolution of heating homes using the sun progressed slowly until the 1930s, when different American architects joined to explore solar heating [5]. Evidently, solar heating was very popular back then, but it was not until the 1970s, where many architectural newspapers were very critical of the standard ways of constructing buildings at that time [1, 5].

The oil crisis in 1973 led to the development of alternative innovations such as the *Trombe wall* [1, 5]. In addition to this, the world experienced historical events that made many ideas re-calibrate, including how to change architecture to take advantage of renewable energy sources [6]. Consequently, many magazines such as *Architecture d'Aujourd'hui*, published different buildings and their influence with solar energy [1]. In this magazine, the first uses of 'Trombe Wall detached house' in Odeillo, France, designed by architect Jacques Michel, were detailed (Figure 3).

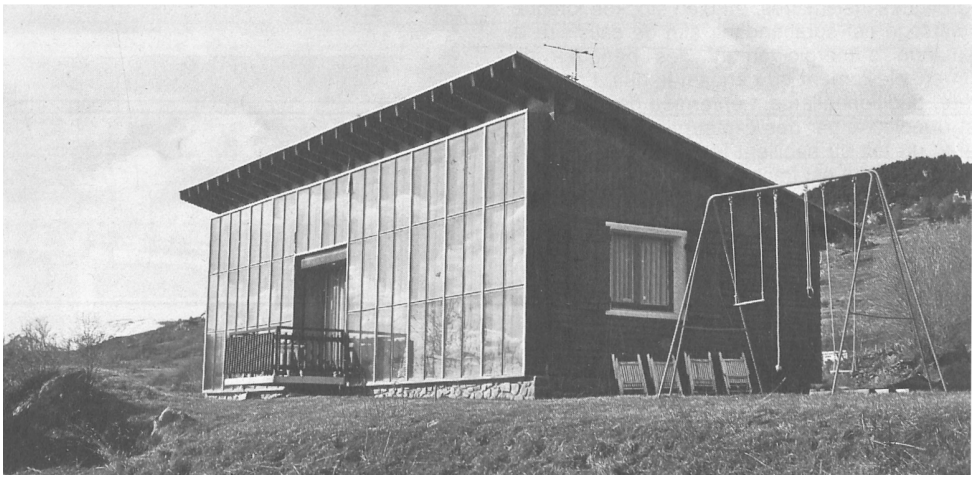

Figure 3: *Detached house with Trombe wall, built in 1970s in Odeillo, France. Reproduced from [1]*

Years later, after extensive work, the French engineer Felix Trombe demonstrated that the panels installed on the vertical walls of the structure were more productive and efficient than external collector devices placed on the roof [1], as illustrated in the first sketch of Figure 4. Since then this type of passive heating system has often been called *Trombe wall*.

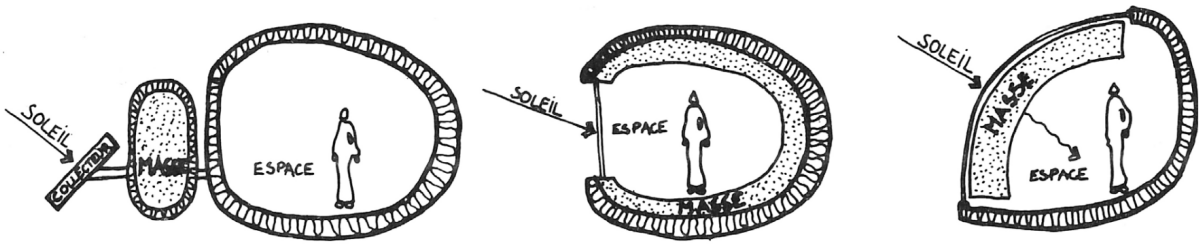

Figure 4: *Bio-climatic architecture hand-drawn diagrams: solar collector external to the building; glass façade and thermal mass inside the building; Trombe Wall. Reproduced from [1]*

As society experiences changes such as fuel shortages and various energy crises, harnessing solar energy has been a valuable asset in recent years [1]. The *Trombe wall* has become one of the most remarkable advances for many years that is still used today due to its benefits for the environment and also for users. Clearly, the integration of passive energy systems makes a significant contribution to sustainable development, so it is hoped that today's buildings can achieve an environmentally friendly and energy efficient design instead of using fossil energy to heating and cooling [7, 8].

2.2 How does a Trombe wall work?

Trombe wall is a passive solar heating system, where thermal energy flows in the system by natural means such as radiation, conduction and convection [8]. The main objective of this wall is to absorb and trap heat to distribute it to the living space in different ways, such as using ventilation vents. These vents allow hot air to enter the house, while cold air comes through a bottom vent and aids in circulation [9, 10]. Various techniques are used to further improve energy efficiency, for example, a dark paint is often used on the sun-facing side of the wall. This causes the solar radiation that penetrates the glazing to heat the wall even more and thus more heat is trapped to accumulate in the narrow air space [3]. Furthermore, in order to ensure high efficiency, the glass must have the highest transmissivity to solar radiation and the lowest emissivity to infrared radiation [6].

It is important to think about where this Trombe wall can be used. In general, Trombe walls are particularly well-suited to sunny climates and it is recommended to orient them towards the equator as it helps to absorb even more solar energy during the day [11].

Figure 5 illustrates the operation of the Trombe wall.

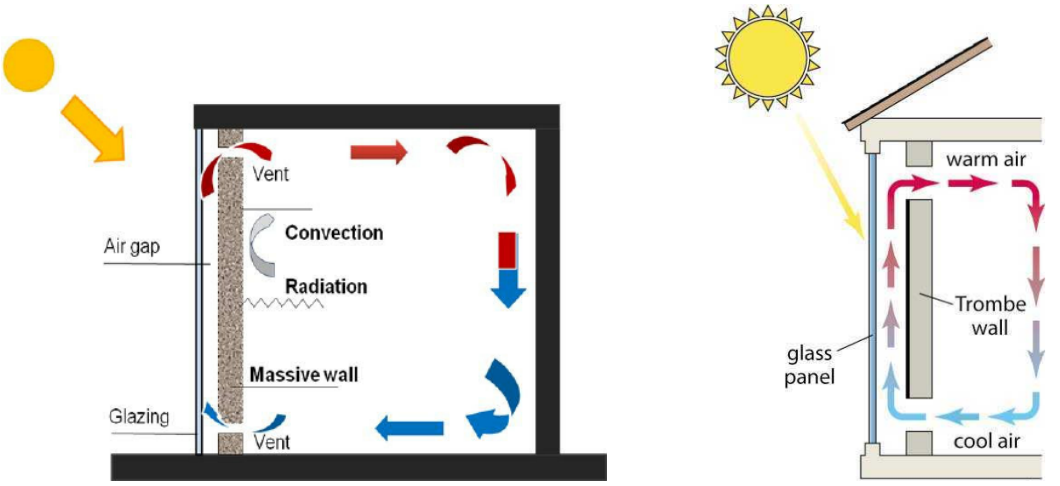

(a) *Reproduced from [12]* **(b)** *Reproduced from [11]*

Figure 5: *Working principle of a traditional Trombe wall*

2.3 Different configurations of Trombe walls

After the great invention of the Trombe wall, various modified versions of that first prototype have appeared. Progress has been made in terms of materials with different characteristics, including more complex geometric modifications in the design of this wall. In this section, the most relevant changes of the different types of Trombe wall that have been developed to date will be discussed.

2.3.1 Adapting to the seasons

The season of the year is one of the important factors to consider. In winter, it is intended to heat a building as much as possible, while in summer it is intended not to overheat it. Here, the importance of having some variations in the design of this type of walls. The most prominent variation when talking about the seasons of the year is the use of facades, overhangs, eaves and other building design elements to evenly balance solar heat delivery [13].

This type of design is considered to help prevent overheating of the building. That is, in winter the sun is at a lower altitude, meaning that it will hit the surface (wall) directly. On the other hand, in summer the sun is usually at a higher altitude, so this causes the sun to fall on the overhang providing a shadow on the surface, and thus preventing the building from overheating.

An example of this type of design can be seen in Figure 6.

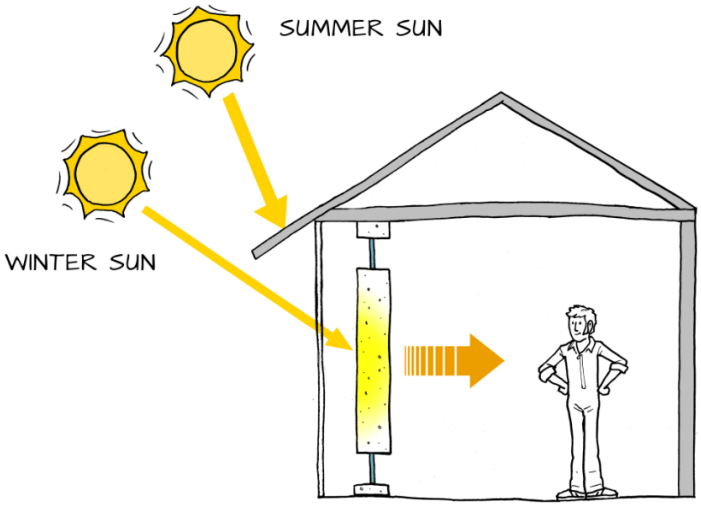

Figure 6: *A Trombe wall with overhang to shade from summer sun. Reproduced from [13]*

2.3.2 Air circulation

On top of that, there are variations in terms of air circulation between the wall and the glass. For instance, Figure 7 shows three different cases:

a) *Non-ventilated solar wall* that basically has no air circulation inside or outside the room.

b) *Trombe wall in winter* that follows the traditional behavior, that is, hot air enters through the top vent and cold air comes out from the bottom.

c) *Trombe wall in summer* that does not allow circulation inside the room to avoid overheating, so the air is expelled to the outside.

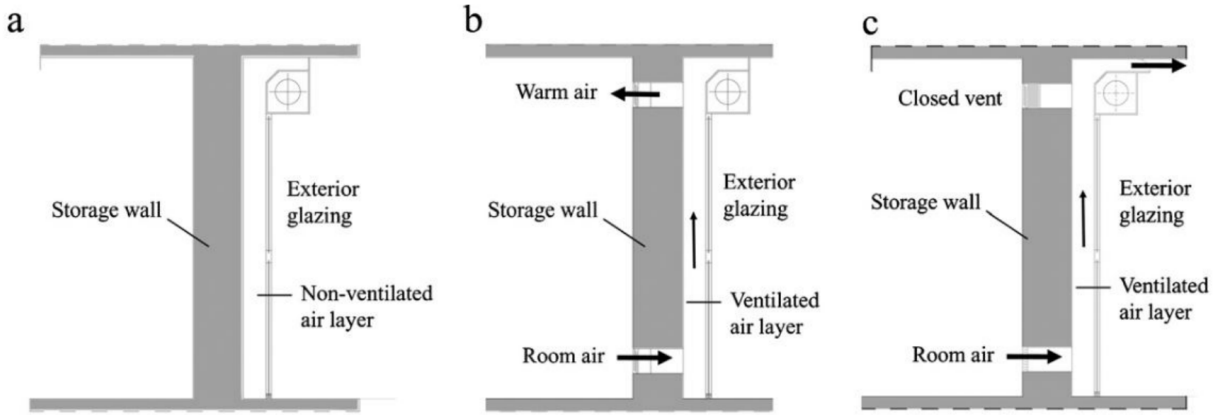

Figure 7: *Different operating schemes: a) Non-ventilated solar wall, b) Trombe wall in winter, and c) Trombe wall in summer, with cross-flow. Reproduced from [14]*

2.3.3 Sunspaces

Attached *sunspaces* are another configuration with the principle of the Trombe wall. This type of design generally has more glazing area than floor area. The difference between the traditional design is that now a living space is created between the glass and the wall. During the nights, the heat loss is not critical, but it is recommended to use double glazing in the case of using this living space at night [13]. In the same way, it is usually possible to play with the vents depending on the time of day. Namely, in the day the vents should be open to get convective and radiative heat transfer. However, at night (especially in low temperatures) the vents are closed to keep the convection going to the proper direction [13, 15].

Figure 8 shows how these attached sunspaces operate

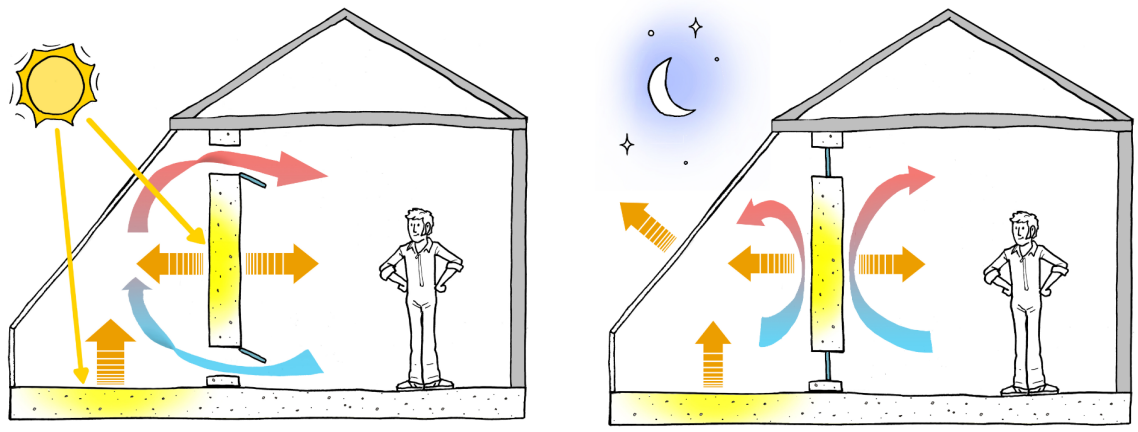

(a) *Daylight* **(b)** *Night*

Figure 8: *A sunspace with vents. Reproduced from [13]*

2.3.4 Water walls

The operation of this variation is similar to the traditional Trombe wall. The main difference is in using water tanks instead of masonry. Heat exchange in this situation has been shown to be more effective since the surface temperature of the water retains heat better than air [16]. Figure 9 depicts that in this configuration, the glass is placed in front of the water tank, which facilitates the flow of radiant solar heat since the water distributes the absorbed heat through convection to the rooms of the building. Therefore, the heat is transferred through the entire thermal mass much faster compared to a masonry wall that relies solely on conduction [13]. Furthermore, the high heat capacity of water compared to building materials means that more thermal energy is conserved using water. The main challenge of this alternative is the difficulty of handling and its limited applications compared to traditional walls [17]. This has made it currently not a relevant option.

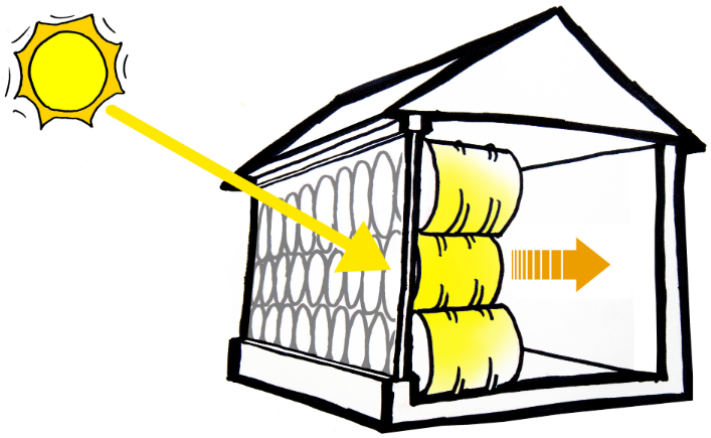

Figure 9: *Water tanks for thermal mass. Reproduced from [13]*

2.4 Pros and Cons

Undoubtedly, the development of an idea like that of a Trombe wall brings many positive points, such as the reduction of energy consumption to maintain certain temperatures. However, it is important to mention its limitations and problems against its positive points to think if it is really worth investing in this type of passive technology. The most important points are highlighted below.

Pros

- ***Reliability***: Reliable solution to reduce heating bills.
- ***Construction***: Relatively easy to incorporate into building structure and its materials are relatively inexpensive.
- ***Designs***: Available designs for different situations, e.g. winter, summer.
- ***Passive technology***: No moving parts are needed and essentially no maintenance is required.
- ***Applications***: Ideal for living spaces, such as home offices, living rooms, and bedrooms.

Cons

- ***Extra costs***: Trombe walls can increase construction costs due to additional components such as glazing.
- ***Heat transfer***: The amount of heat stored is unpredictable due to changes in solar intensity, so heat transfer is always uncertain.
- ***Low thermal resistance***: During night or in cloudy weather, the heat flux is transferred from the interior to the exterior of the building.

3 Numerical methods background

This section aims to introduce and describe the numerical techniques commonly used to transform Partial Derivative Equations (PDE) into a system of algebraic equations in a discrete domain. Although this is an extensive topic, the most relevant points used for the development of this report will be discussed.

3.1 Spatial discretization

3.1.1 Mesh

When working with numerical methods, the core idea is to discretize a domain in space. For this, it is necessary to divide it into *sufficiently* small parts called elements. In the Finite Volume Method (FVM) the variables of interest are usually assigned to the central node of each element meaning that the more elements are used, the greater the precision of the analysis [18]. This set of elements makes up the commonly called *mesh*. Depending on the complexity of the problem to be analyzed, this mesh can be used at convenience. Therefore, the following is intended to *briefly* describe the most relevant meshes in the numerical analyses.

- **Structured mesh:** A structured mesh is composed of regular and uniform elements that are arranged in a logical pattern. This means that the nodal connectivity can be expressed as a matrix of constant dimensions. Besides that, it is characterized by having the same number of neighboring nodes for each node. Structured meshes are relatively simple to generate, so the computational resources are less compared to other types of complex meshes. Nevertheless, it has limitations when working with complex shapes, so they are often used on simple geometries. This type of mesh can be found in two different forms.
  - **Orthogonal mesh:** This mesh has the same geometry and structure, meaning that the grids are uniform.

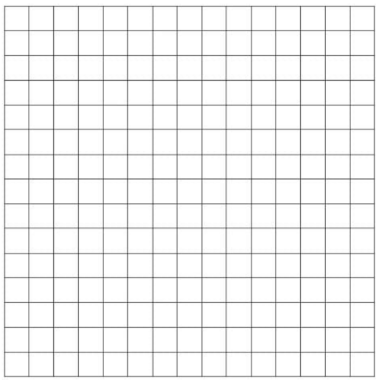

Figure 10: *Structured mesh – Orthogonal type. Reproduced from [19]*

– **Non-orthogonal mesh:** In this type of mesh, the fluxes through the faces are not normal to the faces of the control volume. The most outstanding point of this type is that they can be adapted to complex surfaces.

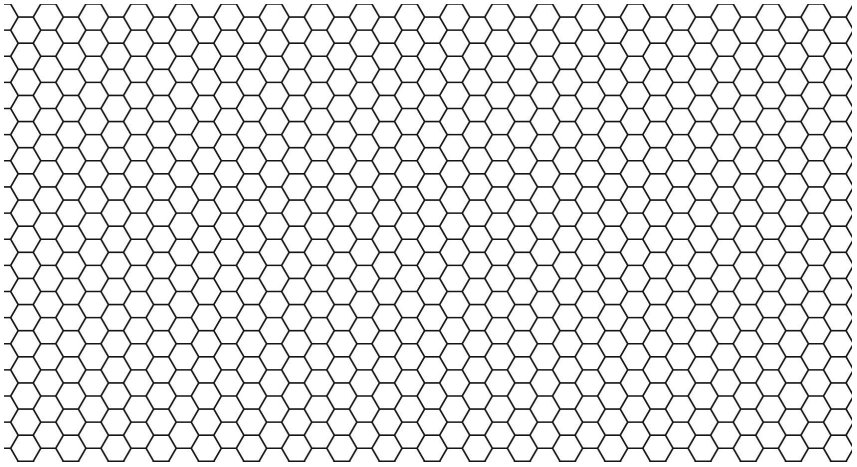

Figure 11: *Structured mesh – Non-orthogonal type. Reproduced from [20]*

- **Unstructured mesh:** Unstructured meshes contain elements that can be joined in a different order. This makes these meshes more flexible and adaptable as they can be used in different geometry and topology including holes, cracks, and the like. Effectively, this means that it does not have coding advantages as in the case of structured meshes and that simulations with this type of mesh are more expensive since the resolution process is more difficult.

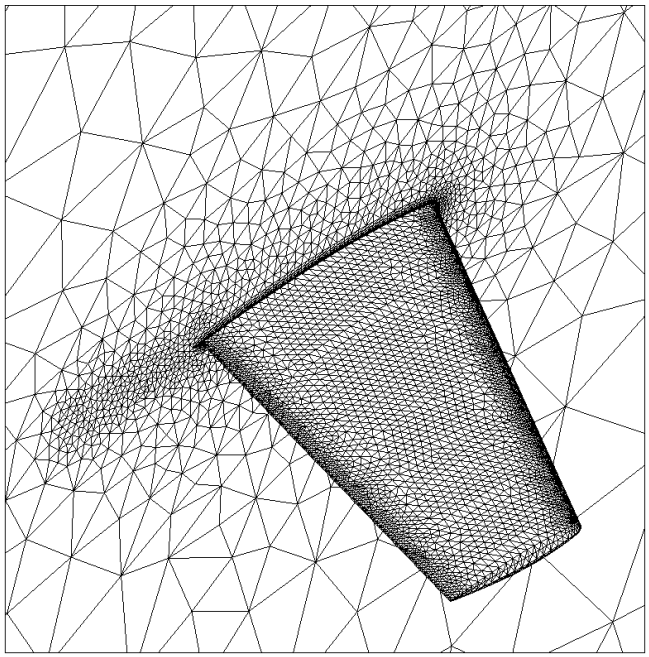

Figure 12: *Sample of unstructured mesh of a compressible steady turbulent flow over an ONERA M6 wing. Reproduced from [21]*

- **Collocated mesh:** A collocated mesh is a type of grid where the main variables of the fluid, such as pressure, density, velocity, etc., are stored in the same positions.

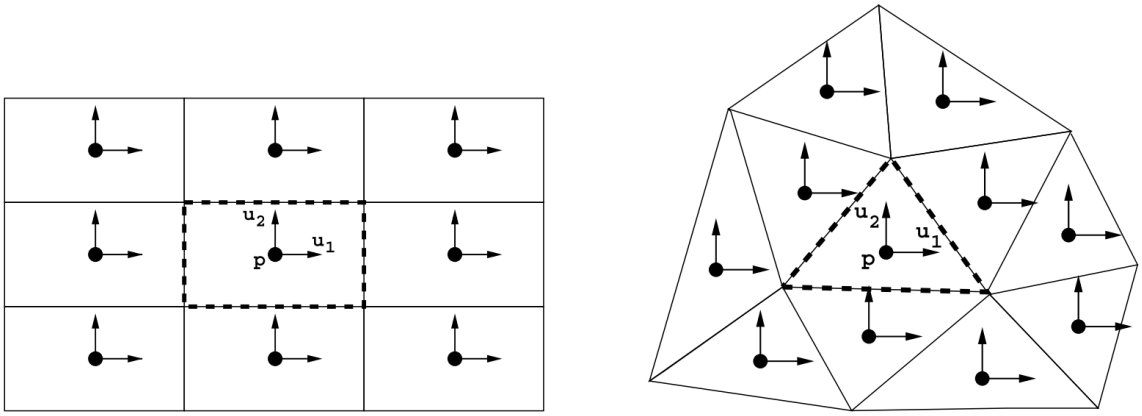

Figure 13: *Arrangement for a collocated-mesh. Reproduced from [22]*

- **Staggered mesh:** The main difference with the collocated grid arrangement is that a staggered grid stores the scalar variables (pressure, density, etc.) in the centers of the cells of the control volumes (CVs), while the velocity or moment variables are stored on the faces of each cell. This way of storing information in different places makes it more difficult to handle different CVs for different variables. The biggest advantage of the staggered grid arrangement is the coupling of pressure and velocities and avoids convergence problems [23]. This type of arrangement is mainly used when solving the incompressible Navier-Stokes to avoid the pressure-velocity decoupling problem.

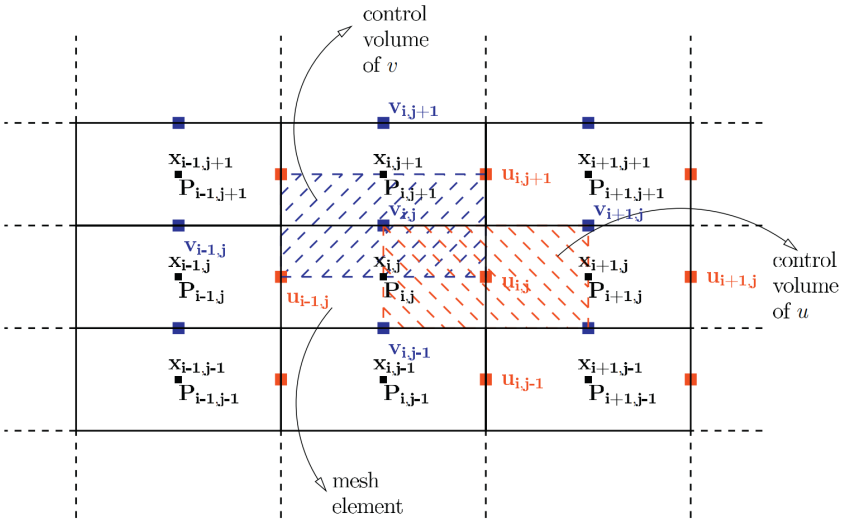

Figure 14: *Arrangement for a staggered-mesh. Reproduced from [23]*

3.1.2 Finite Volume Method

The Finite Volume Method (FVM) is a numerical method used to evaluate complex Partial Differential Equations (PDEs) in the form of algebraic equations [24]. Although there are some alternative techniques such as the Finite Difference Method (FDM) and the Finite Element Method (FEM), this report will be prepared using FVM. This means that a domain will be divided into a finite number of control volumes (see Figure 15 and 16). Unlike the aforementioned classical techniques that approximate derivatives in finite differences, FVM converts volume integrals into a surface integral using the divergence theorem. That is why this method *essentially* relies on the Gauss divergence theorem which is valid for any type of mesh and reads

Theorem 1 (Gauss divergence theorem) *The vector's outward flux through a closed surface is equal to the volume integral of the divergence over the area within the surface [25].*

$$\int_{\Omega} (\nabla \cdot \vec{F}) dV = \int_{\partial\Omega} \vec{F} \cdot \vec{n} dS$$

Then, the fluxes across the surfaces of the control volumes are approximated by means of integral over each cell. Furthermore, this method divides the spatial domain into elements whose properties are assumed to remain constant and they are assigned at a central node. Besides this, FVM is considered as a conservative method given that the flow entering to a given control volume is identical to the flow leaving the adjacent volume.

As in most numerical techniques, there are points to consider. Namely, some truncation errors appear in the evaluation of properties on the faces on the control volumes. This can be counteracted using numerical schemes that estimate the value of a given property on the cell surface knowing information from neighboring nodes. Moreover, estimating the solution in higher orders is not easy, which is a drawback compared to other methods such as FDM that approximates the derivatives to finite differences using Taylor approximations [26].

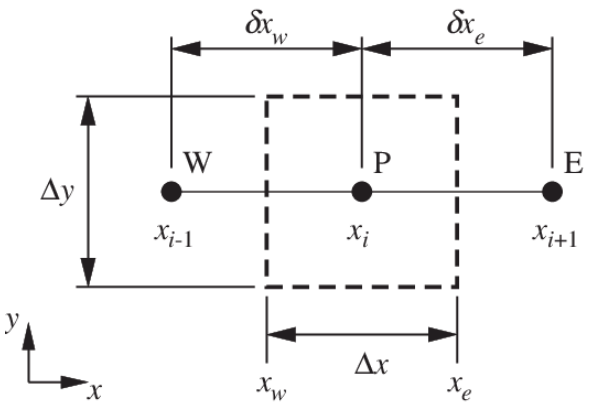

Figure 15: *One-dimensional control volume. Reproduced from [27]*

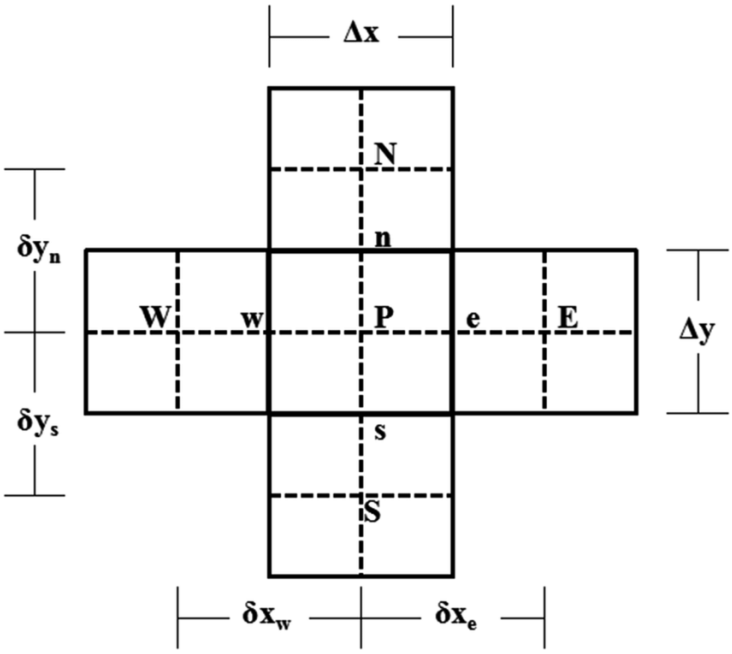

Figure 16: *Two-dimensional control volume. Reproduced from [28]*

3.2 Temporal discretization

The studies in this report are unsteady, which means that time variations of the governing equations are also considered. For this, let us consider an arbitrary generic time dependent differential equation

$$\frac{\partial \varphi}{\partial t}(x,t) = F(\varphi)$$

where φ is a generic variable and $F(\varphi)$ is a function dependant of that variable.

This will be the starting point to explain the following schemes. Even though the objective of this report focuses on the implicit scheme, other schemes that are also relevant to this temporal discretization are detailed below.

3.2.1 Explicit scheme

This first-order approximation scheme evaluates the value of the property at the new time step using only information from the previous time step. The explicit scheme does not need to solve a system of equations, which means that it requires less computational resources. However, this scheme is *conditionally* stable, meaning that there might be some stability problems if a large time step is used. This problem can be solved by setting a specific time step value that satisfies the CFL condition.

The mathematical formulation of an explicit scheme yields

$$\varphi^{n+1} = \varphi^n + \Delta t F(\varphi^n) \tag{1}$$

3.2.2 Implicit scheme

This first-order approximation scheme evaluates the value of the property in the new time step using information from the previous and new time steps. This causes the implicit scheme to have to solve a system of equations, which means that computational resources are increased because a solver is needed. Consequently, a great advantage is that this scheme is unconditionally stable for any time step. Therefore, this high stability and the possibility of using larger time steps make them the preferred solution for users when it comes to studying unstable cases.

The mathematical formulation of an implicit scheme follows

$$\varphi^{n+1} = \varphi^n + \Delta t F(\varphi^{n+1}) \tag{2}$$

3.2.3 Crank-Nicolson scheme

This second-order approximation scheme evaluates the value of the property at the new time step using information from the old and new time steps. Its function value depends on the previous and next time instant, unlike the previous schemes. This makes this scheme a high-order type, which means that its precision is higher than the schemes mentioned above. Certainly this type of scheme has to solve a system of equations making it more complex to implement.

The mathematical formulation of a Crank-Nicolson scheme yields

$$\varphi^{n+1} = \varphi^n + \frac{1}{2}\Delta t \left(F(\varphi^n) + F(\varphi^{n+1})\right) \tag{3}$$

3.3 Solvers

Discretizing a certain geometry in several elements makes it necessary to solve systems of algebraic equations to calculate a certain parameter. As discussed before, properties are assigned to the center of each element, and these values are influenced by the values of neighboring nodes. This means that frequently this system of equations is coupled. In addition to this, many problems usually require a large amount of calculations, so it is very important to implement a solver capable of solving this system effectively.

The system of equations is normally expressed as

$$A \cdot \boldsymbol{x} = b \tag{4}$$

where A is the matrix of $N \times N$ dimensions formed by the depedent coefficients, $\boldsymbol{x}$ is the row vector of the variable of the study with N components, and b is the non-dependent coefficient.

Arguably, the easiest way to solve a type of system of equations like the one shown in equation 4 is by taking the inverse of matrix A. However, this is not realistic since for systems of many equations

the computational costs are extremely high. This makes it necessary to look for other ways to solve such systems. Therefore, solvers can be divided into two types.

- **Iterative solvers:** This type of solvers tries to solve the system of equations by means of successive approximations to the solution. An initial estimated value is the starting point for these solvers to start the calculations. Note that iterative algorithms do not obtain exact solutions, unlike direct methods. Rather, they get closer and closer to the solution the more they work [29]. After each iteration, the calculated values are compared with the last iteration until the error between them is smaller than the previous defined *convergence criteria*. Note that the precision of the final solution depends to a large extent on this convergence criteria established by the user. Some of these iterative solvers are Jacobi and Gauss-Seidel.

- **Direct solvers:** These solvers attempt to deliver an exact solution of the system of equations in a finite number of steps. An initial estimate is no longer needed because these solvers calculate all the variables at once. Although direct solvers are usually much faster than iterative solvers, they are more difficult to implement and require more computer memory space. Some of these direct solvers are LU and TDMA.

The two solvers that will be used in this report are briefly detailed below.

3.3.1 Gauss-Seidel

The Gauss-Seidel (GS) method consists of giving an initial approximation to then solving the system of equations point-by-point. The convergence of this method is only guaranteed if the matrix A is diagonally-dominant or symmetric and positive definite [30]. This method is based on the Jacobi algorithm, but the main difference is that Gauss-Seidel uses the new values of each x_i as soon as they are known. This makes this method to convergence much faster than Jacobi's.

The following formulation is obtained for each node

$$\phi_P{}^{n+1} = \frac{a_E\phi_E{}^n + a_W\phi_W{}^n + a_N\phi_N{}^n + a_S\phi_S{}^n + b_P}{a_P} \tag{5}$$

Note that ϕ stands for the solution of the system which is expressed by $\boldsymbol{x}$ in equation 4.

After calculating $\phi_P{}^{n+1}$ for all nodes, the convergence criterion must be evaluated. Note that in an unsteady case, this condition must be true for each time step.

3.3.2 TDMA

The Tridiagonal Matrix Algorithm (TDMA) is a direct method for solving systems of tridiagonal equations. The matrix A in these systems is characterized by having nonzero elements on the main diagonal and on the first diagonal below and above the main. This method is useful for

one-dimensional problems but for more dimensions it is not applicable. For higher dimensions, a line-by-line solver is generally used which is a modification of the TDMA method.

The discretized equations are written as follows

$$a_P\phi_P = a_E\phi_E + a_W\phi_W + b_P \tag{6}$$

This equation can be rewritten as follows

$$a_P\phi_P - a_E\phi_E - a_W\phi_W = b_P \tag{7}$$

The variable ϕ_i is found by using some linear combination

$$\phi_P = P_P\phi_E + R_P \tag{8}$$

$$\phi_W = P_W\phi_P + R_P \tag{9}$$

By substituting the equation 9 into the equation 6, the following is obtained

$$a_P\phi_P = a_E\phi_E + a_W(P_W\phi_P + R_W) + b_P \tag{10}$$

Manipulating this equation gives

$$(a_P - a_W P_W)\phi_P = a_E\phi_E + a_W R_W + b_P \tag{11}$$

$$\phi_P = \frac{a_E}{a_P - a_W P_W}\phi_E + \frac{a_W R_W\phi_W + b_P}{a_P - a_W P_W} \tag{12}$$

By comparing the equation 8 with the equation 12, the coefficients P_P and R_P are found

$$P_P = \frac{a_E}{a_P - a_W P_W} \qquad R_P = \frac{a_W R_W + b_P}{a_P - a_W P_W} \tag{13}$$

Note that TDMA basically consists of two parts: i) forward elimination phase – remove the a_W diagonal, and ii) backward substitution phase – find T_{i-1} based on T_i.

3.4 Dimensionless Numbers

Dimensionless numbers have great utility in the world of heat transfer. These are useful for reducing dependencies, extrapolating results to other situations (e.g. fluids), and for establishing geometric similarity relationships between different situations. They are also used to correlate heat transfer coefficients, such as the expressions used in this project. Accordingly, the non-dimensional numbers used in this report will be discussed briefly.

- **Reynolds number:** The dimensionless Reynolds number, referred to as Re, correlates the inertial forces to the viscous forces. This means that it plays an important role in predicting

patterns in the behaviour of a fluid. Therefore, it is used to determine whether the fluid flow is laminar or turbulent. Re is defined as

$$Re = \frac{\textit{inertial forces}}{\textit{viscous forces}} = \frac{\rho v L}{\mu} \tag{14}$$

where ρ is the density of the fluid, v is the flow speed, L is the characteristic linear dimension and μ is the dynamic viscosity of the fluid.

- **Prandtl number:** The dimensionless Prandtl number, called Pr, correlates the momentum diffusivity (kinematic viscosity) to the thermal diffusivity. Therefore, it describes how well heat is conducted and transported by the flow. Pr depends on the fluid properties and is defined as follows

$$Pr = \frac{\textit{momentum diffusivity}}{\textit{thermal diffusivity}} = \frac{\nu}{\alpha} = \frac{\mu c_p}{\lambda} \tag{15}$$

where μ is the dynamic viscosity of the fluid, c_p is the specific heat capacity and λ is the thermal conductivity of the fluid. Note that these properties change with temperature, so the Prandtl number will also change.

- **Nusselt number:** The dimensionless Nusselt number, referred as Nu, is a measure of the ratio between heat transfer by convection and heat transfer by conduction within a fluid. Therefore, it is used to indicate how much heat transfer occurs due to convection compared to conduction. Nu is defined as

$$Nu = \frac{\textit{convective heat transfer}}{\textit{conductive heat transfer}} = \frac{\alpha L}{\lambda} \tag{16}$$

where α is the convective heat transfer coefficient of the flow, L is the characteristic linear dimension and λ is the thermal conductivity of the fluid

- **Grashof number:** The dimensionless Grashof number, called Gr, is defined as the ratio of buoyant forces to viscous forces. This is commonly used to determine the flow regime of fluid boundary layers in laminar systems. Gr is defined as follows

$$Gr = \frac{\textit{buoyant forces}}{\textit{viscous forces}} = \frac{g\beta(T_{wall} - T_\infty)L^3}{\nu^2} \tag{17}$$

where g is the acceleration due to Earth's gravity, β is the coefficient of thermal expansion, T_{wall} is the wall temperature, T_∞ is the bulk temperature, L is the vertical characteristic length and ν is the kinematic viscosity.

- **Rayleigh number:** The dimensionless Rayleigh number, referred as Ra, is defined as the product of the Gr and Pr number. This means that it describes the relationship between momentum diffusivity and thermal diffusivity. In other words, it indicates the presence and strength of convection within a fluid body. Therefore, it is commonly used to measure the "amount of convection" in a flow. Ra is defined as

$$Ra = GrPr \tag{18}$$

4 Numerical resolution

The procedure followed to obtain the core equations is presented in this section. They are essential in the development of numerical models to study different situations of Heat and Mass Transfer. The main objective is to obtain the temperatures of the different elements acting in the system.

4.1 Traditional wall

When this report refers to a *traditional wall*, it is an enclosed volume with a south-facing wall. This wall has a normal composition, that is to say that no modification is given to it. The following physical-mathematical model to be simulated is based on the following hypotheses:

- The model will be treated in a transitory regime.
- All the walls, roof, and floor of the volume are adiabatic except for the south-facing wall.
- In principle, the composition of the wall will be made of a single material (concrete), but the in-house numerical code created can include other materials if necessary.
- Thermophysical properties are considered constant due to their low variability.
- Any fluid motion is only caused by natural means, so only *natural convection* is relevant.[1]

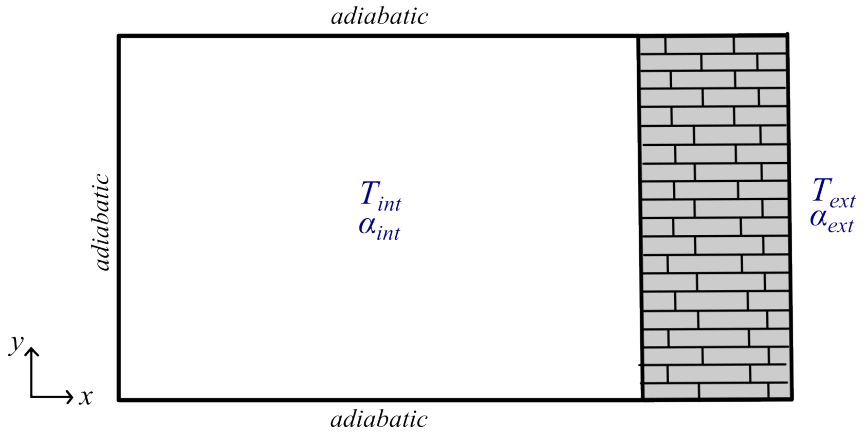

Figure 17: *Traditional wall scheme*

4.1.1 Mathematical formulation

4.1.1.1 Energy balance in the fluid

An energy balance can be made on the mass of air inside the volume in order to determine the

[1] In real life this is not always the case, but this decision has been made based on the fact that implementing forced convection would mean using different correlations, that is, the procedure followed would not vary much. Hence, it has been preferred to include other more relevant variations such as the energy consumed or the influence of air infiltration.

equation that allows calculating the temperature inside this volume. Figure 18 shows the main factors involved in the concrete wall to be studied.

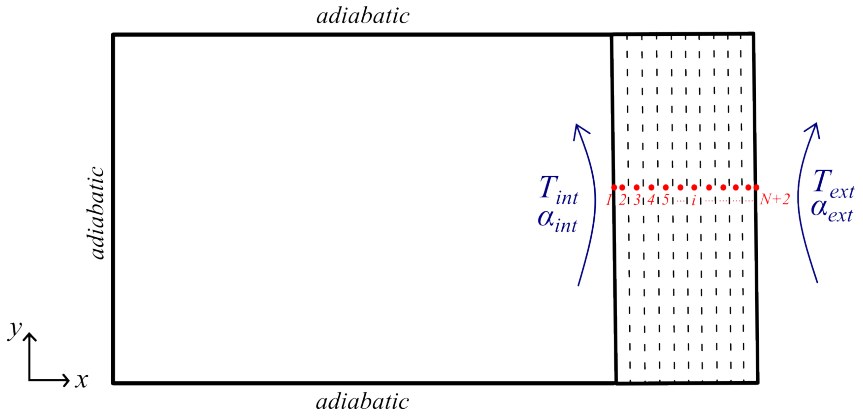

Figure 18: *Energy balance in the fluid – Traditional wall*

Note that radiation is a non-participating medium, meaning that it does not influence the fluid balance. Hence, this energy balance is expressed as follows

$$\{Accumulation\} = \{In\} - \{Out\} + \{Generation\} \tag{19a}$$

$$\frac{mc_{p,air}}{\Delta t}\left({T_{int}}^{n+1} - {T_{int}}^{n}\right) = {\alpha_{int}}^{n}\left(T^n[1] - {T_{int}}^{n}\right)S \tag{19b}$$

This expression is equivalent to

$$\frac{\rho_{air}Vc_{p,air}}{\Delta t}\left({T_{int}}^{n+1} - {T_{int}}^{n}\right) = {\alpha_{int}}^{n}\left(T^n[1] - {T_{int}}^{n}\right)S \tag{19c}$$

Solving for the internal temperature inside the room gives

$${T_{int}}^{n+1} = {T_{int}}^{n} + \frac{\Delta t}{\rho_{air}Vc_{p,air}}\left[{\alpha_{int}}^{n}\left(T^n[1] - {T_{int}}^{n}\right)S\right] \tag{19d}$$

where S and V are the heat transfer area and the volume of the enclosure, respectively.

Using the equation 19d, the temperature inside the enclosed volume can be determined. It must be taken into account that this expression can be expanded if different scenarios are considered. For instance, if it is intended to maintain a desired temperature range, a device can be placed inside the room that gives power P. Alternatively, air infiltration into the room can also be taken into account. These two examples of variations follow the already derived expression with certain modifications detailed as follows

- If there is a device giving a power P inside the room **without** air infiltration, the previous expression becomes

$${T_{int}}^{n+1} = {T_{int}}^{n} + \frac{\Delta t}{\rho_{air}Vc_{p,air}}\left[{\alpha_{int}}^{n}\left(T^n[1] - {T_{int}}^{n}\right)S \pm P\right] \tag{20}$$

where P is the power supplied. Note that the equation 20 can take a positive or negative value for the power P depending on whether the device is heating or cooling the volume.

- If there is now a device giving a power P inside the room **with** air infiltration, the following expression holds

$$T_{int}{}^{n+1} = T_{int}{}^{n} + \frac{\Delta t}{\rho_{air} V c_{p,air}} \left[\rho_{air} \dot{V} c_{p,air} \left(T_{ext} - T_{int}{}^{n} \right) + \alpha_{int}{}^{n} \left(T^{n}[1] - T_{int}{}^{n} \right) S \pm P \right] \tag{21}$$

where $\dot{V}$ is the volumetric air flow.

In this way, general expressions have been obtained that can be used to analyze the different case studies proposed in the following sections.

4.1.1.2 Thermal radiation

To calculate thermal radiation, it is necessary to determine the view factors.

View factors

Figure 19 shows the situation to be analyzed. Notice that there is a large yard near the wall.

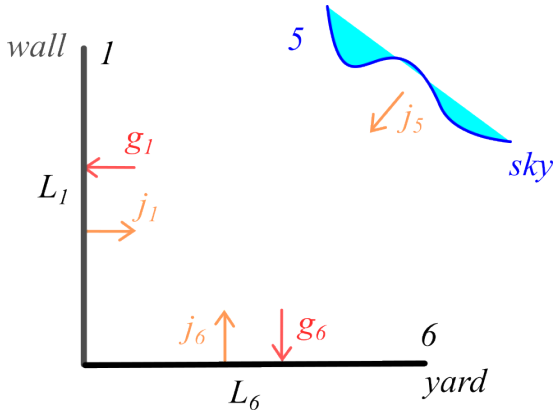

Figure 19: *View factors scheme for a traditional wall*

The view factors for each surface[2] are as follows

- **Surface 1:**

$$F_{11} = 0; \qquad F_{15} = 1 - F_{11} - F_{16}; \qquad F_{16} = \frac{L_1 + L_6 - d_{16}}{2L_1} \tag{22}$$

[2]Note that for **surface 5**, the view factors are not needed since the sky is considered as a black-body ($\varepsilon_5 = 1$) and thus the radiosity j_5 relation can be found directly.

where L_1 and L_6 are the length of the wall and yard, respectively.

The distance d_{16} is defined as $d_{16} = \sqrt{{L_1}^2 + {L_6}^2}$

- **Surface 6:**

$$F_{61} = \frac{A_1}{A_6} F_{16}; \qquad F_{65} = 1 - F_{61} - F_{66}; \qquad F_{66} = 0 \tag{23}$$

where A_x is the cross-sectional area of the elements and is found as $A_x = L_x W$.

Irradiosity and radiosity relations

The expressions for irradiosity (g_k) and radiosity (j_k) yields

- **Surface 1:**

$$j_1 = \varepsilon_1 \sigma {T_1}^4 + (1 - \varepsilon_1) g_1 \tag{24a}$$

$$g_1 = F_{11} j_1 + F_{15} j_5 + F_{16} j_6 \tag{24b}$$

- **Surface 5:**

$$j_5 = \sigma {T_{sky}}^4 \tag{25}$$

- **Surface 6:**

$$j_6 = \varepsilon_6 \sigma {T_6}^4 + (1 - \varepsilon_6) g_6 \tag{26a}$$

$$g_6 = F_{61} j_1 + F_{65} j_5 + F_{66} j_6 \tag{26b}$$

where σ is the Stefan-Boltzmann constant, ε_k is the emissivity of the surface k and T_k is the temperature of the surface k.

Note that T_1 is the wall temperature that will be determined based on a numerical analysis detailed in the following sections. T_6 is the yard temperature and is an input data. Finally, T_{sky} is calculated based on the ambient temperature following this expression [31]

$$T_{sky} \approx 0.0552 {T_{amb}}^{1.5} \tag{27}$$

Finally, the net rate of heat transfer by thermal radiation is calculated as follows

$$\dot{q}_{rad,k} = j_k - g_k \tag{28}$$

4.1.1.3 Solid analysis

Based on the assumptions used for this analysis, the solid analysis only considers the *south-facing wall*. Other elements, such as the roof and the floor, are left out, since they have been considered adiabatic.

Wall

The numerical methodology followed before implementing it in the in-house numerical code is as follows

- **Discretization:** This analysis uses an uniform mesh, which means that the surface and volume for every control volume (CV) is assumed to be constant.
  - **CV length**

$$\Delta x = \frac{D}{N} \tag{29a}$$

    where D is the wall thickness and N is the number of nodes.
  - **CV position**

$$x_{cv}[i] = (i-1)\Delta x \tag{29b}$$

  - **Node position**

$$x_p[i] = \frac{x_{cv}[i] + x_{cv}[i-1]}{2} \tag{29c}$$

  - **Node distance**

$$d_p[i] = x_p[i+1] - x_p[i] \tag{29d}$$

  Figure 20 shows this discretization.

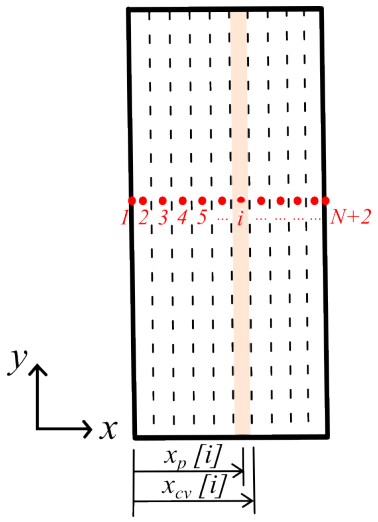

Figure 20: *Spatial discretization for a traditional wall*

- **Discretization equations**
  - **Internal nodes:** The internal nodes for this analysis range from $i = 2$ to $N + 1$. Figure 21 displays the energy balance which can be written as follows

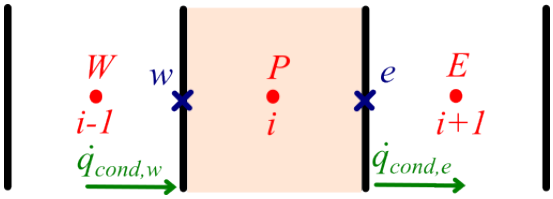

Figure 21: *Energy balance in the internal nodes*

$$\{Accumulation\} = \{In\} - \{Out\} + \{Generation\} \tag{30a}$$

$$\frac{\partial}{\partial t}\int_{V_p} u\rho dV = \dot{q}_{cond,w} - \dot{q}_{cond,e} \tag{30b}$$

$$\rho_p V_p \int_{t^n}^{t^{n+1}} \frac{\partial u_p}{\partial t} dt = \int_{t^n}^{t^{n+1}} \sum \dot{Q}_p dt \tag{30c}$$

By definition, the internal energy at the center of the control volume follows

$$\vec{u}_p = \frac{1}{V_p}\int_{V_p} u\, dV \approx u_p \tag{31a}$$

$$du = c_p dT \tag{31b}$$

Using these relations and rewriting yields to

$$\rho_p c_{p,p} V_p ({T_p}^{n+1} - {T_p}^{n}) = \left[\beta \sum {\dot{Q}_p}^{n+1} + (1-\beta)\sum {\dot{Q}_p}^{n}\right]\Delta t \tag{32}$$

where β depends on the time-integration scheme to be used. As previously discussed, the implicit scheme is employed in this analysis, hence $\beta = 1$. Therefore, equation 32 can be rewritten as follows

$$\rho_p c_{p,p} V_p ({T_p}^{n+1} - {T_p}^{n}) = \left[-\lambda_w \left(\frac{T_P - T_W}{d_{PW}}\right) S_w + \lambda_e \left(\frac{T_E - T_P}{d_{PE}}\right) S_e\right]^{n+1} \Delta t \tag{33}$$

The general equation of coefficient is given by

$$a_P {T_P}^{n+1} = a_E {T_E}^{n+1} + a_W {T_W}^{n+1} + b_P \tag{34}$$

After comparing the equation 33 and 34, the coefficients for the internal nodes are found

$$a_E = {\lambda_e}^{n+1} \frac{S_e}{d_{PE}} \tag{35a}$$

$$a_W = {\lambda_w}^{n+1} \frac{S_w}{d_{PW}} \tag{35b}$$

$$a_P = a_E + a_W + \frac{\rho_p c_{p,p} V_p}{\Delta t} \tag{35c}$$

$$b_P = \frac{\rho_p c_{p,p} V_p}{\Delta t} {T_P}^{n} \tag{35d}$$

– **Node i = 1:** A similar analysis is followed, the main difference is that this first node is affected by the temperature inside the volume T_{int}. Figure 22 shows the energy balance and is expressed as follows

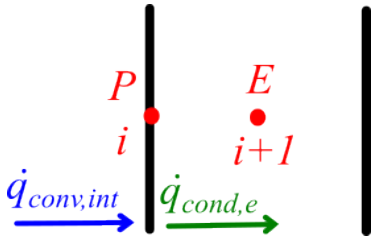

Figure 22: *Energy balance in the first node*

$$\dot{q}_{conv,int}^{n+1} = \dot{q}_{cond,e}^{n+1} \tag{36a}$$

$$\alpha_{int}{}^{n+1}\left(T_{int}{}^{n+1} - T_P{}^{n+1}\right) = -\lambda_e{}^{n+1}\left(\frac{T_E{}^{n+1} - T_P{}^{n+1}}{d_{PE}}\right) \tag{36b}$$

By comparing this last expression with the equation 34 the following coefficients are obtained for the first node.

$$a_E = \frac{\lambda_e{}^{n+1}}{d_{PE}} \tag{37a}$$

$$a_W = 0 \tag{37b}$$

$$a_P = a_E + a_W + \alpha_{int}{}^{n+1} \tag{37c}$$

$$b_P = \alpha_{int}{}^{n+1}\, T_{int}{}^{n+1} \tag{37d}$$

– **Node i = N+2:** By following the same procedure, the coefficients for the last node can be found. Note that this node is affected by radiation and external temperature T_{ext}. Figure 23 depicts the energy balance and is given by

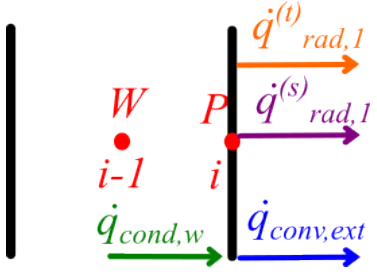

Figure 23: *Energy balance in the last node (Traditional)*

$$\dot{q}_{cond,w}^{n+1} = \dot{q}_{rad,1}^{(t)\,n+1} + \dot{q}_{rad,1}^{(s)\,n+1} + \dot{q}_{conv,ext}^{n+1} \tag{38}$$

with

$$\dot{q}_{cond,w}^{n+1} = -{\lambda_w}^{n+1}\left(\frac{{T_P}^{n+1} - {T_W}^{n+1}}{d_{PW}}\right) \tag{39a}$$

$$\dot{q}_{rad,1}^{(t)\,n+1} = {j_1}^{n+1} - {g_1}^{n+1} \tag{39b}$$

$$\dot{q}_{rad,1}^{(s)\,n+1} = I_T \alpha_s \tag{39c}$$

$$\dot{q}_{conv,ext}^{n+1} = {\alpha_{ext}}^{n+1}\left({T_P}^{n+1} - {T_{ext}}^{n+1}\right) \tag{39d}$$

where I_T is a value obtained from meteorological data containing global and diffuse radiation at different times of the day and α_s is the absorption coefficient.

Rewriting and comparing with the equation 34 yields to

$$a_E = 0 \tag{40a}$$

$$a_W = \frac{{\lambda_w}^{n+1}}{d_{PW}} \tag{40b}$$

$$a_P = a_E + a_W + {\alpha_{ext}}^{n+1} + \varepsilon_1 \sigma T_P^{3\,n} \tag{40c}$$

$$b_P = {\alpha_{ext}}^{n+1}\,{T_{ext}}^{n+1} + \varepsilon_1 {g_1}^{n+1} + I_T \alpha_s \tag{40d}$$

4.1.1.4 Heat transfer coefficients

The hypothesis mentioned before indicates that only *natural convection* is considered in this study. Based on the literature, for a vertical plate the following correlations can be used to find the heat transfer coefficients inside and outside the volume [31].

- **Laminar flow:** $10^3 < Ra < 10^9$

$$C = 0.8 \tag{41a}$$

$$n = 1/4 \tag{41b}$$

$$K = \left[1 + \left(1 + \frac{1}{\sqrt{Pr}}\right)^2\right]^{-1/4} \tag{41c}$$

- **Turbulent flow:** $Ra \geq 10^9$

$$C = 0.0246 \tag{42a}$$

$$n = 2/5 \tag{42b}$$

$$K = \left[\frac{Pr^{1/6}}{1 + 0.494 Pr^{2/3}}\right]^{2/5} \tag{42c}$$

After determining the type of flow, the Nusselt number can be calculated as follows

$$Nu = C Ra^n K \tag{43}$$

Finally, the heat transfer coefficient can be found by solving the equation 16 for α

$$\alpha = \frac{Nu\lambda}{X} \tag{44}$$

where X is the characteristic length, which in this case is the wall height H.

4.2 Trombe wall

When this report refers to a *Trombe wall*, it is an enclosed volume with a south-facing wall that is usually painted a dark color to absorb thermal energy. This wall is covered with external glazing with an insulating air-gap between the glass and the wall. This physical-mathematical model is simulated based on the following hypotheses:

- The model will be treated in a transitory regime.
- All the walls, roof, and floor of the volume are adiabatic except for the south-facing wall.
- The external glazing is considered thin enough, so it can be modeled using a single node.
- Different number of control volumes will be used to discretized the wall thickness.
- In principle, the composition of the wall will be made of a single material (concrete), but the in-house numerical code created can include other materials if necessary.
- The glass is considered to be transparent to solar radiation and opaque to thermal radiation.
- Thermophysical properties are considered constant due to their low variability.
- Any fluid motion is only caused by natural means, so only *natural convection* is relevant.[3]
- The air-gap between the glass and the wall is considered as *air cavity*, so based on the literature, new empirical correlations are used to calculate the heat transfer coefficient in this small gap.
- Radiation is considered as a non-participating medium, so it does not influence the energy balance in the fluid.

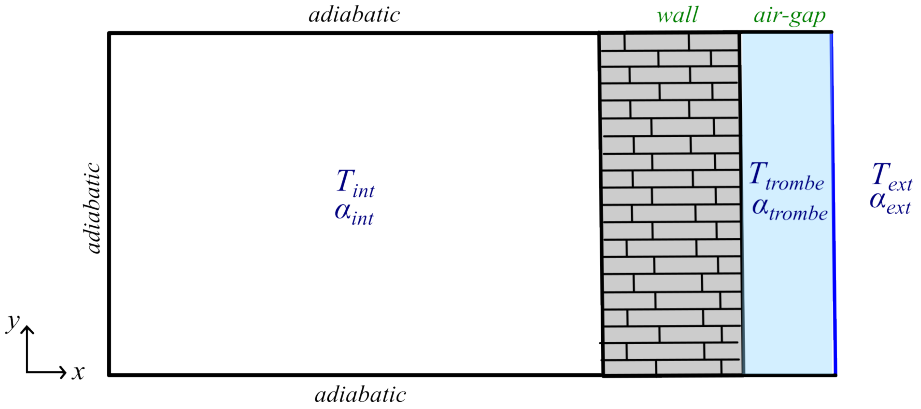

Figure 24: *Trombe wall scheme*

[3] See footnote 1.

4.2.1 Mathematical formulation

4.2.1.1 Energy balance in the fluid

A similar energy balance on the air mass inside the volume can be done on the Trombe wall. Figure 25 indicates the parameters involved in this case.

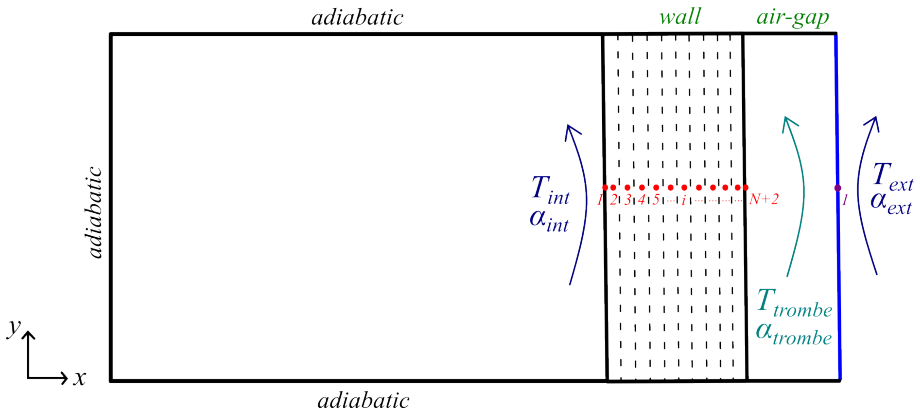

Figure 25: *Energy balance in the fluid – Trombe wall*

The mass balance is expressed exactly as discussed in Section 4.1.1.1. For the sake of completeness, the expressions for calculating the temperature inside the volume are shown here

- Trombe wall in a closed volume:

$$T_{int}{}^{n+1} = T_{int}{}^{n} + \frac{\Delta t}{\rho_{air} V c_{p,air}} \left[\alpha_{int}{}^{n} \left(T^{n}[1] - T_{int}{}^{n} \right) S \right] \tag{45}$$

- Trombe wall in a closed volume with heating/cooling device:

$$T_{int}{}^{n+1} = T_{int}{}^{n} + \frac{\Delta t}{\rho_{air} V c_{p,air}} \left[\alpha_{int}{}^{n} \left(T^{n}[1] - T_{int}{}^{n} \right) S \pm P \right] \tag{46}$$

- Trombe wall in a volume with air infiltration and heating/cooling device:

$$T_{int}{}^{n+1} = T_{int}{}^{n} + \frac{\Delta t}{\rho_{air} V c_{p,air}} \left[\rho_{air} \dot{V} c_{p,air} \left(T_{ext} - T_{int}{}^{n} \right) + \alpha_{int}{}^{n} \left(T^{n}[1] - T_{int}{}^{n} \right) S \pm P \right] \tag{47}$$

4.2.1.2 Thermal radiation

A procedure similar to that of the traditional wall is followed.

View factors

Figure 26 illustrates the situation to be analyzed.

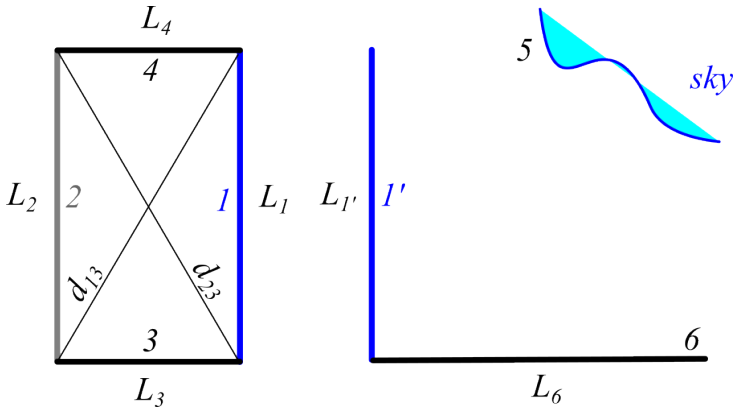

Figure 26: *View factors scheme for a Trombe wall*

Then, the view factors for each surface[4] are expressed as follows

- **Surface 1:**

$$F_{11} = 0;\ F_{12} = \frac{d_{13} + d_{23} - 2L_1}{2L_1};\ F_{13} = \frac{L_1 + L_3 - d_{13}}{2L_1};\ F_{14} = 1 - F_{11} - F_{12} - F_{13} \quad (48)$$

- **Surface 2:**

$$F_{21} = \frac{A_1}{A_2}F_{12};\quad F_{22} = 0;\quad F_{23} = \frac{L_2 + L_3 - d_{23}}{2L_2};\quad F_{24} = 1 - F_{21} - F_{22} - F_{23} \quad (49)$$

- **Surface 3:**

$$F_{31} = \frac{A_1}{A_3}F_{13};\quad F_{32} = \frac{L_2 + L_3 - d_{23}}{2L_3};\quad F_{33} = 0;\quad F_{34} = 1 - F_{31} - F_{32} - F_{33} \quad (50)$$

- **Surface 4:**

$$F_{41} = \frac{A_1}{A_4}F_{14};\quad F_{42} = \frac{A_2}{A_4}F_{24};\quad F_{43} = \frac{A_3}{A_4}F_{34};\quad F_{44} = 0 \quad (51)$$

- **Surface 1':**

$$F_{1'1'} = 0;\qquad F_{1'5} = 1 - F_{1'1'} - F_{1'6};\qquad F_{1'6} = \frac{L_1 + L_6 - d_{16}}{2L_1} \quad (52)$$

- **Surface 6:**

$$F_{61'} = \frac{A_{1'}}{A_6}F_{1'6};\qquad F_{65} = 1 - F_{61'} - F_{66};\qquad F_{66} = 0 \quad (53)$$

where A_x and L_x is the cross-sectional area and the length of the element x, respectively.

The distance d_{xy} is defined as $d_{xy} = \sqrt{{L_x}^2 + {L_y}^2}$ and the area A_x is given by $A_x = L_x W$.

[4] See footnote 2.

Note that the rectangular space is not very wide, which means that L_3 and L_4 are small compared to the other dimensions. In this case, surface 1 and surface 2 can be considered to be in a one-to-one relationship. Hence, the view factors for surfaces 3 and 4 are negligible, which means that temperatures T_3 and T_4 are not needed. The view factors for surfaces 1 and 2 are simplified as

- **Surface 1:**

$$F_{11} = 0; \qquad F_{12} = 1 \tag{54}$$

- **Surface 2:**

$$F_{21} = 1; \qquad F_{22} = 0 \tag{55}$$

Irradiosity and radiosity relations

Trombe wall technology introduces a new element: external glazing. Therefore, the analysis of these parameters is divided into the interior and exterior zone.

- **Interior zone:** This zone comprises the rectangular enclosure between the wall and the glass. This scheme is shown in Figure 27.

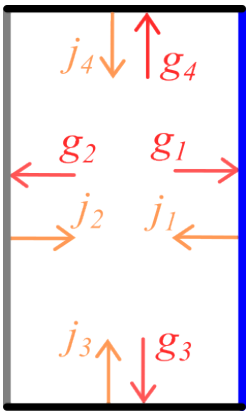

Figure 27: *Internal irradiosity and radiosity scheme for a Trombe wall*

The general expressions for irradiosity (g_k) and radiosity (j_k) holds

  - **Surface 1:**

$$j_1 = \varepsilon_1 \sigma {T_1}^4 + (1 - \varepsilon_1) g_1 \tag{56a}$$

$$g_1 = F_{11} j_1 + F_{12} j_2 + F_{13} j_3 + F_{14} j_4 \tag{56b}$$

  - **Surface 2:**

$$j_2 = \varepsilon_2 \sigma {T_2}^4 + (1 - \varepsilon_2) g_2 \tag{57a}$$

$$g_2 = F_{21} j_1 + F_{22} j_2 + F_{23} j_3 + F_{24} j_4 \tag{57b}$$

– **Surface 3:**

$$j_3 = \varepsilon_3 \sigma {T_3}^4 + (1 - \varepsilon_3) g_3 \tag{58a}$$

$$g_3 = F_{31} j_1 + F_{32} j_2 + F_{33} j_3 + F_{34} j_4 \tag{58b}$$

– **Surface 4:**

$$j_4 = \varepsilon_4 \sigma {T_4}^4 + (1 - \varepsilon_4) g_4 \tag{59a}$$

$$g_4 = F_{41} j_1 + F_{42} j_2 + F_{43} j_3 + F_{44} j_4 \tag{59b}$$

Note that these expressions can be rewritten considering (again) that L_3 and L_4 are small compared to the other dimensions. Hence, the simplified expressions yields to

– **Surface 1:**

$$j_1 = \varepsilon_1 \sigma {T_1}^4 + (1 - \varepsilon_1) g_1 \tag{60a}$$

$$g_1 = F_{11} j_1 + F_{12} j_2 = j_2 \tag{60b}$$

– **Surface 2:**

$$j_2 = \varepsilon_2 \sigma {T_2}^4 + (1 - \varepsilon_2) g_2 \tag{61a}$$

$$g_2 = F_{21} j_1 + F_{22} j_2 = j_1 \tag{61b}$$

- **External zone:** This zone basically consists of the interaction of external conditions with the glass. This scheme is displayed in Figure 27.

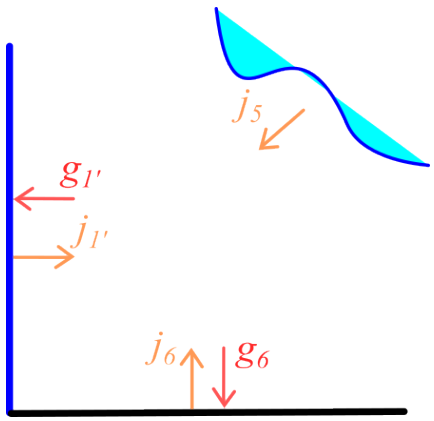

Figure 28: *External irradiosity and radiosity scheme for a Trombe wall*

The general expressions for irradiosity (g_k) and radiosity (j_k) yields to

– **Surface 5:**

$$j_5 = \sigma {T_{sky}}^4 \tag{62}$$

– **Surface 6:**

$$j_6 = \varepsilon_6 \sigma {T_6}^4 + (1 - \varepsilon_6) g_6 \tag{63a}$$

$$g_6 = F_{61} j_1 + F_{65} j_5 + F_{66} j_6 \tag{63b}$$

where σ is the Stefan-Boltzmann constant, ε_k is the emissivity of the surface k and T_k is the temperature of the surface k.

Note that T_1 is the glass temperature and T_2 is the wall temperature to be determined based on a numerical analysis detailed in the following sections. T_6 is the yard temperature and is an input data. Finally, the sky temperature T_{sky} and the net rate of heat transfer by thermal radiation $\dot{q}_{rad}$ are calculated using the equation 27 and 28, respectively.

4.2.1.3 Solid analysis

The analysis of the solids is similar to the case of the traditional wall, the main difference is that now the glass is added and must also be analyzed.

External glass

The external glass is considered to be transparent[5] to solar radiation, and opaque[6] to thermal radiation. Thus, the mass balance in the glass is expressed as follows

$$\{Accumulation\} = \{In\} - \{Out\} + \{Generation\} \tag{64a}$$

$$\frac{\rho_{glass} V_{glass} c_{p,glass}}{\Delta t} \left({T_{glass}}^{n+1} - {T_{glass}}^{n} \right) = \dot{q}_{conv,trombe} - \dot{q}^{(t)}_{rad,1} - \dot{q}^{(t)}_{rad,1'} - \dot{q}_{conv,ext} \tag{64b}$$

with

$$\dot{q}_{conv,trombe} = \alpha_{trombe} \left(T_{wall}[N+2] - {T_{glass}}^{n} \right) S_{glass} \tag{64c}$$

$$\dot{q}^{(t)}_{rad,1} = (j_1 - g_1) S_{glass} \tag{64d}$$

$$\dot{q}^{(t)}_{rad,1'} = (j_{1'} - g_{1'}) S_{glass} \tag{64e}$$

$$\dot{q}_{conv,ext} = \alpha_{ext} \left({T_{glass}}^{n} - T_{ext} \right) S_{glass} \tag{64f}$$

Substituting and solving for the glass temperature gives

$$\begin{aligned} {T_{glass}}^{n+1} = {T_{glass}}^{n} + \frac{\Delta t}{\rho_{glass} V_{glass} c_{p,glass}} \Big[& \alpha_{trombe} \left(T_{wall}[N+2] - {T_{glass}}^{n} \right) S_{glass} \\ & - (j_1 - g_1) S_{glass} - (j_{1'} - g_{1'}) S_{glass} - \alpha_{ext} \left({T_{glass}}^{n} - T_{ext} \right) S_{glass} \Big] \end{aligned} \tag{64g}$$

where S_{glass} and V_{glass} are the heat transfer area and the volume of the external glazing, respectively.

[5] Glass allows the greatest possible visible light to pass through ($\dot{q}^{(s)}_{rad} = 0$).

[6] Glass does not allow transmission of light waves ($\tau = 0$).

Wall

The procedure followed is exactly the same as the one discussed in Section 4.1.1.3. This means that the discretization used in the traditional wall is the same for the Trombe wall.

Note that the discretization coefficients of the first node ($i = 1$) and of the intermediate nodes ($2 \leqslant i \leqslant N + 1$) are exactly the same. However, for the last node ($i = N + 2$), the coefficients must be modified since now this node is no longer in contact with the ambient conditions but with the small air-gap between the wall and the glass.

- **Node i = N+2:** Figure 29 shows the energy balance and is expressed as follows

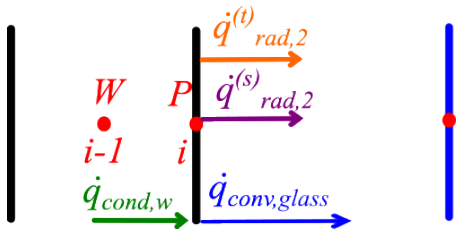

Figure 29: *Energy balance in the last node (Trombe)*

$$\dot{q}^{n+1}_{cond,w} = \dot{q}^{(t)\ n+1}_{rad,1} + \dot{q}^{(s)\ n+1}_{rad,1} + \dot{q}^{n+1}_{conv,glass} \tag{65}$$

with

$$\dot{q}^{n+1}_{cond,w} = -{\lambda_w}^{n+1} \left(\frac{{T_P}^{n+1} - {T_W}^{n+1}}{d_{PW}} \right) \tag{66a}$$

$$\dot{q}^{(t)\ n+1}_{rad,2} = {j_2}^{n+1} - {g_2}^{n+1} \tag{66b}$$

$$\dot{q}^{(s)\ n+1}_{rad,2} = I_T \alpha_s \tag{66c}$$

$$\dot{q}^{n+1}_{conv,glass} = {\alpha_{trombe}}^{n+1} \left({T_P}^{n+1} - {T_{glass}}^{n+1} \right) \tag{66d}$$

where I_T is a value obtained from meteorological data containing global and diffuse radiation and α_s is the absorption coefficient.

Rewriting and comparing with the equation 34 gives

$$a_E = 0 \tag{67a}$$

$$a_W = \frac{{\lambda_w}^{n+1}}{d_{PW}} \tag{67b}$$

$$a_P = a_E + a_W + {\alpha_{trombe}}^{n+1} + \varepsilon_2 \sigma {T_P^3}^n \tag{67c}$$

$$b_P = {\alpha_{trombe}}^{n+1} {T_{glass}}^{n+1} + \varepsilon_2 {g_2}^{n+1} + I_T \alpha_s \tag{67d}$$

4.2.1.4 Heat transfer coefficients

Internal and external

The aforementioned hypotheses indicate that this study also considers only *natural convection*. Consequently, to determine the internal and external heat transfer coefficients, the expressions discussed in Section 4.1.1.4 can be used.

Air-gap

Besides that, the Trombe wall includes an air space between the wall and the glass that can be considered as a small cavity. It is reported in literature that in order to determine the heat transfer coefficient in this cavity α_{trombe}, the following expressions apply to a cavity of this type with isothermal vertical walls and with an adiabatic top and bottom, which clearly fits this problem [31].

$$Nu_L = 0.42 Ra_L^{1/4} Pr^{0.012} \left(\frac{H}{L}\right)^{-0.3} \quad \text{if} \begin{cases} 10 \lesssim \frac{H}{L} \lesssim 40 \\ 1 \lesssim Pr \lesssim 2 \times 10^4 \\ 10^4 \lesssim Ra_L \lesssim 10^7 \end{cases} \tag{68}$$

$$Nu_L = 0.046 Ra_L^{1/3} \quad \text{if} \begin{cases} 1 \lesssim \frac{H}{L} \lesssim 40 \\ 1 \lesssim Pr \lesssim 20 \\ 10^6 \lesssim Ra_L \lesssim 10^9 \end{cases} \tag{69}$$

where, H and L are the height and length of the cavity, respectively.

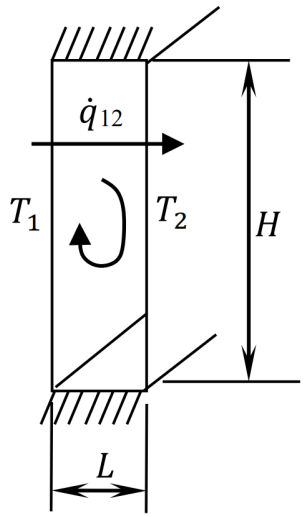

Figure 30: *Cavity with isothermal vertical walls. Reproduced from [31]*

4.3 Algorithm

The algorithm for solving the traditional and Trombe wall is the following

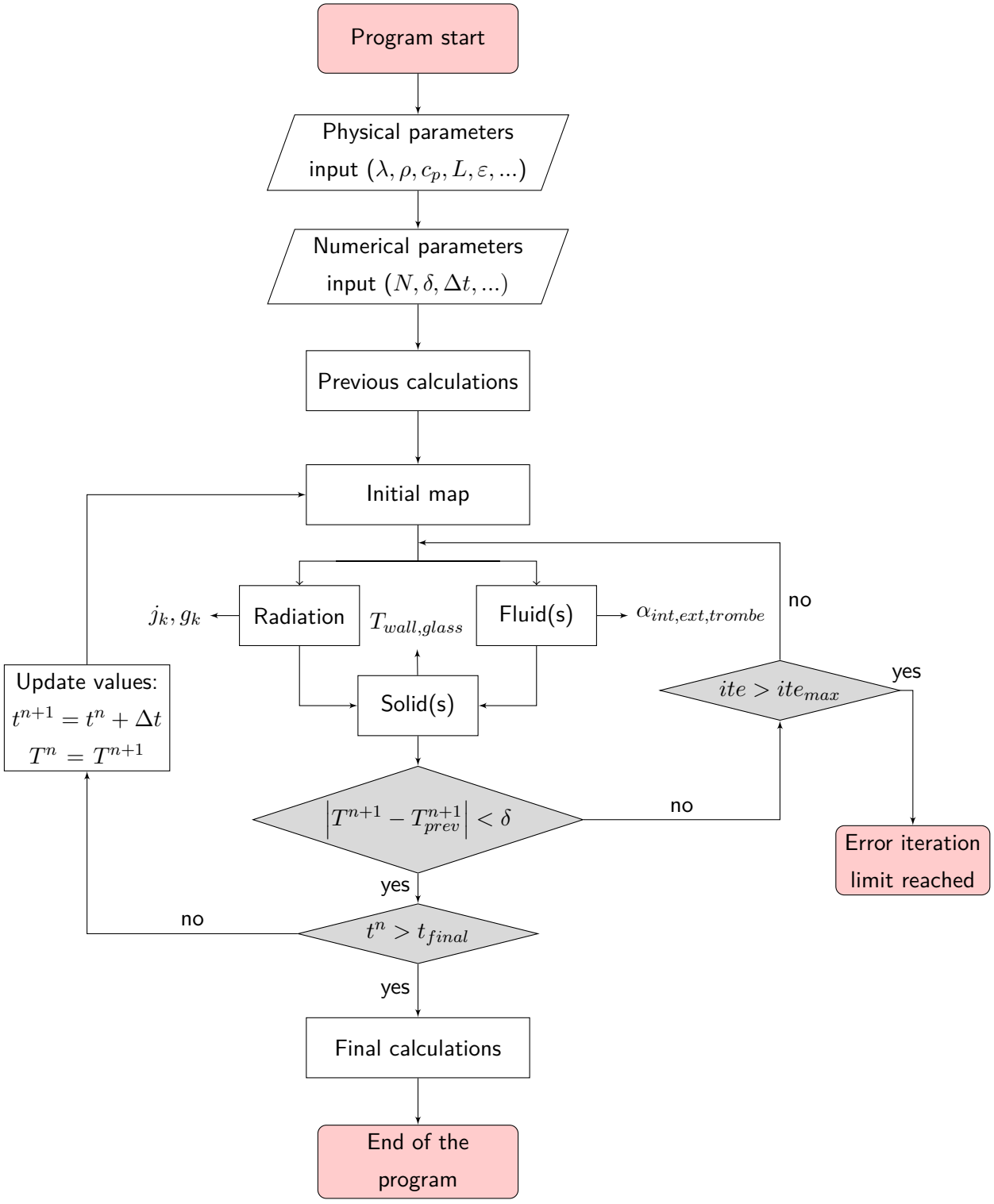

Figure 31: *Flow chart for numerical solution procedure*

5 Verification studies of the heat conduction model

In order to get used with programming code in the C++ environment, simple cases have been simulated to implement the Finite Volume Method (FVM). This was very useful before starting to solve the case studies proposed in this report, since in addition to exploring the main features of C++, this is the base that can later be extended to study more complex cases. In the same way, this has made it possible to check if the results coincide with the analytical solution or with solutions proposed in the literature.

5.1 Heat conduction problem

The heat conduction equation is shown in equation 70. This equation indicate how the temperature of a given region evolves over time.

$$\rho c_p \frac{\partial T}{\partial t} = \nabla \cdot (\lambda \nabla T) + \dot{q}_v \tag{70}$$

where ρ, c_p and λ are the density, specific heat capacity and the thermal conductivity of the material. T is the temperature and $\dot{q}_v$ the internal volumetric heat source.

Note that the temperature is a function of x and t, i.e. $T(x,t)$. Thus, this previous work consists of studying the spatial part, and the temporal part. To do this, the C++ developed code is structured in several parts. First, a declaration of the variables used in this problem. Second, declaration of the main functions to perform the calculations. Finally, the main function of the program where the calculation functions are called. This main function follows the algorithm shown in Figure 31, which basically consists of using a FVM discretization of centered nodes to then obtain the discretization coefficients, and solve them using a solver (GS or TDMA).

Likewise, it is aimed to study the results when a certain domain is composed of one and two materials. Therefore, it is important to consider how the nodes close to the point where material 1 and material 2 connect can be treated. In the case where their properties are very different, either very high or low, there could be inconsistencies in the results.

That is why, the harmonic mean (eq. 71) is implemented given that it is useful when dealing with discontinuities.

$$\phi_X = \frac{d_{PX}}{\frac{d_{Px}}{\phi_P} + \frac{d_{xX}}{\phi_X}} \tag{71}$$

5.1.1 Spatial study

In order to study the spatial part, the analytical equation of heat conduction for a flat plate is used.

$$T(x) = -\frac{\dot{q}_v}{2\lambda}x^2 + C_1 x + C_2 \tag{72}$$

where C_1 and C_2 are constants that depend on the boundary conditions of the problem.

The objective is to compare the results of the implemented code with the results obtained with this analytical solution. It can be seen that equation 72 is applicable for one-dimensional permanent problems. Hence, the C++ code used is run for a very long time such that the steady state is reached.

The input data used for this case are as follows:

- Numerical parameters: $N = 100$ and $\Delta t = 100\, s$.
- Temperatures: $T_{left} = 373.15\, K$ and $T_{right} = 373.15\, K$.
- Heat transfer coefficients: $\alpha_{left} = 4\, W/(mK)$ and $\alpha_{right} = 4\, W/(mK)$.
- Material 1 (copper) thermophysical properties: $\rho = 8900\, kg/m^3$, $c_p = 390\, J/(kgK)$, $\lambda = 300\, W/(mK)$ and $\dot{q}_v = 1500\, W/m^3$.
- Material 2 (fiberglass) thermophysical properties: $\rho = 2000\, kg/m^3$, $c_p = 700\, J/(kgK)$, $\lambda = 0.04\, W/(mK)$ and $\dot{q}_v = 0\, W/m^3$.

Figure 32 and 33 shows the one and two-material study, respectively.

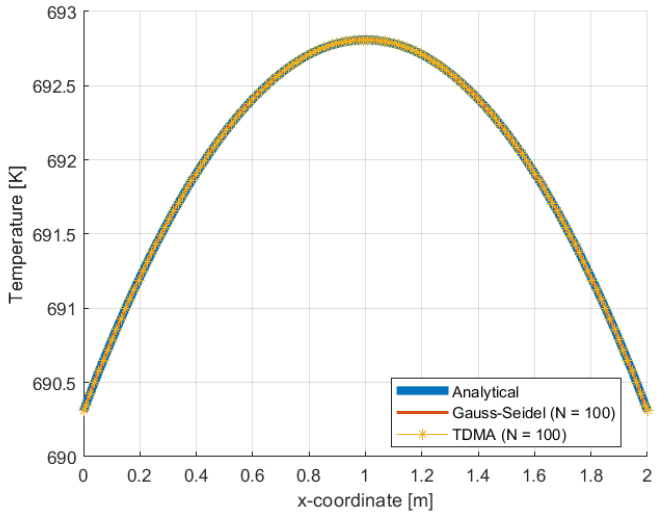

Figure 32: *Comparison between analytical and numerical results for one-material steady heat conduction using the following geometry:* $L = 2\, m$, $H = 1m$, *and* $W = 1\, m$

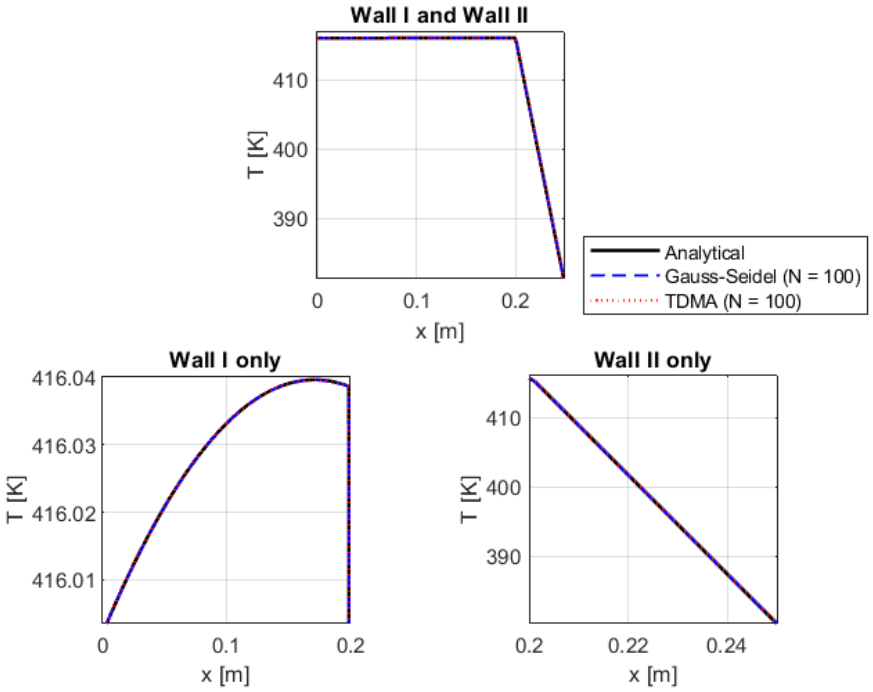

Figure 33: *Comparison between analytical and numerical results for 1D steady heat conduction case using the following geometry:* $L_{mat,1} = 20\ cm$, $L_{mat,2} = 5\ cm$, $H = 1\ m$, *and* $W = 1\ m$

5.1.2 Temporal study

Although the above results match the analytical solution, it is important to check the temporal part as well. The main challenge is that a transient problem has no analytical solution. Advantageously, in the literature one can find cases where for certain boundary conditions a Partial Difference Equation (PDE) with dimensionless variables is proposed. Thus, it has been decided to take one of these cases and adapt the numerical code according to the boundary conditions. In this way, it will be possible to compare the results of the C++ code with those reported in the literature.[7]

This case consists of a copper bar, shown in Figure 34, whose sides are adiabatic, and the left and right ends have fixed temperatures.

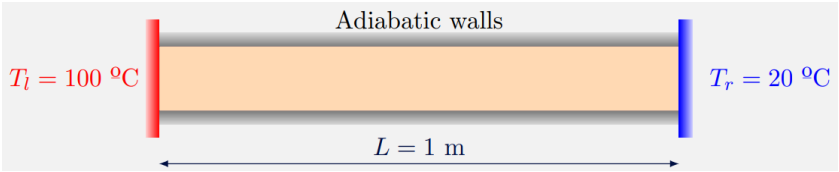

Figure 34: *1D transient conduction case. Reproduced from [33]*

[7] For more details, see references [32, 33]

The following nondimensionalization of the variables is proposed

$$t^* = t\frac{D}{L^2}; \qquad x^* = \frac{x}{L}; \qquad u \equiv T^* = \frac{T - T_{left}}{T_{right} - T_{left}} \tag{73}$$

The PDE proposed with dimensionless variables is

$$u(x^*, t^*) = u_1 x^* + \frac{4u_0}{\pi} \sum_{n=1,3,5,\ldots}^{\infty} \left(\frac{sin(n\pi x^*)}{n} e^{-n^2\pi^2 t^*} \right) + \frac{2u_1}{\pi} \sum_{n=1}^{\infty} \left((-1)^n \frac{sin(n\pi x^*)}{n} e^{-n^2\pi^2 t^*} \right) \tag{74}$$

In order to solve this set of equations, the following input data is used [33].

- Boundary conditions: $u_0 = 0$ and $u_1 = 1$.
- Numerical parameters: $n = 1000$ and $\Delta t = 100\ s$.
- Temperatures: $T_{left} = 100\,°C$, $T_{right} = 20\,°C$ and $T_0 = 30\,°C$.
- Heat transfer coefficients: $\alpha_{left} = 100\,W/(mK)$ and $\alpha_{right} = 100\,W/(mK)$.
- Material (copper) thermophysical properties: $\rho = 8960\ kg/m^3$, $c_p = 380\ J/(kgK)$, $\lambda = 400\,W/(mK)$ and $D = 1.1748 \cdot 10^{-4}\ m^2/s$.

Having this information it is possible to determine the temperature in different positions at different times. Below is an example of how this can be done if the temperature is calculated at $x = 0.5\,m$ and $t = 300\ s$.

$$t^* = t\frac{D}{L^2} = 300\left(\frac{1.1748 \cdot 10^{-4}}{1^2}\right) = 0.0352$$
$$x^* = \frac{x}{L} = \frac{0.5}{1} = 0.5$$
$$u_0 = T_0^* = \frac{T_0 - T_{left}}{T_{right} - T_{left}} = \frac{30 - 100}{20 - 100} = 0.875$$

Substituting these values into equation 74 gives

$$u(x^* = 0.5, t^* = 0.0352) = 0.8303$$

Finally, the temperature is found as follows

$$T(x = 0.5, t = 300) = T_{left} + u(T_{right} - T_{left}) = 33.5798\,°C$$

After doing the same for arbitrary positions and times, the following results were obtained for $T(x,t)$.

	$T(0.15, 100)$ $[°C]$	$T(0.3, 175)$ $[°C]$	$T(0.5, 300)$ $[°C]$	$T(0.75, 600)$ $[°C]$
Analytical	52.9453	39.7255	33.5798	28.0878
Numerical	52.9421	39.7223	33.5781	28.0869

Table 1: *Comparison between analytical and numerical results for 1D transient conduction case*

6 Meteorological data

For the next case studies, meteorological data from the city of Barcelona is used. These data have been obtained from the *Meteonorm® version 7.3.2* for Barcelona. The most relevant data used in this report are temperature and radiation. It is important to highlight that this information is available on an hour-by-hour basis. Therefore, interpolation has been used to run the simulations for different time steps desired by the user.

For the sake of simplicity, it has been decided to study a particular month. January is the month chosen to have a notion of how different cases would work in real life. For more information on these meteorological data in other months, see *Meteonorm®*.

6.1 Temperature

The evolution of the external temperature T_{ext} over time in January can be seen in Figure 35.

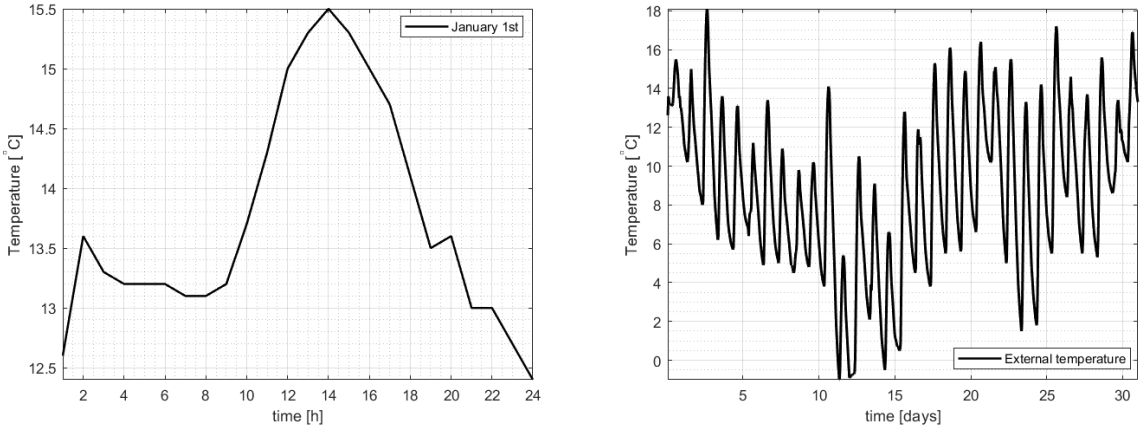

(a) *1 day* **(b)** *31 days*

Figure 35: *Evolution of the external temperature in January*

It can be concluded that there are not very high temperatures, which makes sense since it is a winter month.

6.2 Radiation

The evolution of the *total* radiation over time in January is shown in Figure 36. This total radiation contains the global and diffuse contribution for an inclined surface (90° facing south).

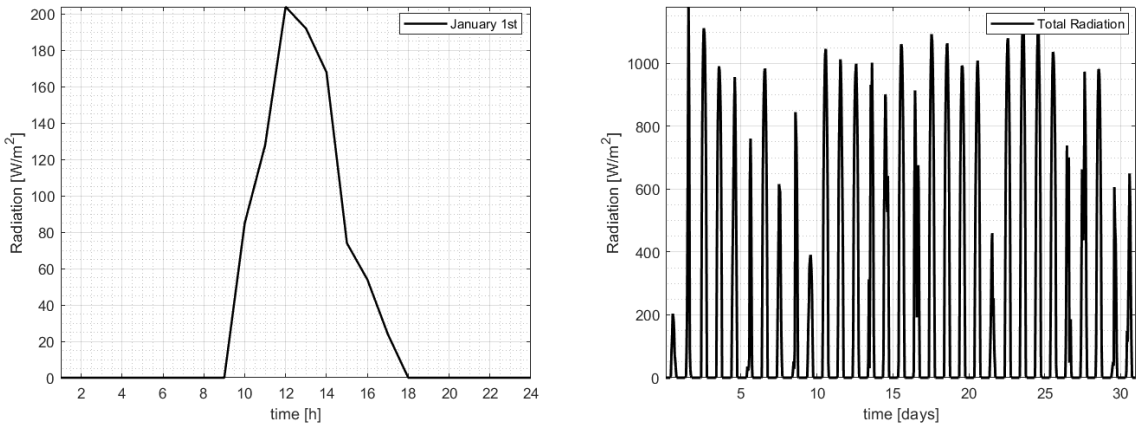

(a) *1 day* **(b)** *31 days*

Figure 36: *Evolution of the total radiation in January*

Although it is not expected to have high radiation values in such a winter month, it is seen that for some particular moments the radiation reaches high peaks. Yet, these are immediately reduced at the next time instant.

7 Case 1: Enclosure

Case objective: *To study the thermal behaviour of a volume located in Barcelona-Spain with a south-facing traditional wall and the rest of the walls, roof and floor adiabatic. Besides this, analyze the influence of the most optimal numerical parameters to be used in the rest of this study.*

7.1 Problem description

The problem consists of analyzing a volume $L \times W \times H$ located in Barcelona, Spain. This volume is characterized by having a roof, floor and walls that are considered completely adiabatic, with the exception of the wall facing south. This wall has a thickness D and is made of concrete. For this case, it has been decided that the external face of this wall is covered by an optical coating *SOLKOTE HI/SORB-II* that is specifically formulated for solar thermal applications. This coating is characterized by its high temperature tolerance, humidity resistance and its high capacity for absorption and adhesion to wall surfaces [34].

The study of this enclosure uses real data for the month of January of a specific year in Barcelona. The surface in contact with the outdoor ambient is exchanging energy by convection with an external temperature T_{ext} that varies at each instant desired by the user. The exterior heat transfer coefficient α_{ext} is calculated at each instant assuming that the air velocity is negligible, so that only natural convection is relevant. This means that the empirical formulations discussed previously are used. Furthermore, there is an exchange of energy due to radiation. Direct and diffuse radiation are taken into account, and the sky temperature T_{sky} is a function of the exterior temperature T_{ext} which is determined by using the expression 27. Finally, it is assumed that the enclosure is completely empty and there is only dry air with an initial temperature of 10°C at the first instant of the day.

Figure 37 depicts this case study.

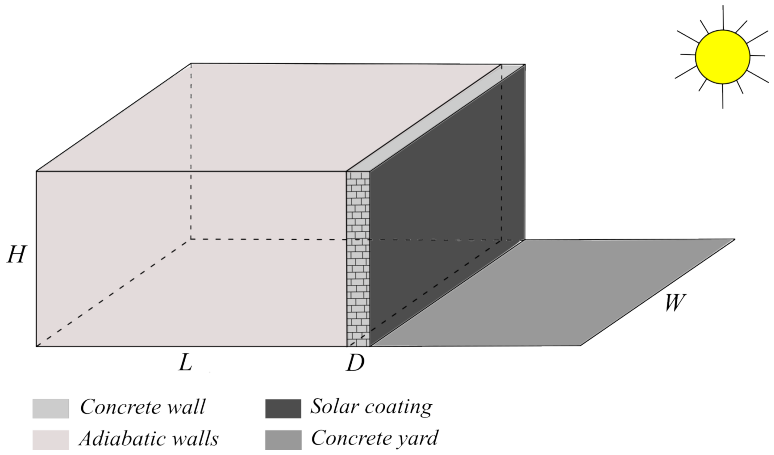

Figure 37: *Case 1 – Enclosure*

7.2 Influence of numerical parameters

In order to evaluate the performance of the code and the consequences of modifying different inputs – such as solver tolerance, mesh size and time step – on the computation time and final results, it has been decided to carry out a study modifying the most important numerical parameters. This study will help to find the most optimal inputs in such a way that realistic results are obtained, without having to increase the computational time. In general, it is sought to reduce this time as much as possible; otherwise, it would end up affecting the costs of the simulation.

7.2.1 Solver tolerance

The code developed in C++ contains two solvers – Gauss Seidel (GS) and Tri-diagonal Matrix Algorithm (TDMA). Although most of the results discussed were obtained using TDMA, it is important to discuss the influence of the tolerance imposed on the code when using GS.[8] This parameter determines if the solution is capable of converging or not. It also affects the processing time because if a very low tolerance is imposed, a high computational time is needed.

For this case, the following parameters were set: $N_x = 102$ and $\Delta t = 5\,min = 300\,s$. The results can be found in Figure 38 and 39.

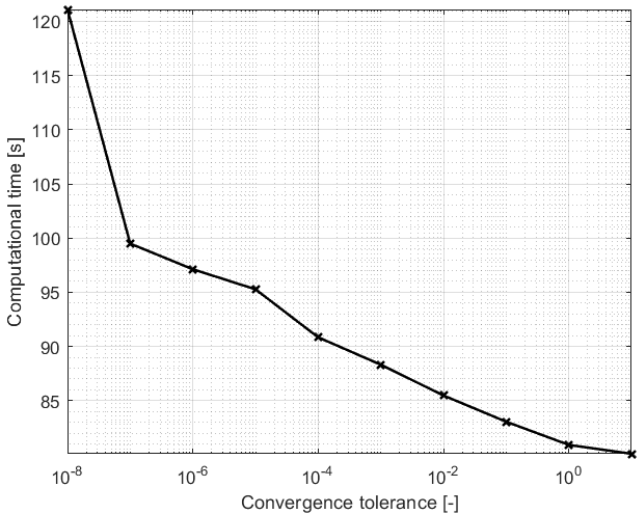

Figure 38: *Computational time as a function of convergence tolerance for a 31-day simulation using GS, holding constant N_x and Δt*

As expected, the smaller the tolerance, the longer the computation time. Also, by increasing the

[8] Note that this tolerance parameter does not affect the TDMA solver since it is a direct method.

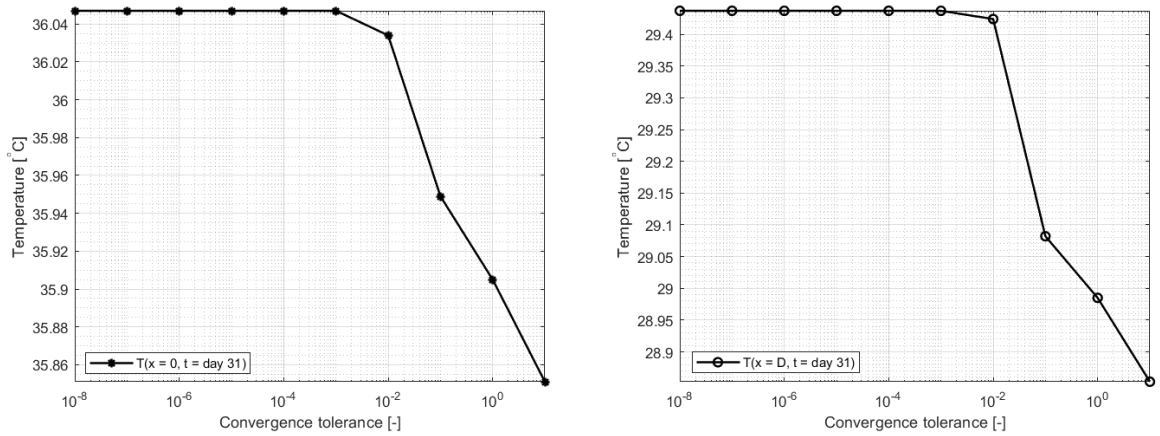

(a) *Inward-facing side* $(x = 0)$ **(b)** *Outward-facing side* $(x = D)$

Figure 39: *Wall temperature (at* $x = 0$ *and* $x = D$*) on day 31 as a function of convergence tolerance, holding constant* N_x *and* Δt

solver tolerance, the final results deviate a bit from the expected ones. These changes become relevant after increasing the tolerance more than 10^{-3}. Hence, it can be concluded that a tolerance less than or equal to 10^{-3} is enough for this case study. This would help reducing the computation time by a factor of ~ 1.4.

7.2.2 Time step

The time step is another relevant parameter that determines the precision of the final results of the numerical simulation. In this case, it is intended to study a month that contains 31 days, which is equivalent to 2 678 400 seconds. Someone may argue that using an increment of one-second would be a good option to get realistic results. Although this statement is true, the computational cost of studying a month with a second-to-second increment is very high. The C++ code created is capable of giving the outputs for different instants. Therefore, it is intended to study the optimal time step that gives acceptable results and does not compromise computational time.

For this case, the following parameters were set: $N_x = 102$ and $\delta = 10^{-3}$. The results can be seen in Figure 40 and 41.

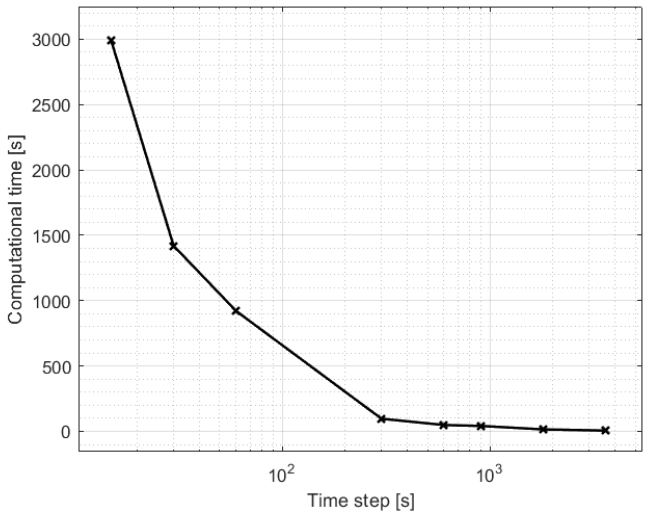

Figure 40: *Computational time as a function of time step for a 31-day simulation using TDMA, holding constant* N_x

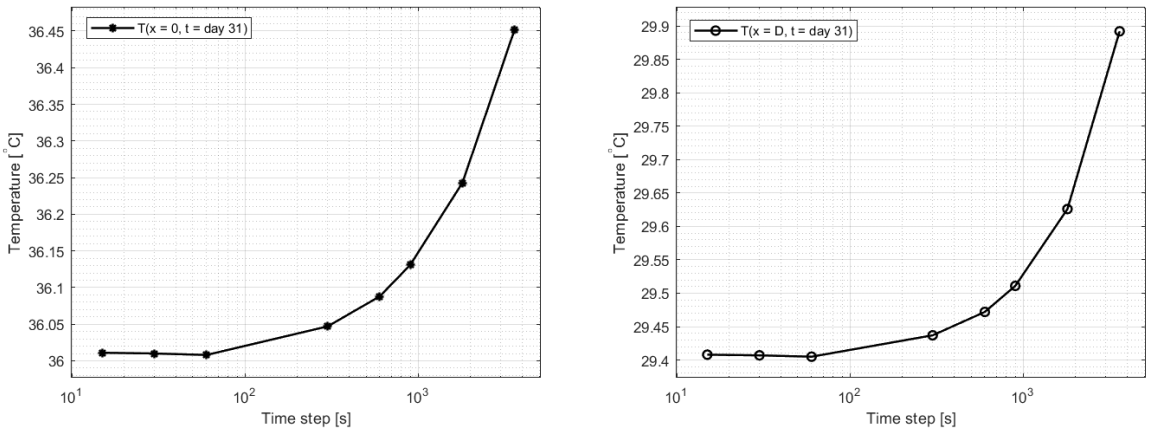

(a) *Inward-facing side* $(x = 0)$ **(b)** *Outward-facing side* $(x = D)$

Figure 41: *Wall temperature (at* $x = 0$ *and* $x = D$*) on day 31 as a function of time step, holding constant* N_x

From these results it is clear that if the time increment increases, the computation time is significantly reduced. Nonetheless, when the time increment is higher and higher, the results deviate from the actual value. For instance, when the time increment is less than one minute (60 seconds), the results are pretty much the same. However, when the value is more than 10 minutes (600 seconds), there is a deviation of the results. There is a small change in the results when Δt is in the range of 1 and 5 minutes, this is not relevant, so any value within this time range could be a good option in order to reduce the computation time by a maximum factor of ~ 9.

7.2.3 Mesh size

The number of nodes to discretize a domain – which in this case is a concrete wall – is another relevant parameter to analyze. Given that in this study the thickness of the wall is 20 cm, it has been decided to vary the number of nodes from 5 to 202.

The following parameters were set: $\Delta t = 5\,min$ and $\delta = 10^{-3}$. The results obtained are available Figure 42 and 43.

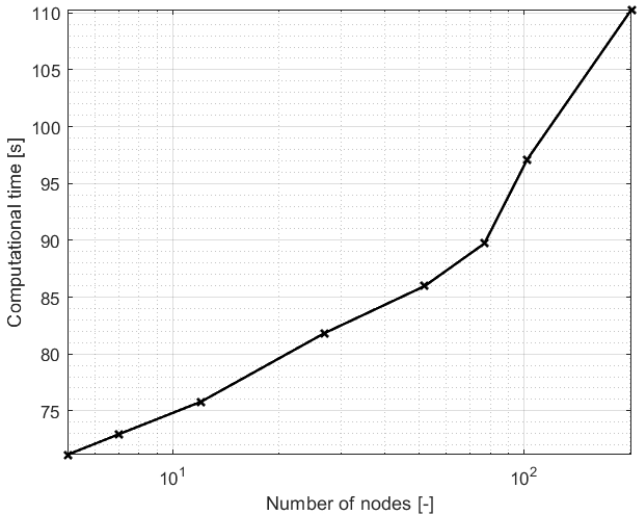

Figure 42: *Computational time as a function of the number of nodes for a 31-day simulation using TDMA, holding constant* Δt

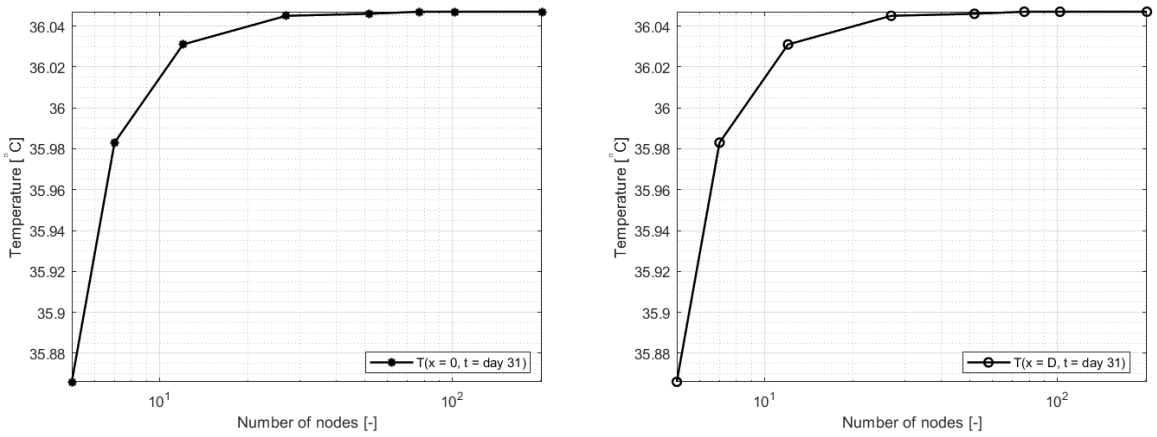

(a) *Inward-facing side* $(x = 0)$ **(b)** *Outward-facing side* $(x = D)$

Figure 43: *Wall temperature (at* $x = 0$ *and* $x = D$*) on day 31 as a function of the number of nodes, holding constant* Δt

Figure 42 displays the strong relationship between the number of nodes and the computation time, it can be seen that when more nodes are used, the processing time increases. Besides this, Figure 43 shows that when the number of nodes is less than 27, the results deviate away from the real ones. Therefore, for this type of wall geometry, a number greater than 27 nodes would be the most optimal.

7.3 Results and discussion

7.3.1 Input data

The input data used for this case study is detailed below

- **Physical data**
  - Geometry: $L = 10\,m, \quad W = 10\,m, \quad H = 4\,m, \quad D = 20\,cm$
  - Thermophysical properties: $\rho = 2200\,kg/m^3, \quad \lambda = 1.6\,W/(mK), \quad c_p = 1000\,J/(kgK)$
  - Optical properties
    - Concrete: $\varepsilon_{concrete} = 0.88, \quad \alpha_{s,concrete} = 0.60$ [31]
    - Solar coating: $\varepsilon_{coating} = 0.49, \quad \alpha_{s,coating} = 0.94$ [34]
- **Numerical data** [9]
  - Number of nodes: $N_x = 52$
  - Time step: $\Delta t = 150\,s = 2.5\,min$
  - Initial map: $T^o = 10°C = 283.15\,K$

7.3.2 Wall temperature distribution

The temperature distribution in the wall at different instants of time can be seen in Figure 44.

For the time intervals in which the sun does not rise or is hidden, it is seen that the temperature of the inward-facing side $(x = 0)$ is high compared to the outward-facing side $(x = D)$. This is because the external temperature is relatively low. On the other hand, during sunny hours, the temperature of the wall increases due to the high temperatures and the radiation that is produced. The parabolic shape of this temperature distribution indicates the accumulation of heat in the wall. Results demonstrate that the recorded temperatures are quite high, this can be attributed to the fact that this wall is made of concrete that is characterized by its high specific heat capacity c_p that indicates the ability to store heat. To this must be added the fact that an optical coating is

[9] These values were chosen before studying the influence of numerical parameters.

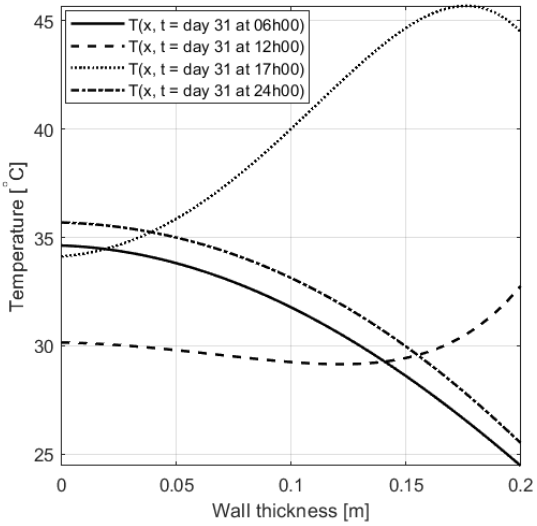

Figure 44: *Temperature distribution on the coated wall on day 31, using* $\Delta t = 150s$ *and* $N_x = 52$

being used on the external surface of this wall. This coating is characterized by its high absorption coefficient that oscillates between 0.88 and 0.94 [34].

7.3.3 Internal temperature

After knowing the temperature of the first node of the wall, the interior temperature T_{int} is calculated using the expression 19d which is recalled as follows

$$T_{int}{}^{n+1} = T_{int}{}^{n} + \frac{\Delta t}{\rho_{air} V c_{p,air}} \left[\alpha_{int}{}^{n} \left(T^{n}[1] - T_{int}{}^{n} \right) S \right]$$

For comparison purposes, the evolution of the internal temperature has been simulated without using a coating as well. These results can be found in Figure 45.

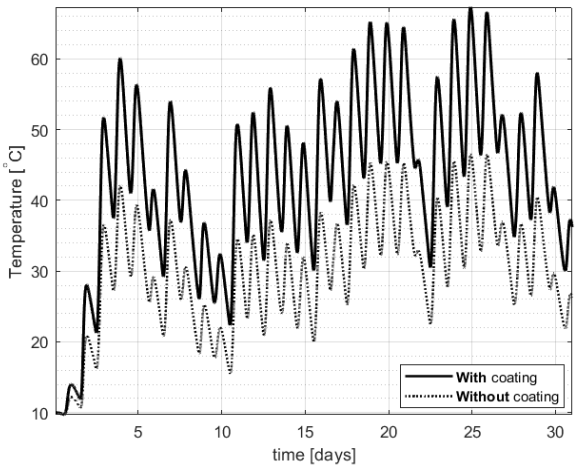

Figure 45: *Evolution of the internal temperature in January, using* $\Delta t = 150\ s$ *and* $N_x = 52$

It is observed that the temperatures inside the volume are relatively high. In the case of using a coating, these temperatures are even higher. Both the wall material and the coating have properties that allow them to absorb most of the radiation, which explains why the temperatures are high. If the coating had not been implemented, the temperature is reduced by about 20 degrees. This reduction is noticeable, but the temperature inside the volume is still high. Trying to find a reason for this, one could argue that most of the volume is considered adiabatic, leading to high temperatures inside. In addition to this, the meteorological data used indicates relatively high level of radiation for this particular month.

7.3.4 Heat transfer coefficients

The heat transfer coefficients can be found in Figure 46. They are calculated using the empirical formulations for natural convection discussed in Section 4.1.1.4. In fact, they are seen to be changing every instant as expected and are within the range of air in natural convection.

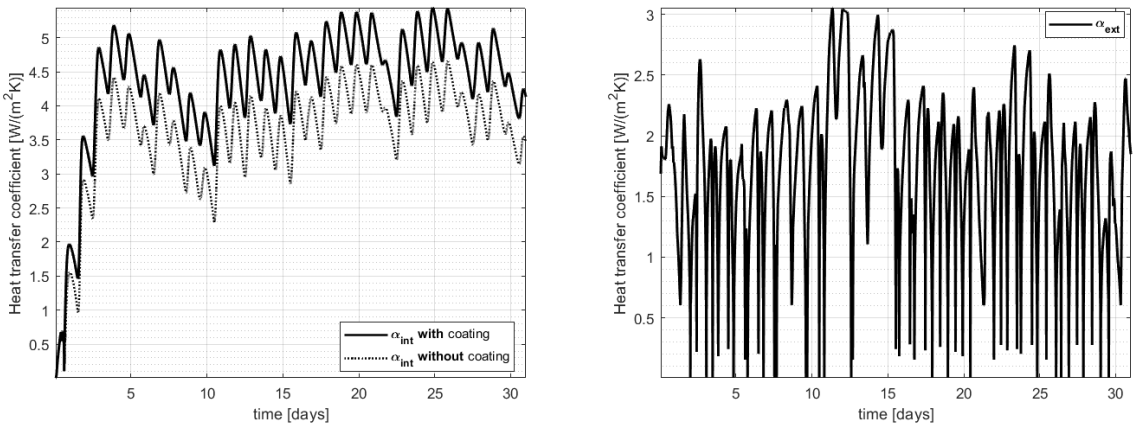

(a) *Internal* **(b)** *External*

Figure 46: *Evolution of the heat transfer coefficients in January, using* $\Delta t = 150\ s$ *and* $N_x = 52$

8 Case 2: Energy needed in an enclosure

Case objective: *To study the energy required to maintain a certain range of temperatures within a volume located in Barcelona-Spain with a traditional wall facing south and the rest of the walls, roof and floor adiabatic. For this, the behavior of the different power sources and the time step will be analyzed.*

8.1 Problem description

The problem follows exactly the same scenario as discussed in Section 7. For this case, it is intended to study how much energy is needed to maintain a certain temperature range within the volume $L \times W \times H$ located in Barcelona, Spain. Therefore, the main modification that has been made is to add a device inside the volume that is capable of giving a power P to heat or cool as needed. This device is expected to check the temperature at every given time instant and decide what to do in order to maintain a given temperature range.

It is reported in literature that a comfortable room temperature for most people is usually between 18 and 20°C [35]. This certainly depends on the individual, but for this case study, this is the range that is intended to be achieved. Reaching the right temperature is always essential for various reasons, such as physical comfort. The volume proposed in this study is meant to be any room in a house. So being too warm can impact the ability to concentrate, whilst being too cold may increase the risk of getting sick. Additionally, the costs of maintaining a certain temperature range might also be an important factor to consider when choosing the appropriate room temperature.

Without further ado, the situation to be studied in this case is illustrated in Figure 47.

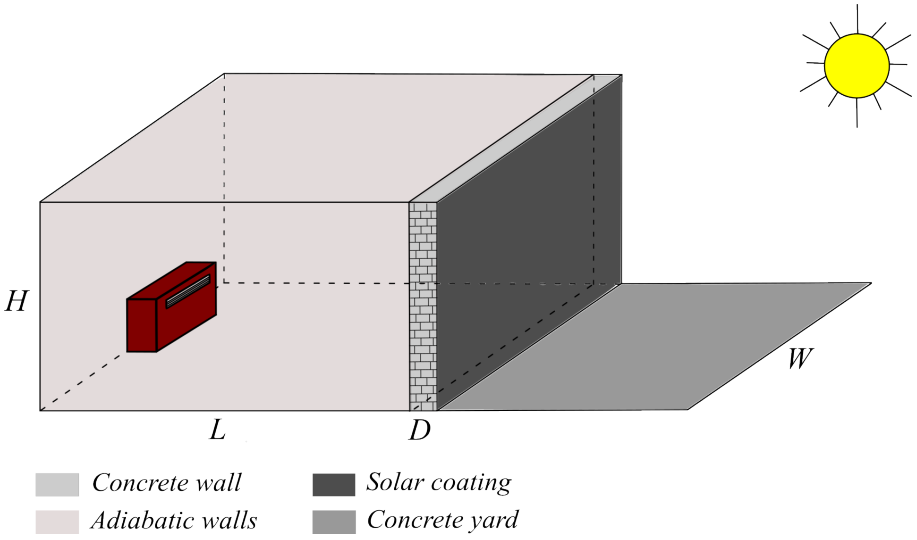

Figure 47: *Case 2 – Enclosure with a heating/cooling device*

8.2 Results and discussion

8.2.1 Input data

The input data used for this case study is detailed below

- **Physical data**
  - Geometry: $L = 10\,m, \quad W = 10\,m, \quad H = 4\,m, \quad D = 20\,cm$
  - Thermophysical properties: $\rho = 2200\,kg/m^3, \quad \lambda = 1.6\,W/(mK), \quad c_p = 1000\,J/(kgK)$
  - Optical properties
    - Concrete: $\varepsilon_{concrete} = 0.88, \quad \alpha_{s,concrete} = 0.60$ [31]
    - Solar coating: $\varepsilon_{coating} = 0.49, \quad \alpha_{s,coating} = 0.94$ [34]
  - Temperature range: $18°C \leq T_{int} \leq 20°C$
  - Power provided by the device: $P = 1\,kW, \quad P = 2\,kW, \quad P = 3\,kW, \quad P = 4\,kW$
- **Numerical data** [10]
  - Number of nodes: $N_x = 27$
  - Time step: $\Delta t = 150\,s = 2.5\,min$
  - Initial map: $T^o = 10°C = 283.15\,K$

8.2.2 Internal temperature

Although the internal temperature has been previously discussed, the effect of having a device providing different power is studied. This T_{int} can be found using the equation 20 which is recalled as follows

$$ {T_{int}}^{n+1} = {T_{int}}^{n} + \frac{\Delta t}{\rho_{air} V c_{p,air}} \left[{\alpha_{int}}^{n} \left(T^n[1] - {T_{int}}^{n} \right) S \pm P \right] $$

Note that this equation can take a positive or negative value for the power P. In case the device detects that the internal temperature is below the range, it will provide heat and therefore a positive value for P. On the other hand, when cooling a negative value for P is required. Furthermore, in the case of $P = 0\,kW$, this expression becomes the equation 19d.

Figure 48 illustrates how the internal temperature inside a volume would change for different power sources, and with a wall using a coating.

[10] These numerical parameters are the most optimal, see Section 7.2.

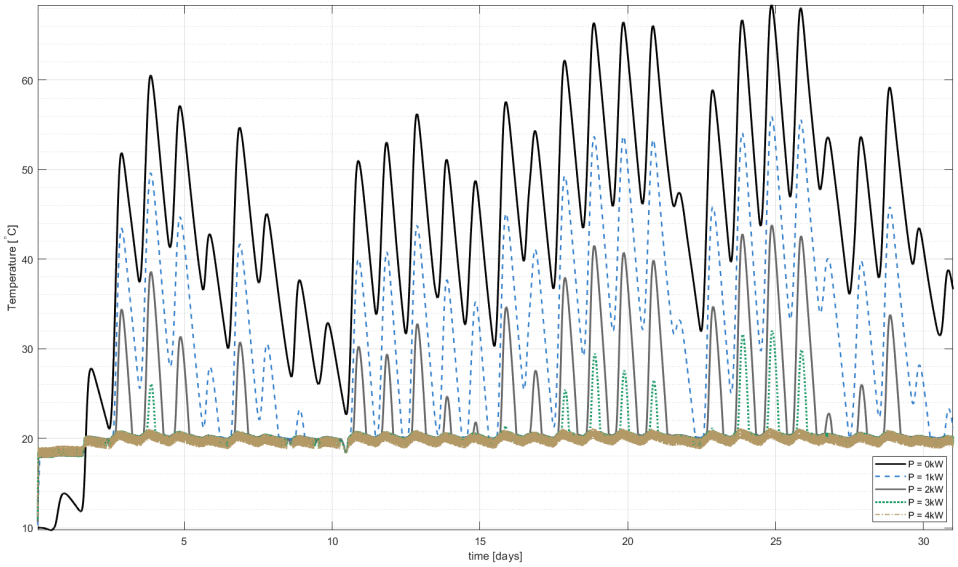

Figure 48: *Evolution of the internal temperature in January for different power sources, using a coating,* $\Delta t = 150s$ *and* $N_x = 27$

The solid black line represents the results for $P = 0\,kW$, this means that the heating/cooling device is basically turned off, leading to the same outcome discussed in the previous section. Overall, the internal temperature is observed to drop as more power is applied. Namely, for $P = 1\,kW$ (dark-gray dashed line), the temperature has decreased but it is still not within the desired range. Since the objective is to reach temperatures between 18 and 20 °C, applying a power of $P = 3\,kW$ may be considered as a valid option; however, there are some peaks for certain instants of the month. Slightly better results are achieved when using $P = 4\,kW$, displayed by the light-gray concentration shown above. Hence, for the rest of this study $P \geq 4\,kW$ are considered the best option.[11]

Even though the results shown in this chapter follow the most optimal numerical parameters and are in agreement with what was expected, it would be interesting to see what is the effect of using a small time step on the heating/cooling system. So far, a time step of $\Delta t = 150\,s$ has been used. This means that every 150 seconds the device checks the temperature and decides to heat, cool or just do nothing (in case the temperature is already in the desired range). A timestep can be thought as a way of examining the data over a given time interval. So if Δt is small, it means that the device inside the room will check the temperature more frequently, which might help to get better results.

Figures 49 and 50 display the results if the air-conditioning system works every 150 and 10 seconds

[11] Higher power values will certainly help to reach lower temperatures.

respectively.

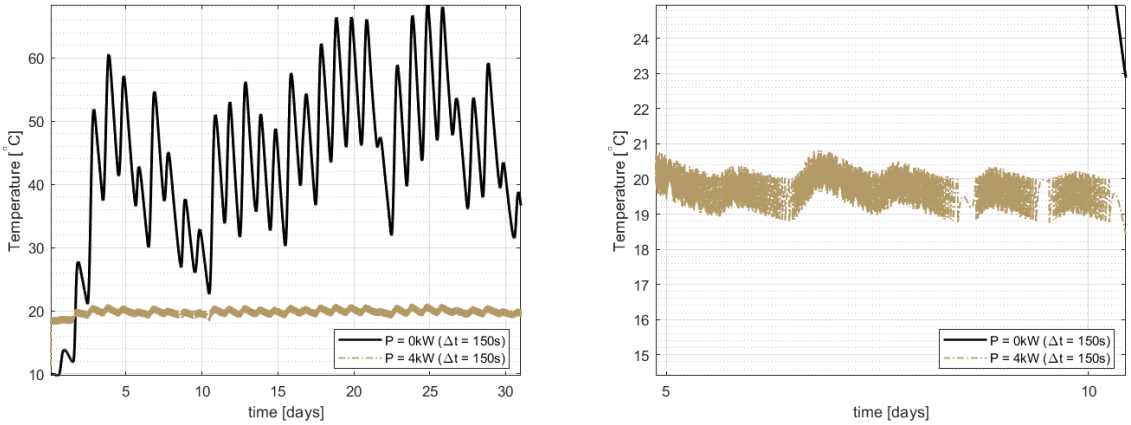

(a) *Standard view* **(b)** *Zoom view*

Figure 49: *Evolution of the internal temperature in January, using a coating,* $\Delta t = 150\,s$*,* $N_x = 27$ *and* $P = 4\,kW$

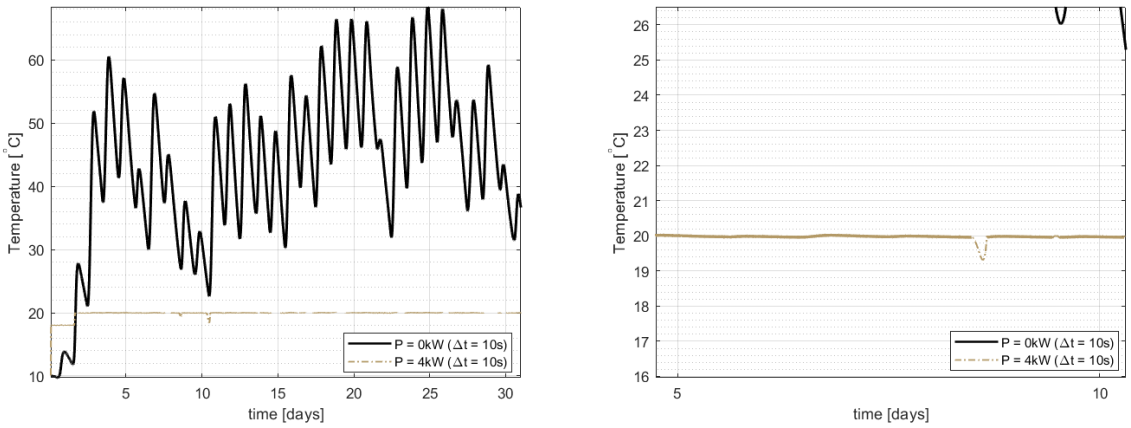

(a) *Standard view* **(b)** *Zoom view*

Figure 50: *Evolution of the internal temperature in January, using a coating,* $\Delta t = 10\,s$*,* $N_x = 27$ *and* $P = 4\,kW$

By comparing both results, it is clear that using a small time step gives better results while providing the same power source. This simply can be attributed to the fact that the device checks the temperatures more frequently. Consequently, when talking about air-conditioning is better to use small time steps; however, this could affect simulation costs. Therefore, an optimal balance between these parameters is a must.

8.2.3 Energy needed

It has been discussed in Section 7 that the temperatures inside the volume are indeed very high. However, at this point, this has been fixed by using a device capable of heating or cooling. For this case, it has been determined that this device should give a power of $P \geq 4\,kW$ to maintain the temperatures in a desired range, but it remains to be discussed how much energy would be spent each day (or in a month) in order to achieve this.

The amount of electrical energy used depends on the total power P used and the period of time during which it is used. Since this report deals with numerical methods, the period of time is equivalent to the time step Δt. Hence, the required energy in joules (J) can be found as follows

$$E = P\Delta t \tag{76}$$

or in kilowatt hour (kWh)

$$E = \frac{P\Delta t}{3.6 \cdot 10^6} \tag{77}$$

For comparison purposes, the energy used per day for two different time steps is studied and can be found in Figure 51.

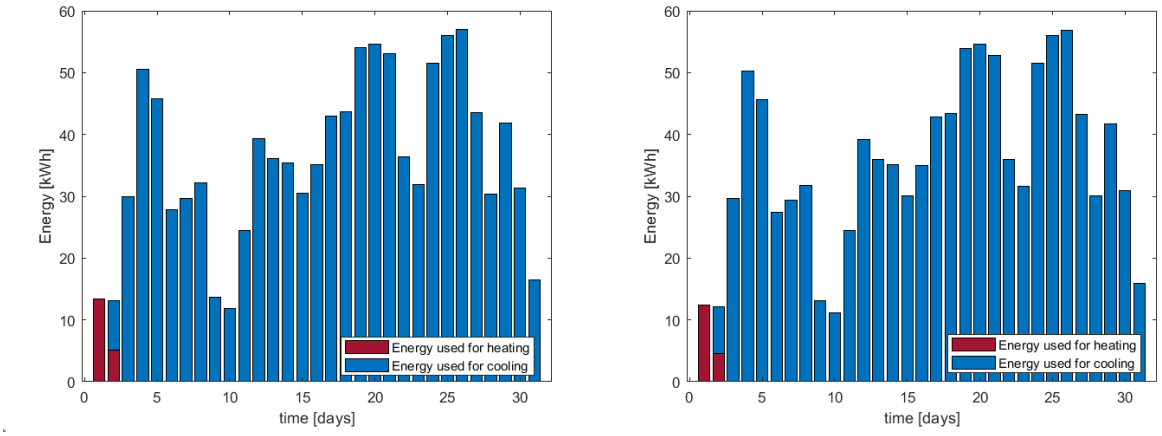

(a) $\Delta t = 150\ s$ **(b)** $\Delta t = 10\ s$

Figure 51: *Amount of energy used to heat/cool a volume located in Barcelona in January, using a coating and* $N_x = 27$ *and* $P = 4\,kW$

The results confirm that for $4\,kW$, regardless of the time step used, the amount of energy needed will be basically the same. Consequently, it can be concluded that any time step value between 10 and 150 seconds would give realistic results in terms of energy used. Now it remains to be determined which time step is preferred by the user when implementing an air-conditioning system. Let us

remember that by using a small time increment, it has been possible to reduce temperatures to the desired range (Figure 50). However, this has implied high computational costs.

A final study is performed to better understand how the time step influences the final results when *relatively* higher power is applied. Figure 52 shows what is the energy expended when using $40\,kW$ as a power source for two different time steps.

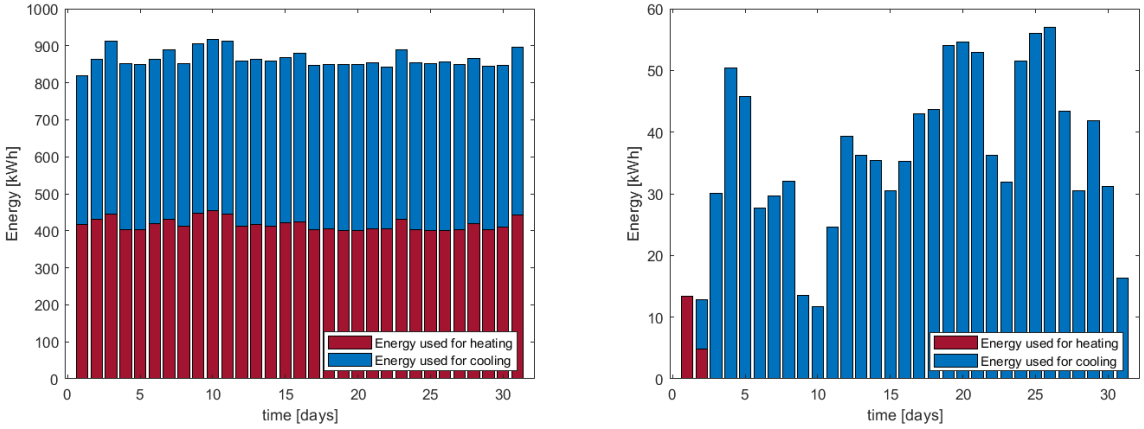

(a) $\Delta t = 150\ s$ **(b)** $\Delta t = 10\ s$

Figure 52: *Amount of energy used to heat/cool a volume located in Barcelona in January, using a coating and* $N_x = 27$ *and* $P = 40\,kW$

The idea of this analysis is to study if a long time step is still suitable for high powers. Based on Figure 52a, it is clear that applying a power of $40\,kW$ every 150 seconds is not the best option as it deviates a lot from realistic results. The same amount of energy is expected to be used regardless of the power source used by the air conditioner. This strange behavior is due to the fact that applying higher power for relatively longer intervals causes it to either cool down or heat up more than it needs to, expending more energy to counteract this effect and thus leading to incorrect results. Something very different is shown in Figure 52b, where it is seen that using a smaller time step for high powers provides a much more similar result to the ones presented before. Therefore, this helps to conclude that when using relatively high power sources, it is important to consider reducing the time step to less than 150 seconds.

Section 7 detailed the most optimal numerical parameters when studying the thermal behavior inside a volume. Nevertheless, it has just been shown that when talking about air-conditioning, the time step should be modified depending on the type of power supplied. All this may raise concerns about what is the optimal time step for both the numerical simulation itself and also for the air-conditioning system. This can be addressed by implementing a smart system that can provide different power sources for different temperature ranges.

Although this is outside the scope of this master's thesis, the findings – at this stage of understanding – are summarized as follows:

- Regardless of the time step used, the energy expended must be the same for any given energy source.
- Using higher power sources means choosing a small time step to track the temperature range correctly. Keep in mind that this would end up affecting computational costs, but it is necessary if air conditioning is implemented.

To check the results in more detail, see Table 2.

Wall type	**Coating**	P $[kW]$	Δt $[s]$	$E_{heating}$ $[kWh]$	$E_{cooling}$ $[kWh]$	E_{total} $[kWh]$
Traditional	Yes	4	150	18.50	1092.67	1111.17
Traditional	Yes	4	10	16.98	1086.88	1103.86
Traditional	Yes	40	150	12915.00	13851.70	26766.70
Traditional	Yes	40	10	18.22	1094.22	1112.44

Table 2: *Summary of the energy used to heat/cool a volume located in Barcelona in January, using* $N_x = 27$ *in a traditional wall for low and high power sources for different times steps*

9 Case 3: Trombe

Case objective: *To analyze and verify the influence of adding a south-facing Trombe wall in a volume located in Barcelona-Spain with the rest of the walls, roof and floor adiabatic. In addition to this, the energy required to maintain a range of temperatures within this volume will be studied.*

9.1 Problem description

The problem consists of studying a volume $L_1 \times W \times H$ located in Barcelona, Spain. This volume is characterized (again) by having a roof, floor and walls that are considered completely adiabatic, with the exception of the *Trombe wall* facing south. Trombe walls are a type of technology that can be installed in homes to passively heat them [9]. This reduces the need to heat a certain volume with traditional methods such as heaters, which certainly reduces the amount of energy used.

In this case, the wall has a thickness D and is made of concrete. A common feature to this type of wall has been implemented – the use of an optical coating *SOLKOTE HI/SORB-II*. This wall is then covered with external glazing with an air-gap L_2 between the wall and the glass, helping to trap sunlight like a small greenhouse. For convenience, it is assumed that this air does not circulate inside the room. Note that the glass surface in contact with the external environment is exchanging energy by radiation and convection with an external temperature T_{ext} and sky temperature T_{sky}.

Regarding the volume, it is assumed that there is a device that is capable of giving a power P to heat or cool, and that there is only dry air with an initial temperature of 10°C at the first instant of the day. The meteorological data of this study correspond to the month of January of a particular year as detailed in Section 6.

Figure 53 illustrates the Trombe wall.

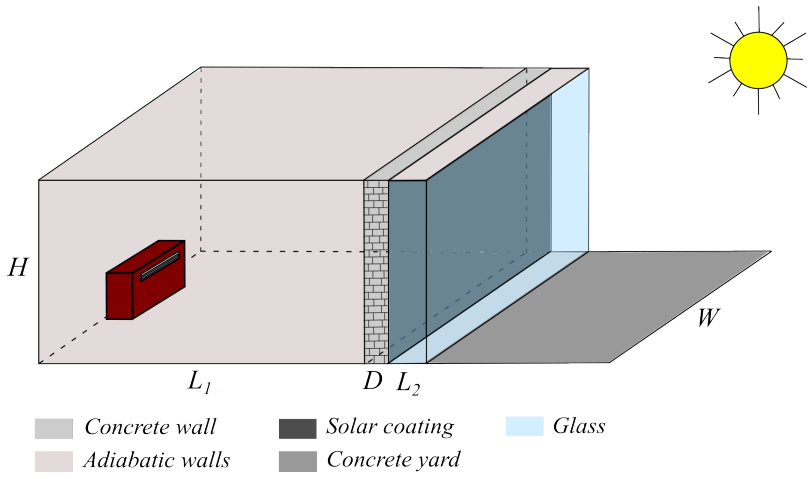

Figure 53: *Case 3 – Enclosure with a Trombe wall*

9.2 Results and discussion

9.2.1 Input data

The input data used for this case study is detailed below

- **Physical data**
  - Geometry: $L_1 = 10\,m, \quad W = 10\,m, \quad H = 4\,m, \quad D = 20\,cm, \quad L_2 = 20\,cm$
  - Thermophysical properties: $\rho = 2200\,kg/m^3, \quad \lambda = 1.6\,W/(mK), \quad c_p = 1000\,J/(kgK)$
  - Optical properties
    - Concrete: $\varepsilon_{concrete} = 0.88, \quad \alpha_{s,concrete} = 0.60$ [31]
    - Solar coating: $\varepsilon_{coating} = 0.49, \quad \alpha_{s,coating} = 0.94$ [34]
  - Temperature range: $18°C \leq T_{int} \leq 20°C$
  - Power provided by the device: $P = 0\,kW, \quad P = 4\,kW \quad P = 7\,kW$
- **Numerical data** [12]
  - Number of nodes: $N_x = 27$
  - Time step: $\Delta t = 150\,s = 2.5\,min$
  - Initial map: $T^o = 10°C = 283.15\,K$

9.2.2 Wall temperature distribution

The temperature distribution in the Trombe wall at different instants of time can be seen in Figure 44. For comparative purposes, the temperature distribution in the traditional wall is added as well.

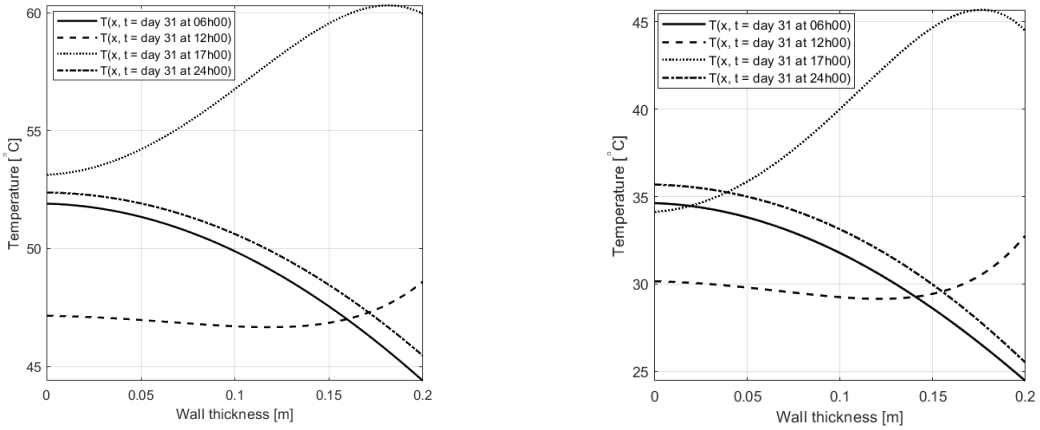

(a) *Trombe wall* **(b)** *Traditional wall*

Figure 54: *Temperature distribution at different instants on a south-facing coated wall on day 31, using* $\Delta t = 150\,s$, $N_x = 27$ *and* $P = 0\,kW$

[12] These numerical parameters are the most optimal, see Section 7.2.

When comparing these results, a similar behavior is observed in both cases, confirming that the findings are directly in line with previous results. Similarly, it is demonstrated that a Trombe wall can indeed help to heat a certain volume without consuming energy. This is an important finding in the understanding of why it is commonly used for heating without using any mechanical or electrical assistance. Namely, it is seen that the wall temperature has increased by a factor of about 1.33, which yields to expect higher temperatures inside of volume as well. As discussed, these high temperatures are due to the fact that most of the walls have been considered adiabatic and the type of coating used.

9.2.3 Internal temperature

The internal temperature T_{int} is calculated using the expression 19d which is recalled as follows

$$T_{int}{}^{n+1} = T_{int}{}^{n} + \frac{\Delta t}{\rho_{air} V c_{p,air}} \left[\alpha_{int}{}^{n} \left(T^{n}[1] - T_{int}{}^{n} \right) S \right]$$

The evolution of the internal temperature as a function of time in a sotuh-facing traditional and Trombe wall using a coating is displayed in Figure 55.

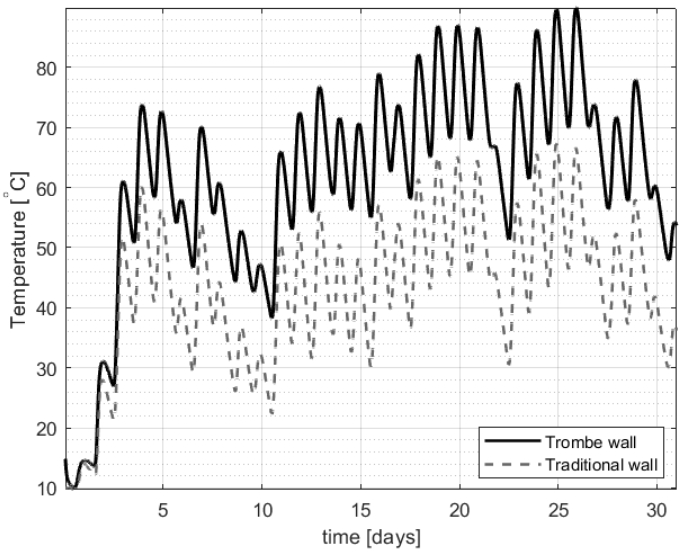

Figure 55: *Evolution of the internal temperature of a coated wall in January, using* $\Delta t = 150\ s$, $N_x = 27$ *and* $P = 0\ kW$

From these results it is clear that by using this kind of passive solar heating technology, higher temperatures are achieved inside the volume compared to when a traditional wall is used. Apart from advantages such as simple structure and convenient operation, the Trombe wall seems to be a good choice in cold regions due to its high efficiency. All this is in agreement with what has been reported in the literature [1].

At the domestic level, these temperatures are not the most optimal, so it is intended to reduce them in the range of 18 and 20°C. In Section 8, it was shown that adding a device that is capable of heating or cooling helps reduce these temperatures. Similarly, previous findings show that applying $4\,kW$ in a volume with a traditional wall using coating helps achieve this temperature range. Clearly more energy is expected to be expended in a volume with a Trombe wall as higher temperatures were recorded.

In order to calculate these new temperatures when air-conditioning is implemented, equation 20 is used which is recalled as follows

$$ {T_{int}}^{n+1} = {T_{int}}^{n} + \frac{\Delta t}{\rho_{air} V c_{p,air}} \left[{\alpha_{int}}^{n} \left(T^{n}[1] - {T_{int}}^{n} \right) S \pm P \right] $$

Figures 56 and 57 show how the internal temperature varies when a power supply is applied in two cases: *(a)* coated Trombe wall and *(b)* uncoated Trombe wall.

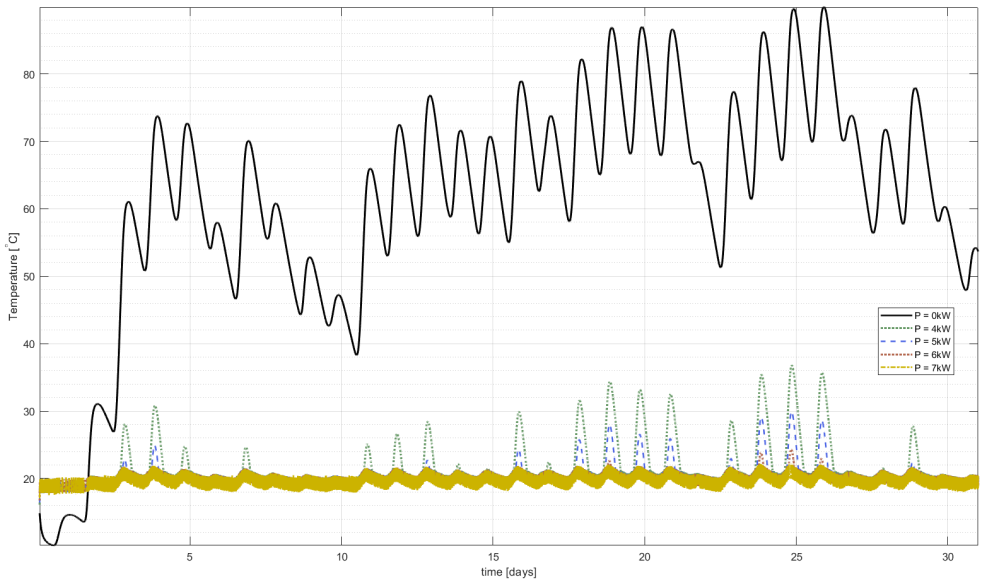

Figure 56: *Evolution of the internal temperature in January for different power sources in a volume located in Barcelona with a coated Trombe wall, using* $\Delta t = 150\ s$ *and* $N_x = 27$

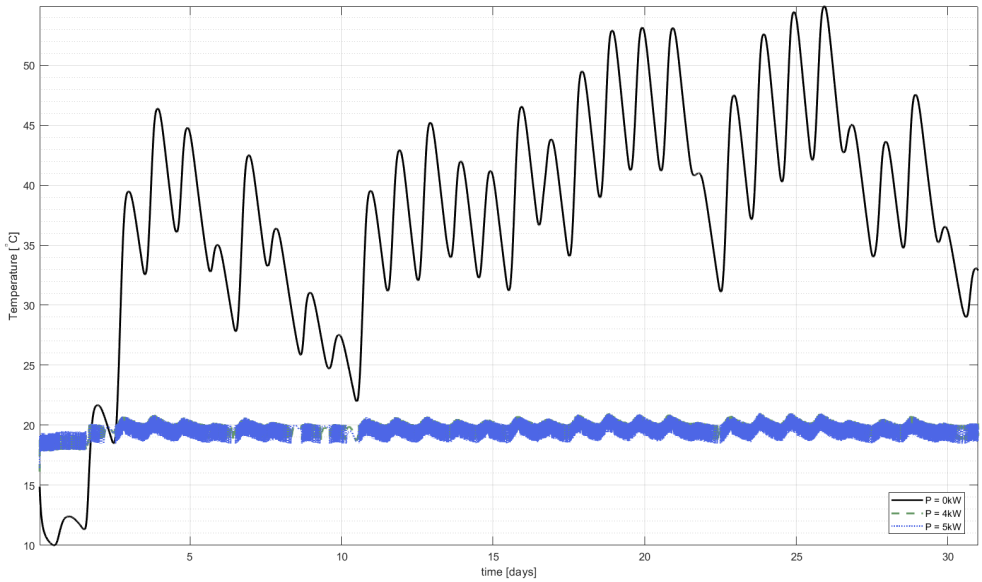

Figure 57: *Evolution of the internal temperature in January for different power sources in a volume located in Barcelona with an uncoated Trombe wall, using* $\Delta t = 150\ s$ *and* $N_x = 27$

The results now provide evidence that applying $P \geq 5\ kW$ to a volume with an uncoated Trombe wall is sufficient to reduce temperatures to the desired range. Nevertheless, for a Trombe wall with coating, $5\ kW$ does not seem to be enough for some days of the month. It is seen that for some instants of time, the internal temperature is within the range; however, there are still some peaks at certain instants, which means that a higher power supply should have been applied.[13] Therefore, the device should give a power $P \geq 7\ kW$ to maintain the temperatures in a desired range in a volume with a Trombe wall.

9.2.4 Energy needed

Having determined the minimum power supply for the two situations, it is possible to calculate the amount of electrical energy required to operate this device. This can be done by using the equations 76 and 77 discussed previously.

The results are shown in Figure 58, where it can be seen how much energy is needed to cool or heat in the case of using a Trombe wall with and without coating.

[13] Using a small time step will certainly help reduce further the temperatures as the air conditioner applies power more frequently, see Section 8.2.2.

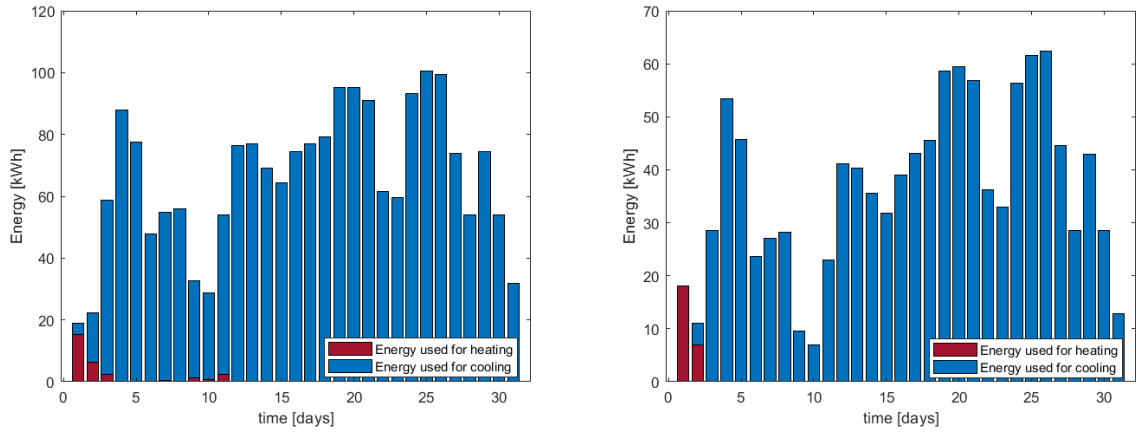

(a) *Trombe wall with coating and* $P = 7\,kW$ **(b)** *Trombe wall without coating and* $P = 5\,kW$

Figure 58: *Amount of energy used to heat/cool a volume located in Barcelona with a Trombe wall in January, using* $\Delta t = 150\,s$ *and* $N_x = 27$

Likewise, for comparison purposes, Figure 59 displays the amount of energy needed in the case of using the traditional wall and the Trombe wall, both using coating.

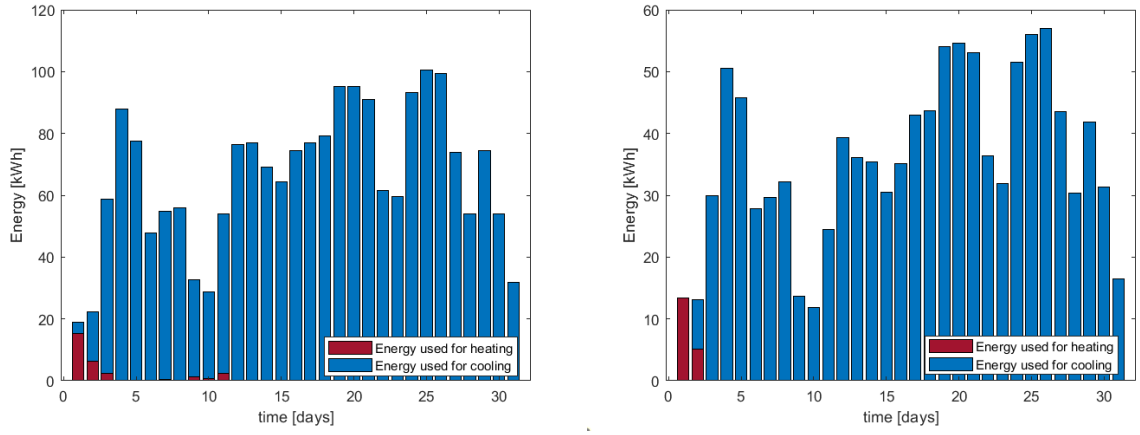

(a) *Trombe wall with coating and* $P = 7\,kW$ **(b)** *Traditional wall with coating and* $P = 4\,kW$

Figure 59: *Amount of energy used to heat/cool a volume located in Barcelona with two wall structures in January, using* $\Delta t = 150\,s$ *and* $N_x = 27$

In general, it is demonstrated that more energy is used in the case of using a Trombe wall. Even more energy is needed if the Trombe wall uses an optical coating. This all makes sense because the temperature inside the volume has increased compared to when using a traditional wall. Moreover, as a general comment, it is worth mentioning that these results have used a time increment of 150 seconds given that the power supply is closed to $4\,kW$. Let us remember that this time step has

been shown to give realistic values for nearby power sources.[14]

Table 3 details the results of this energy analysis using the most optimal power sources discussed above.

Wall type	**Coating**	P $[kW]$	Δt $[s]$	$E_{heating}$ $[kWh]$	$E_{cooling}$ $[kWh]$	E_{total} $[kWh]$
Traditional	Yes	4	150	18.50	1092.67	1111.17
Traditional	Yes	4	10	16.98	1086.88	1103.86
Trombe	Yes	7	150	28.29	2008.12	2036.41
Trombe	Yes	7	10	23.94	1989.04	2012.98

Table 3: *Summary of the energy used to heat/cool a volume located in Barcelona in January, using $N_x = 27$ in two types of walls, and the most optimal power sources for different time steps*

9.2.5 Heat transfer coefficients

This particular case study includes a parameter of interest, this is the heat transfer coefficient α_{trombe} in the air gap between the wall and the glass.

As shown in Figure 53, there is a small amount of air at a given length L_2 that influences the temperature of the wall and glass. Therefore, new correlations are needed to determine the value of α_{trombe}. Note that this air-gap can be seen as a small cavity. Section 4.2.1.4 discussed some expressions valid for a cavity with isothermal vertical walls and with an adiabatic top and bottom. These features clearly fits the problem, so those expressions are valid for this study.

By checking the input data for this case, it is determined that both expressions could be applied. However, **the results discussed in this section were obtained using expression 69** due to the following reasons:

- The range of the H/L ratio is wider, so it is applicable to different cavity dimensions.
- The Prandtl number Pr obtained is very closed to 1, so higher values are not needed for this parameter.
- The Rayleigh number Ra is of the order of 10^6 (or higher). Both expressions met this requirement but the chosen equation covers a wide range of Ra numbers.

[14] This time step must be reduced when using higher powers (e.g. $40\,kW$) as discussed in Section 8.2.3.

Figure 60 shows the evolution of the cavity heat transfer coefficients α_{trombe} over time, calculated using both Nusselt expressions.

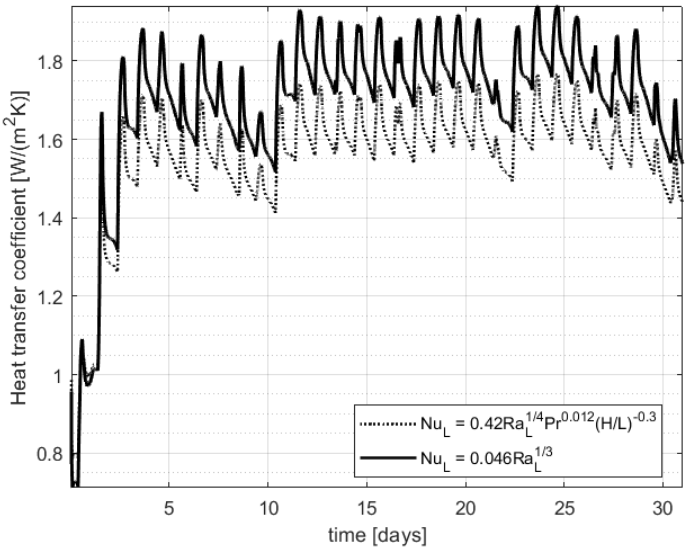

Figure 60: *Evolution of the heat transfer coefficient in the air gap in January, using* $\Delta t = 150s$, $N_x = 27$ *and* $P = 0kW$

Note that these coefficients are quite similar when both expressions are used. Thus, the final results are expected to be no different. In order to verify this, Figure 61 shows the wall temperature distribution when both Nusselt number correlations are used.

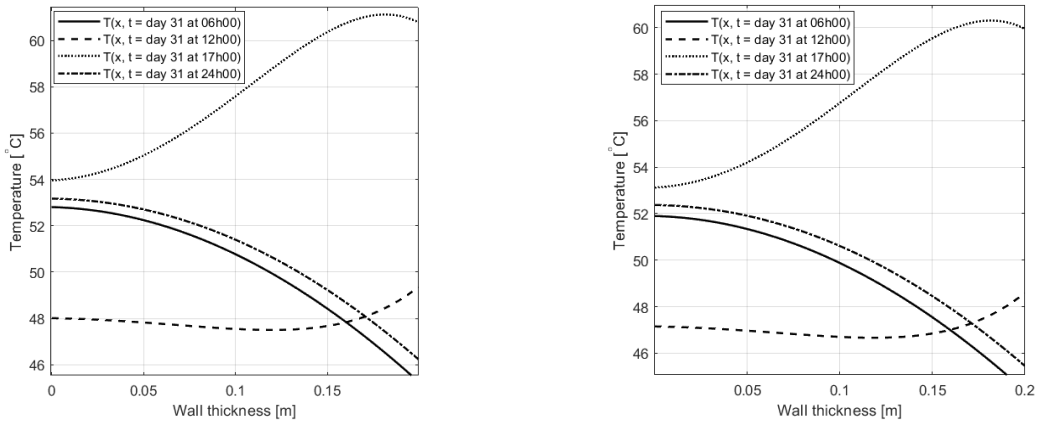

(a) *Using eq. 68* **(b)** *Using eq. 69*

Figure 61: *Wall temperature distribution on the Trombe coated wall on day 31 using two different Nusselt expressions,* $\Delta t = 150s$, $N_x = 27$ *and* $P = 0kW$

Similarly, the amount of energy expended is compared and detailed in Table 4

Wall type	Coating	Nusselt	P $[kW]$	Δt $[s]$	$E_{heating}$ $[kWh]$	$E_{cooling}$ $[kWh]$	E_{total} $[kWh]$
Trombe	Yes	Eq. 68	7	150	29.17	2019.62	2048.79
Trombe	Yes	Eq. 68	7	10	24.03	1997.18	2021.21
Trombe	Yes	Eq. 69	7	150	28.29	2008.12	2036.41
Trombe	Yes	Eq. 69	7	10	23.94	1989.04	2012.98

Table 4: *Summary of the energy used to heat/cool a volume located in Barcelona with a coated Trombe wall in January, using $N_x = 27$, two different Nusselt expressions, and the most optimal power sources for different time steps*

For the sake of completeness, the glass temperature T_{glass} is also plotted as it is influenced by α_{trombe} as shown in the equation 64g. Note that this glass has been considered small enough that it has been treated as a single point when it comes to numerical simulations.

Figure 62 shows the evolution of the glass temperature along the time.

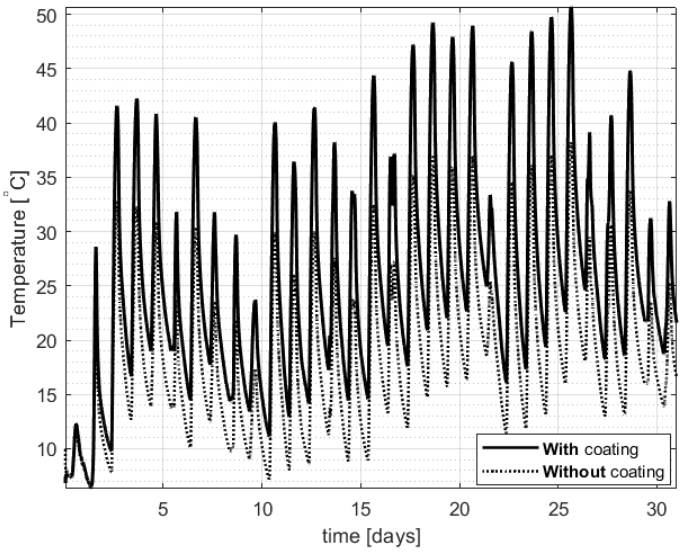

Figure 62: *Evolution of the glass temperature in January, using $\Delta t = 150s$, $N_x = 27$ and $P = 0kW$*

10 Case 4: Airflow

Case objective: *To study how the use of the external air helps to save the energy necessary to maintain a range of temperatures in a volume located in Barcelona-Spain with a Trombe wall facing south and the rest of the walls, roof and floor adiabatic. For this, an attempt will be made to take advantage of the outside air to heat or cool the volume.*

10.1 Problem description

The problem follows exactly the same scenario as discussed in Section 9. For this case, it is intended to study how much energy can be saved if a volumetric air flow $\dot{V}$ is added to one side of the wall. The same temperature range is expected to be achieved within the volume $L_1 \times W \times H$ located in Barcelona, Spain. Therefore, the idea is to use the outside air to heat or cool. In this way, it will be possible to study how much energy can be saved by using both the device (already implemented in the previous case studies) and the volumetric airflow in parallel. Let us remember that this device gives a power P and checks the temperature at each instant of time to decide what to do to maintain a given temperature range.

Without further ado, the situation to be studied in this case is depicted in Figure 63.

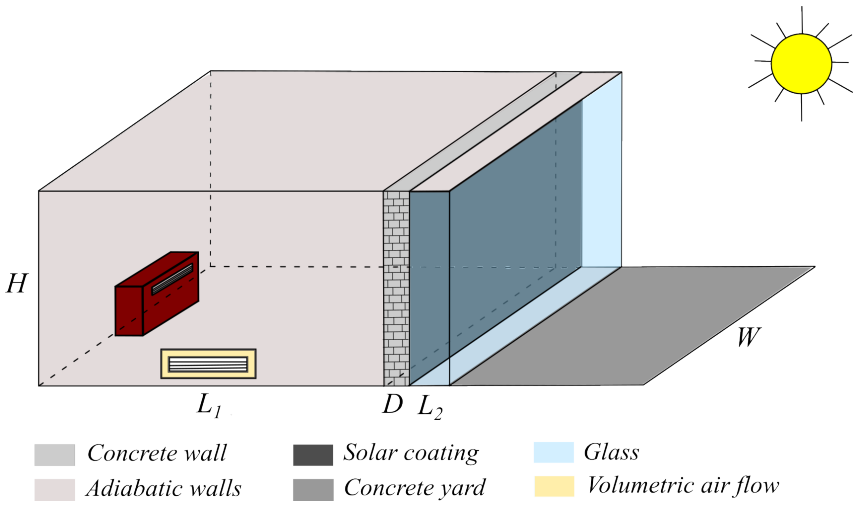

Figure 63: *Case 4 – Enclosure with a Trombe wall, a heating/cooling device and volumetric air flow*

The algorithm[15] implemented in the C++ code to take advantage of the outside air in combination with the power source is detailed below.

[15]Note that this algorithm is a simple way to take advantage of outside air, but clearly it can be further optimized. Namely, different temperature ranges can be chosen to which different power ranges and volumetric airflows are applied.

In case of trying to **heat up the volume**, the following conditions must be met:

if $T_{int} < 18°C$ **then**
  if $T_{ext} > 20°C$ **then**
    ${T_{int}}^{n+1} = {T_{int}}^{n} + \frac{\Delta t}{\rho_{air} V c_{p,air}} \left[\rho_{air} \dot{V} c_{p,air} \left(T_{ext} - {T_{int}}^{n}\right) + {\alpha_{int}}^{n} \left(T^{n}[1] - {T_{int}}^{n}\right) S + P\right]$
  else
    if $T_{ext} < 18°C$ **then**
      ${T_{int}}^{n+1} = {T_{int}}^{n} + \frac{\Delta t}{\rho_{air} V c_{p,air}} \left[{\alpha_{int}}^{n} \left(T^{n}[1] - {T_{int}}^{n}\right) S + P\right]$
    end
  end
end

Algorithm 1: Heating condition

In case of trying to **cool down the volume**, these are the conditions to be met:

if $T_{int} > 20°C$ **then**
  if $T_{ext} > 20°C$ **then**
    ${T_{int}}^{n+1} = {T_{int}}^{n} + \frac{\Delta t}{\rho_{air} V c_{p,air}} \left[{\alpha_{int}}^{n} \left(T^{n}[1] - {T_{int}}^{n}\right) S - P\right]$
  else
    if $T_{ext} < 18°C$ **then**
      ${T_{int}}^{n+1} = {T_{int}}^{n} + \frac{\Delta t}{\rho_{air} V c_{p,air}} \left[\rho_{air} \dot{V} c_{p,air} \left(T_{ext} - {T_{int}}^{n}\right) + {\alpha_{int}}^{n} \left(T^{n}[1] - {T_{int}}^{n}\right) S - P\right]$
    end
  end
end

Algorithm 2: Cooling condition

If **none of these conditions** is met, the internal temperature is calculated as in the simplest case

$$ {T_{int}}^{n+1} = {T_{int}}^{n} + \frac{\Delta t}{\rho_{air} V c_{p,air}} \left[{\alpha_{int}}^{n} \left(T^{n}[1] - {T_{int}}^{n}\right) S\right] $$

10.2 Results and discussion

10.2.1 Input data

The input data used for this case study is detailed below

- **Physical data**
  - Geometry: $L_1 = 10\,m, \quad W = 10\,m, \quad H = 4\,m, \quad D = 20\,cm, \quad L_2 = 20\,cm$
  - Thermophysical properties: $\rho = 2200\,kg/m^3, \quad \lambda = 1.6\,W/(mK), \quad c_p = 1000\,J/(kgK)$
  - Optical properties
    - Concrete: $\varepsilon_{concrete} = 0.88, \quad \alpha_{s,concrete} = 0.60$ [31]
    - Solar coating: $\varepsilon_{coating} = 0.49, \quad \alpha_{s,coating} = 0.94$ [34]
  - Temperature range: $18°C \leq T_{int} \leq 20°C$
  - Power provided by the device: $P = 0\,kW, \quad P = 4\,kW \quad P = 7\,kW$
  - Volumetric air flow
    - One air renewal per hour: $\dot{V} = 0.112\,m^3/s$
    - One air renewal per half hour: $\dot{V} = 0.223\,m^3/s$

- **Numerical data** [16]
  - Number of nodes: $N_x = 27$
  - Time step: $\Delta t = 150\,s = 2.5\,min$

10.2.2 Internal temperature

The evolution of the temperature inside the volume for different power sources[17] and air flows are illustrated in Figure 64.

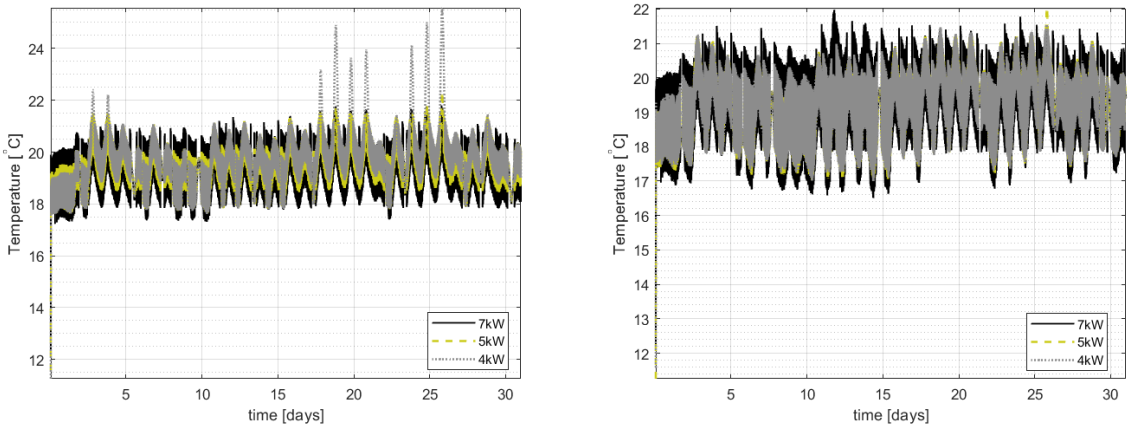

(a) $\dot{V} = 0.112\,m^3/s$ **(b)** $\dot{V} = 0.223\,m^3/s$

Figure 64: *Evolution of the internal temperature in January for different power sources and volumetric air flows in a volume with a coated Trombe wall, using* $\Delta t = 150\,s$ *and* $N_x = 27$

[16] These numerical parameters are the most optimal, see Section 7.2.

[17] These values are based on the main outcomes of the previous case studies.

When there is one air change per hour, it can be seen in Figure 64a that the optimal power value is $P \geq 7\,kW$. If values lower than the latter are used, it is seen that it is not possible to maintain the desired temperature range on certain days. Something different happens when there is one air change every half hour. Figure 64b indicates that with a power of $P \geq 4\,kW$, it is possible to reach the desired temperature range. This makes sense as there are more frequent air changes and therefore this would help to cool or heat the interior of the volume.

At this point, using a more frequent air flow rate would seem to be the best option. However, it must be taken into account that in cases of extreme temperatures, whether they are very high or very low, the volume will become too cool or too hot, accordingly. This will cause the device inside the room to use more energy to maintain the desired temperature range. The objective of this study is to find a way to save energy since maintaining a range of temperatures in a volume that uses a Trombe wall ended up being very costly in terms of energy. Therefore, an energy analysis is a must to reach a conclusion.

10.2.3 Energy needed

Based on the optimal power sources above-mentioned, the amount of energy used can be determined. The results can be seen in Figure 65.

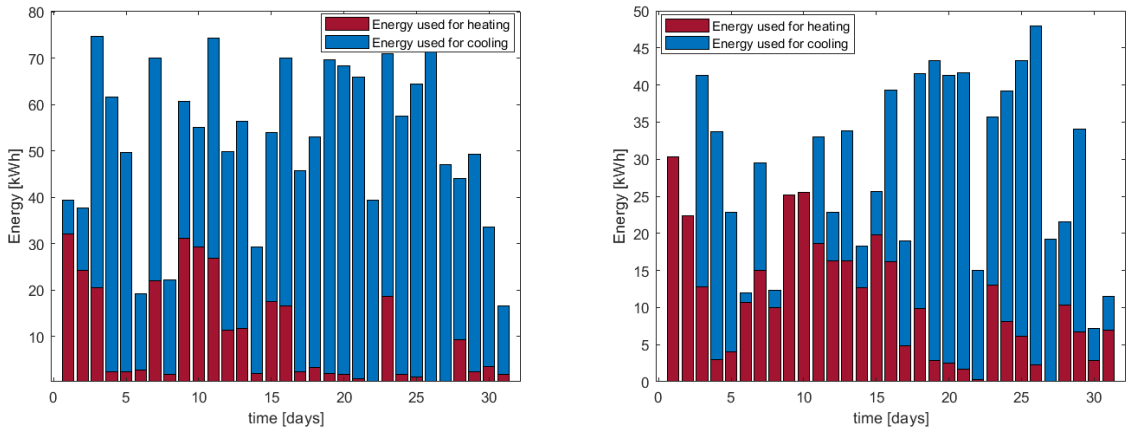

(a) $\dot{V} = 0.112\,m^3/s,\ P = 7\,kW$ **(b)** $\dot{V} = 0.223\,m^3/s,\ P = 4\,kW$

Figure 65: *Amount of energy used to heat/cool a volume located in Barcelona with a coated Trombe wall in January, using* $\Delta t = 150\ s$ *and* $N_x = 27$

As expected, when the volumetric air flow has doubled, it is necessary to heat the volume more times. This is because the temperatures in the month of January are relatively low. Compared to when there was no airflow, it is seen that energy saving for cooling the volume has been achieved. However, at certain times these temperatures make the volume too cold, so now more energy is

needed to heat the volume.

Someone might argue that despite saving energy in cooling, more energy is now needed for heating. Thus, the question of whether overall a reduction in energy consumption was achieved remains open. To answer it, it is necessary to compare the total amount of energy spent on heating and cooling to determine if overall energy savings have been achieved.

Table 5 indicates the results obtained in more detail.

Wall type	$\dot{V}$ $[m^3/s]$	P $[kW]$	Δt $[s]$	**no. times heating**	**no. times cooling**	$E_{heating}$ $[kWh]$	$E_{cooling}$ $[kWh]$	E_{total} $[kWh]$
Trombe	0	4	150	79	11299	13.17	1883.17	1896.34
Trombe	0.112	4	150	488	5992	81.34	998.67	1080.01
Trombe	0.223	4	150	2024	3326	337.34	554.34	891.68
Trombe	0	7	150	97	6885	28.29	2008.12	2036.41
Trombe	0.112	7	150	1038	4527	302.75	1320.38	1623.13
Trombe	0.223	7	150	3051	4226	889.88	1232.58	2122.46

Table 5: *Summary of the energy used to heat/cool a volume located in Barcelona with coated Trombe wall in January, using $N_x = 27$, two different volumetric air flows, and the most optimal power sources*

These results give a pretty good idea of what happens when there is volumetric airflow in the volume with a Trombe wall. On the one hand, it can be seen that by increasing the air flow and the power supply there is a high energy consumption since now more energy is needed to heat the volume. This makes sense because on most days in January the air outside is cold, so if air is allowed to circulate inside the volume, more energy is needed to heat it. On the other hand, increasing the air flow but reducing the power source significantly reduces energy consumption. This means that the outside air helps to maintain the desired temperature range without spending energy to cool or heat. An intermediate solution is found in the case of having one air change per hour for both power sources, where it is seen that the energy used has been reduced but not as in the latter case. Therefore, these findings give a hint that if the volumetric air flow is increased, the power source should be reduced because otherwise it will use more energy than necessary. This suggests that the most optimal configuration is to have one air change every half hour ($\dot{V} = 0.223 m^3/s$) with a power source of $4\,kW$. In this way, energy consumption is reduced by approximately half compared to when there was no air infiltration.

11 Case 5: Non-adiabatic walls

Case objective: *To study how the temperatures change inside the volume located in a cold city like Odeillo-France with a traditional wall and Trombe facing south if the side walls are no longer adiabatic and only the roof and floor are considered adiabatic.*

11.1 Problem description

This case study is a modification of Case 3 discussed in Section 9. The main variation is that the side walls of the volume are no longer adiabatic. This means that only the roof and floor are adiabatic while the side walls and the south-facing wall[18] have convective losses. The latter is assumed to be in direct contact with solar radiation, so there is an exchange of energy by convection and radiation. On the other hand, if it is assumed that the side walls are covered by elements such as trees, it can be said that they are only in contact with the external environment, which means that they exchange energy only by convection.[19]

In addition to this, the volume $L_1 \times W \times H$ is now located in Odeillo, France. This decision has been made because Odeillo is normally a cold place, so very low temperatures are recorded in January. Finally, this enclosure is assumed to be completely empty, so there is no heating/cooling device inside and no outside air infiltration. Figure 66 displays this problem.

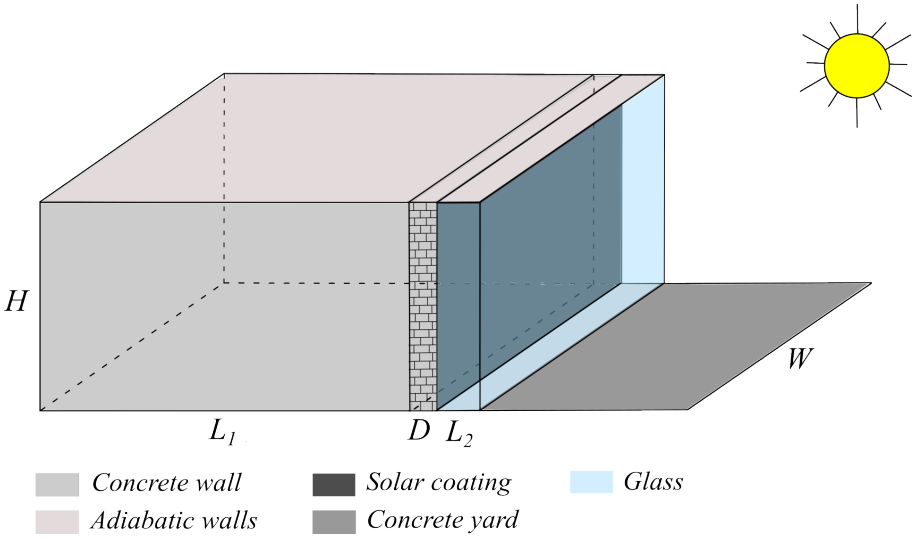

Figure 66: *Case 5 – Enclosure with Trombe wall and non-adiabatic side walls*

[18] The south-facing wall can be a traditional wall or a Trombe wall and must consider energy exchange by convection and radiation.

[19] Although the side walls are covered by trees, diffuse radiation should still be taken into account. However, for comparison purposes this has been ignored.

11.2 Results and discussion

11.2.1 Input data

The input data used for this case study is detailed below

- **Physical data**
  - Geometry: $L_1 = 10\,m$, $W = 10\,m$, $H = 4\,m$, $D = 20\,cm$, $L_2 = 20\,cm$
  - Thermophysical properties: $\rho = 2200\,kg/m^3$, $\lambda = 1.6\,W/(mK)$, $c_p = 1000\,J/(kgK)$
  - Optical properties
    - Concrete: $\varepsilon_{concrete} = 0.88$, $\alpha_{s,concrete} = 0.60$ [31]
    - Solar coating: $\varepsilon_{coating} = 0.49$, $\alpha_{s,coating} = 0.94$ [34]
- **Numerical data** [20]
  - Number of nodes: $N_x = 27$
  - Time step: $\Delta t = 150\,s = 2.5\,min$
  - Initial map: $T^o = 10°C = 283.15\,K$

11.2.2 Internal temperature

So far, the results discussed before considered that the walls, floor, and roof are adiabatic with the exception of the south-facing wall. This was an assumption throughout this study; however, most of the results reported relatively high temperature values that are not very realistic. Although these obtained results agree with what has been reported in the literature, it has been decided to briefly discuss what would have happened if the side walls were not considered adiabatic.

In order to do so, the expression 19d is rewritten as follows

$$\frac{\rho_{air} V c_{p,air}}{\Delta t}\left({T_{int}}^{n+1} - {T_{int}}^{n}\right) = \alpha^n_{int,trombe}\left(T^n_{trombe}[1] - {T_{int}}^{n}\right) S + 3\,\alpha^n_{int,traditional}\left(T^n_{traditional}[1] - {T_{int}}^{n}\right) S \tag{78a}$$

From now on the subscripts *trombe* and *traditional* are called *trom* and *trad*, respectively.

Solving for the internal temperature gives

$${T_{int}}^{n+1} = {T_{int}}^{n} + \frac{\Delta t}{\rho_{air} V c_{p,air}}\left[\alpha^n_{int,trom}\left(T^n_{trom}[1] - {T_{int}}^{n}\right) S + 3\,\alpha^n_{int,trad}\left(T^n_{trad}[1] - {T_{int}}^{n}\right) S\right] \tag{78b}$$

where the term '$\alpha^n_{int,trad}\left(T^n_{trad}[1] - {T_{int}}^{n}\right) S$' represents the convective losses in each side wall.

[20] These numerical parameters are the most optimal, see Section 7.2.

Figure 67 shows the evolution of the temperature inside the volume for two cases:

(i) *Completely adiabatic:* side walls, roof and floor are adiabatic except for the wall facing south.

(ii) *Roof and floor adiabatic*: lateral and south-facing walls have convective losses.

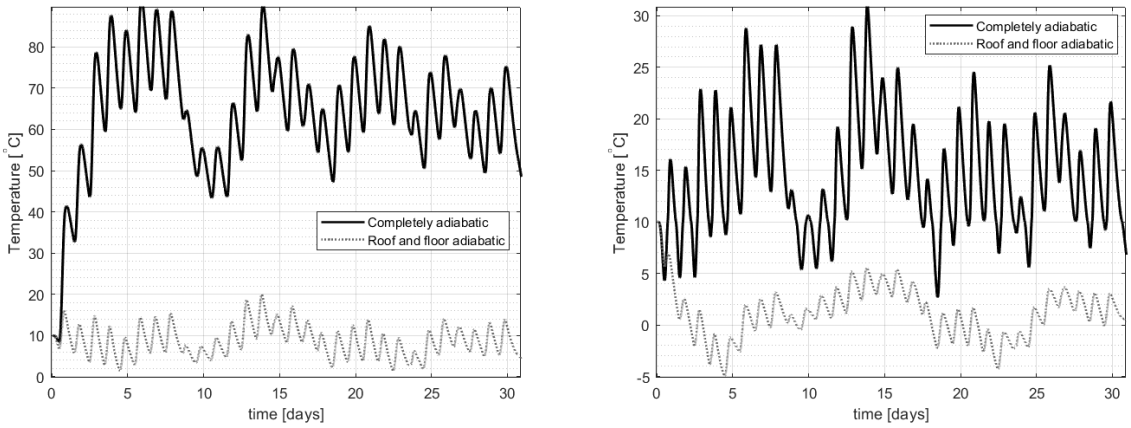

(a) *Coated Trombe wall* **(b)** *Traditional wall*

Figure 67: *Comparison of the internal temperature evolution in January in a volume located in Odeillo with adiabatic and non-adiabatic side walls, using* $\Delta t = 150\ s$ *and* $N_x = 27$

The present study confirms that the assumptions made regarding the adiabatic walls were significant. It has been found that if convective losses are considered in the side walls, more realistic results are obtained. It can be seen that the internal temperatures are now more in line with expectations for a place with a very cold weather. Therefore, as a future recommendation, it is preferable to carry out this type of study considering losses instead of assuming an ideal scenario.

Now it would be interesting to compare the results to find out what is the real influence of a Trombe wall in a cold city if the side walls are no longer adiabatic, that is to say that there are losses due to convection. Figure 68 indicates this scenario.

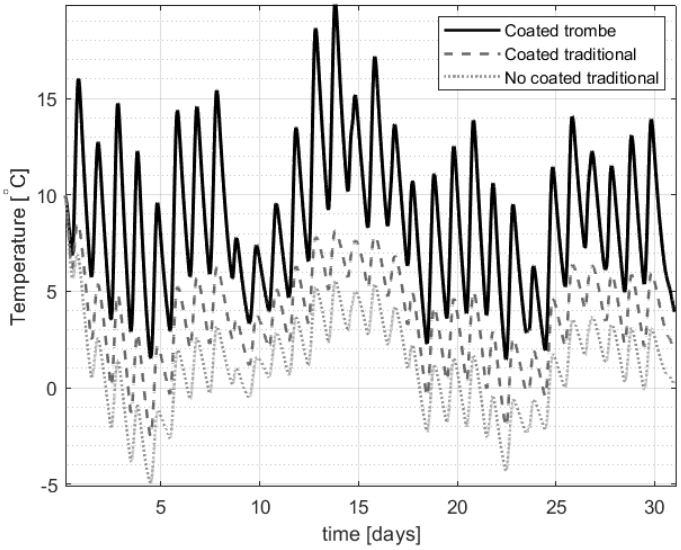

Figure 68: *Evolution of the internal temperature in January in a volume located in Odeillo with two types of south-facing wall and non-adiabatic side walls, using* $\Delta t = 150\ s$ *and* $N_x = 27$

These findings support the importance of using a passive solar-heating system, such as the Trombe Wall. On the one hand, the light gray dotted line represents the internal temperature if the south-facing wall is of the traditional type without using an optical coating. As expected, having a traditional wall does not contribute to heating the room for such a cold climate. Similarly, the dark gray dashed line indicates this latter scenario, but now using an optical coating. It is shown that this partially contributes to increasing the temperature inside the volume, which makes sense because the coating properties help to absorb most of the thermal energy from incident sunlight. On the other hand, the black solid line describes the evolution of the internal temperature when implementing a coated Trombe wall. It is clearly seen that using this type of technology help to increase the temperatures of the enclosure without consuming energy. Hence, once again the importance of having a Trombe wall has been demonstrated.

One of the next steps based on these results may be the study of the energy required to maintain a certain range of temperatures. This will be discussed *briefly* as the procedure is the same as that presented in the previous sections. For this, a Trombe wall with coating and two arbitrary power sources have been taken. Figure 68 shows that the temperatures are not as high or as low compared to the previous case studies; therefore, the chosen power sources are $1\ kW$ and $2\ kW$.

Table 6 details the results of the energy consumed.

Wall type	$\dot{V}$ $[m^3/s]$	P $[kW]$	Δt $[s]$	**no. times heating**	**no. times cooling**	$E_{heating}$ $[kWh]$	$E_{cooling}$ $[kWh]$	E_{total} $[kWh]$
Trombe	0	1	150	17419	13	725.79	0.54	726.33
Trombe	0.112	1	150	17420	7	725.83	0.25	726.08
Trombe	0.223	1	150	17420	5	725.83	0.21	726.04
Trombe	0	2	150	16917	14	1409.75	1.17	1410.92
Trombe	0.112	2	150	16917	9	1409.75	0.75	1410.50
Trombe	0.223	2	150	16920	8	1410.00	0.67	1410.67

Table 6: *Summary of the energy used to heat/cool a volume located in Odeillo with coated Trombe wall in January, using $N_x = 27$, two different volumetric air flows, and two arbitrary power sources*

These results show that in general the energy used is lower compared to the studies that considered the adiabatic walls in a volume located in Barcelona. Also, Odeillo has a lower ambient temperature compared to Barcelona. This makes the outside air not very useful for heating the volume. That is why the total energy practically does not vary if different volumetric air flows are used. Finally, Figure 68 shows that temperatures are generally below $18°C$, this means that the volume must be heated many more times which makes sense with the results detailed above.

12 Economic assessment

The development of this project involves economic costs. Although no financial benefit is expected to be derived from this project, this section is intended to evaluate and estimate financial resources that would have been considered in a professional setting. Note that these costs are not only material but also human resources. Therefore, the total costs can be divided into the following aspects.

- **Human resources:** This aspect considers the economic value of the working hours necessary to fulfill this project. This study has been carried out by a single engineer in a quadrimester. The salary of a junior engineer per hour in Barcelona is around 12€ [36]. The average time spent on this project was 6 working hours in 5 working days. Considering that there are 17 weeks in a quadrimester, the total number of working hours is 510. Taking these aspects into account, the total human costs are approximately 6120.00€.

- **Material resources**

  - **Hardware cost:** The hardware used to perform the project was a laptop with a cost of 800€. A good and oft-used for laptops on straight-line basis is 25% of its cost each year (52 weeks) [37]. Hence, the average cost of the computer is:

$$\textit{Hardware cost} = 800 \cdot 0.25 \cdot \frac{17}{52} = 65.38€ \tag{79}$$

  - **Software cost:** Various software have been used. Some of them include `Matlab` student license (90€), Microsoft Office package (70€), Overleaf-LaTeX(free), Mendeley (free) and `Dev-C++` compiler (free).

$$\textit{Software cost} = 90 + 70 = 160.00€ \tag{80}$$

  - **Energy cost:** The required power supply for the laptop used is $65\,W$. If an average used is 6 hours, the energy result in kilowatt-hours is $0.39\,kWh$. The number of working days in 17 weeks is 85 days. Considering that this project was conducted in a range of hours in which the price of electricity at household in Barcelona, Spain is around $0.21905\,€/kWh$ [38], the total cost of electricity is:

$$\textit{Energy cost} = 85 \cdot 0.39 \cdot 0.21905 = 7.26€ \tag{81}$$

The total costs for the development of this project are summarized in Table 7.

	Human	Hardware	Software	Energy	**Total**
Cost (€)	6120.00	65.38	160.00	7.26	**6352.64**

Table 7: *Total cost estimation*

13 Environmental assessment

One of the concerns in projects is knowing what the environmental impact is. Therefore, this section aims to estimate the impact of this project on the environment.

It is important to mention that it is difficult to accurately quantify the environmental impact since the main source of pollutants has been the electrical energy consumed. Taking into account that there is a great variation in the generation of energy sources in Spain, the amount of CO_2 generated is difficult to estimate. However, since little energy has been needed in this project, it can be affirmed that the environmental impact of the project in terms of electricity consumption has been small. As mentioned in the economic assessment, 510 hours were used in this project. The average consumption of the personal laptop is $65\,W$, so this study has consumed $33.15\,kWh$. It is estimated that each kilowatt-hour produces $0.195\,kg$ CO_2 [39]. Consequently, this project produced $6.46\,kg$ of CO_2.

Besides that, all the material created in this project has been developed on a personal computer, so no additional resources have been needed that could have a negative impact on the environment, such as paper. This means that the environmental impact of this study is negligible compared to other engineering research projects.

Finally, it is essential to highlight that future investigations of this study could further contribute to energy savings through studies that allow optimizing air conditioning in closed spaces, including passive solar heating systems. This means that the investment of resources in this field is quite beneficial for the environment, as it can reduce the number of experiments and comparative tests needed to develop several future engineering projects.

14 Conclusions

The main objective of this project was to consolidate various knowledge about Heat and Mass Transfer. For this, it was decided to take a scenario that is currently of high importance, such as air conditioning in closed spaces. Energy saving and its maximum use is an important issue to be studied in the thermal field. Hence, some in-house numerical codes were developed that allow solving different one-dimensional heat conduction scenarios without the need to solve complex equations. This links to another of the objectives of this project, which consisted of learning to program in a new programming environment such as C++.

This report began by detailing the scope, requirements and objectives during this project. At this stage, it can be confirmed that all these aspects have been successfully achieved. Following this, a brief study was carried out on all the historical events in the evolution of the air conditioning of closed spaces. The Trombe wall turned out to be one of the most useful variations to increase temperatures within a closed volume without the need to consume energy.

Before trying to simulate a Trombe wall, the most important aspects within the world of numerical methods were discussed. This helped to understand how the Finite Volume Method will be implemented and to determine which will be the main tools for this. Once this background was discussed, all the core equations that would be needed were derived in detail in order to simulate a volume with adiabatic walls, roof and floor and the south-facing wall of two types: traditional and Trombe. This practically resulted in solving a combined heat transfer problem, so a global algorithm was detailed.

Having all these tools ready, it was possible to run some simulations. However, trying to fulfill another of the objectives of this project - the introduction to the C++ environment - a previous work was carried out that consisted of solving basic and simple heat conduction problems. This significantly helped to know the main functions of this program to later study two aspects: the spatial and temporal part of some simple cases. On the one hand, to study the spatial part, the created program was run for a long time in such a way that it reaches the steady-state regime to then compared it with its analytical solution. On the other hand, the temporal study was done based on a reference case provided by the CTTC where a solution was proposed.

After having verified that the code for simple cases gives valid results, this code was expanded for more complicated cases. For this, five different case studies were proposed to study various topics of interest.

- ***Case 1:*** Being the first case studied, the thermal behavior of a closed volume with a traditional wall was studied where internal and wall temperatures were discussed. Likewise, this was a good opportunity to study the most optimal numerical parameters in such a way that a given

scenario can be simulated in the fastest way without compromising the final results.

- ***Case 2:*** After having determined the temperature inside the volume, this scenario was introduced. This consisted of adding a device that allows maintaining a given range of temperatures and thus finding how much energy would be spent for this.

- ***Case 3:*** This case was very similar to Case 1, except that now the south-facing wall is Trombe. It was discussed how the internal temperatures increase notably without the need to spend energy. Similarly, in case of wanting to maintain a range of temperatures, the use of different power sources was proposed. Findings showed that the case of using very high power values, the time step should be as small as possible; otherwise, there will be inconsistencies in the final results.

- ***Case 4:*** At this point, it had been found that the energy to cool a volume with a Trombe wall was relatively high if all other walls, roof and floor were adiabatic. Therefore, an attempt was made to use the outside air that allows the interior to be cooled or heated as needed. The results showed that this variant helps to reduce the energy consumed. Something to take into account is that in case of extreme temperatures this could not work perfectly.

- ***Case 5:*** After noticing that the interior temperatures of all the previous cases are relatively high, it was decided to make only the roof and floor adiabatic. This means that all the walls would have convection losses, which is a much more realistic scenario. Besides this, it was decided to locate the volume in a place with much colder temperatures. The results obtained showed that by doing this, the internal temperatures are significantly reduced. Thus, it was concluded that considering adiabatic walls is actually a very relevant assumption.

Note that all these proposed cases have many variations, due to page limits, the most relevant were included. It is important to highlight that there is still room for study that can be complemented in the future. At this point, it was shown that starting from a basic code allowed to develop it to later study more complex thermal problems. Similarly, all the results found make sense and agree with what is reported in the literature.

Finally, this report ends with a brief estimation of the economic and environmental impact of this project. This helped to determine the value that would have been spent on a project of this type and that does not affect significantly the environment. This is because this study consists entirely of simulations with normal computers, which would rather help to obtain reference cases that could be used in the future engineering projects.

15 Future lines

It is important to discuss future lines of research in case it is intended to improve or deepen this project. Therefore, this section details some of the future tasks to be done.

It is essential to mention that at this point the in-house numerical code is capable of solving one-dimensional unsteady heat conduction problems. It must be taken into account that the aim is not to solve a specific building, but to create a learning code on a specific situation that allows studying the behavior of a south-facade. Having said this, the future actions of this project are detailed below.

From the thermal point of view, the future lines are the following:

- ***Models:*** In this report some models have been presented with their respective variations. However, it is important to mention that other (even more complex) models could be considered. Namely, instead of using Trombe technology in a closed space, one of its variants can be used, which consists of letting the air circulate from the air-gap into the interior of the enclosure. In addition to this, the influence of other implementations, such as double glazing, can be studied. Finally, the composition of the south-facing wall can be configured with various materials as it usually is in reality.

- ***CFD:*** The simulation of the cases presented in this report are based on correlations found in the literature that are normally obtained from experiments and that relate some dimensionless numbers. However, what if the heat transfer coefficient has to be determined for a non-standard situation for which no scientific literature is available? A short answer to this is to use CFD&HT (Computational Fluid Dynamics and Heat Transfer). Consequently, one of the points to work on in greater depth is the fact of using open commercial codes. These codes would allow to have CFD simulations tailored to a more specific situation, such as the case studies presented in this report. This will help to have more realistic results instead of assuming certain situations to use information that is available in the literature.

  To get into CFD&HT, it would be important to work on the three-dimensional and transient resolution of heat transfer in walls. In addition, working on the resolution of the equations of conservation of mass, momentum and energy (numerical resolution of the Navier-Stokes equations) for laminar and turbulent flows would also help to acquire the ability to work on new numerical models seeking to reduce the computational costs.

On the other hand, from the point of view of the computational field, the points to be discussed are the following:

- ***C++:*** Improving object-oriented programming skills would help to use an object-oriented

programming methodology. This would allow to have more general and efficient codes that could consider a more complex enclosure, considering the solar radiation on each wall, roof and floor, and taking into account the variation at each instant of time on each face according to orientation, shape and location of the building.

- ***Parallelization:*** Performing some parallelization operations would help to improve the calculation time it would take to analyze a certain problem. The `OpenMP API` could be an option to consider as it supports cross-platform shared memory parallel programming in `C++`.

All these future actions would help to increase my level in thermofluidic engineering since it allows me to approach the study in more detail of the phenomena of Heat Transfer and Fluid Dynamics present in the situations studied. This could lead to obtaining a fairly universal code with claims to compete in the simulation of the thermal behavior of a building. Clearly, it would be necessary to study what already exists in the market and if it would be worth the effort to do it.

16 Acknowledgements

How does a person say 'thank you' when there are many people to thank?

This thesis would not have been possible without the help and encouragement of many people. Hence, I would like to thank all the people that have helped, supported and motivated me not only during my master's degree but also during my life.

Firstly, I would like to express my deepest gratitude to my daily supervisors Carlos David Pérez Segarra and Assensi Oliva Llena for their guidance, support, patience and encouragement during these months. Thank you Carlos David and Assensi for always being available whenever I had questions and for the insightful discussions. I am very grateful that I had the opportunity to work with you. Secondly, I would like to thank the members of the CTTC research group: Jordi Vera and Jesús Castro for their time and their brillant comments and suggestions in various situations of this project. I would also like to thank to my professors in this short but pleasant time at the UPC. Thank you for your valuable feedback during the different courses I took.

I would like to extend my gratitude to my family, not only for their support and encouragement on my life but also for believing in me no matter what project I happen to be working on. I am extremely grateful for the infinite love and support from my parents, grandparents, and brothers. I would like to thank them for believing in me and my dreams and for always standing by my side. I have benefited from many years of support from all of you. In particular, I want my mom and dad to know that I love them. It is a special feeling to know that Lizeth, Angel, Esteban, Adrian and Elian are my greatest fans. A special thanks goes to my grandfather Abdon who offered me his hospitality in this new country.

Last but not least, I would like to thank all the people who have always been there for me during this time away from home. I feel blessed to have them in my life. Thank you all for believing in me and encouraging me to excel both in my professional and personal life in this new phase that I am about to begin.

17 References

[1] P. Medici, "The Trombe wall during the 1970s: Technological device or architectural space? Critical inquiry on the Trombe wall in Europe and the role of architectural magazines," *Spool*, vol. 5, pp. 45–60, 10 2018.

[2] L. Alter, "The Trombe wall: Solar design," 2018. Available online at: https://www.treehugger.com/the-trombe-wall-low-tech-solar-design-makes-a-comeback-4856838 [accessed on 30 May 2023].

[3] Designing Buildings, "Trombe wall," 2020. Available online at: https://www.designingbuildings.co.uk/wiki/Trombe_wall [accessed on 30 May 2023].

[4] C. Karakosta, H. Doukas, and P. John, "EU–MENA energy technology transfer under the CDM: Israel as a frontrunner?," *Energy Policy*, vol. 38, no. 5, pp. 2455–2462, 2010. Greater China Energy: Special Section with regular papers.

[5] N. Lechner, *Heating, Cooling, Lighting*, p. 147–176. Wiley-Interscience, 3rd ed., 2008.

[6] H.-Y. Chan, S. B. Riffat, and J. Zhu, "Review of passive solar heating and cooling technologies," *Renewable and Sustainable Energy Reviews*, vol. 14, no. 2, pp. 781–789, 2010.

[7] J. Dong, Z. Chen, L. Zhang, Y. Cheng, S. Sun, and J. Jie, "Experimental investigation on the heating performance of a novel designed trombe wall," *Energy*, vol. 168, pp. 728–736, 2019.

[8] P. Torcellini and S. Pless, "Trombe walls in low-energy buildings: Practical experiences preprint," 2004. Available online at: https://www.nrel.gov/docs/fy04osti/36277.pdf [accessed on 30 May 2023].

[9] EnviroInc, "What is a Trombe wall and how much does it cost?," 2020. Available online at: https://enviroinc.com/trombe-wall/ [accessed on 30 May 2023].

[10] ArchDaily, "How does a Trombe wall work?," 2021. Available online at: https://www.archdaily.com/946732/how-does-a-trombe-wall-work [accessed on 30 May 2023].

[11] Sun Light & Power, "SLP Series: Modified Trombe wall," 2020. Available online at: https://www.sunlightandpower.com/blog/slp-legacy-series-modified-trombe-wall [accessed on 30 May 2023].

[12] T. Göksal Özbalta and S. Kartal, "Heat gain through trombe wall using solar energy in a cold region of turkey," *Scientific Research and Essays*, vol. 5, pp. 2768–2778, 10 2010.

[13] Venture Well, "Trombe wall and attached sunspace," 2013. Available online at: https://sustainabilityworkshop.venturewell.org/buildings/trombe-wall-and-attached-sunspace.html [accessed on 30 May 2023].

[14] F. Stazi, A. Mastrucci, and C. di Perna, "The behaviour of solar walls in residential buildings with different insulation levels: An experimental and numerical study," *Energy and Buildings*, vol. 47, pp. 217–229, 2012.

[15] GreenSpec, "Passive solar design: Sunspaces," 2022. Available online at: https://www.greenspec.co.uk/building-design/passive-solar-sunspaces/ [accessed on 31 May 2023].

[16] B. K. Agrawal and G. Tiwari, "Building integrated photovoltaic thermal systems," *RSC Energy Series*, pp. 203–207, 2010.

[17] H. L. Simmons, *Olin's Construction: Principles, Materials, and Methods*. Wiley-Interscience, 13th ed., 2012.

[18] NIST, "Finite Volume Method," 2022. Available online at: https://www.ctcms.nist.gov/fipy/documentation/numerical/discret.html#:~:text=A%20mesh%20consists%20of%20vertices,of%20cells%2C%20faces%20and%20vertices. [accessed on 1 June 2023].

[19] SIMSCALE, "What is a mesh?," 2023. Available online at: https://www.simscale.com/docs/simwiki/preprocessing/what-is-a-mesh/ [accessed on 1 June 2023].

[20] Axom, "Mesh types," 2017. Available online at: https://axom.readthedocs.io/en/develop/axom/mint/docs/sphinx/sections/mesh_types.html [accessed on 1 June 2023].

[21] J. Peraire, "Unstructured grid finite-element methods for fluids," *Reports on Progress in Physics*, vol. 61, p. 569, 01 1999.

[22] F. Trias, O. Lehmkuhl, A. Oliva, C. Pérez-Segarra, and R. Verstappen, "Symmetry-preserving discretization of navier–stokes equations on collocated unstructured grids," *Journal of Computational Physics*, vol. 258, pp. 246–267, 2014.

[23] Y. Wang, M. Baboulin, J. Dongarra, J. Falcou, Y. Fraigneau, and O. Le Maître, "A parallel solver for incompressible fluid flows," *Procedia Computer Science*, vol. 18, pp. 439–448, 2013. International Conference on Computational Science.

[24] D. Aleksendrić and P. Carlone, "4 - Soft computing techniques," in *Soft Computing in the Design and Manufacturing of Composite Materials* (D. Aleksendrić and P. Carlone, eds.), pp. 39–60, Oxford: Woodhead Publishing, 2015.

[25] Toppr, "Stokes theorem," 2022. Available online at: https://www.toppr.com/guides/maths/stokes-theorem/#:~:text=The%20Gauss%20divergence%20theorem%20states,net%20flow%20of%20an%20area. [accessed on 2 June 2023].

[26] R. J. LeVeque, "Finite difference methods for differential equations," *In: Draft version for use in AMath 585.6*, pp. 20–22, 1998.

[27] G. Recktenwald, "One dimensional convection: Interpolation models for cfd," *Mechanical and Materials Engineering Department, Portland State University*, 2006.

[28] S. Patankar, *Numerical Heat Transfer and Fluid Flow*. Taylor & Francis Publishers, New York, 1980.

[29] D. A. Spielman, "Iterative solvers for linear equations," *Spectral Graph Theory*, pp. 1–8, 2009.

[30] T. Sauer, *Numerical Analysis*. Pearson Education, Inc., 2nd ed., 2006.

[31] Heat and Mass Transfer Technological Center (CTTC), "Formulae for the resolution of Fluid Dynamics and Heat and Mass Transfer problems," *Polytechnic University of Catalonia*, pp. 1–33, 2022.

[32] M. J. Hancock, "The 1-D Heat Equation," *Linear Partial Differential Equations*, pp. 1–144, 2006.

[33] Heat and Mass Transfer Technological Center (CTTC), "Part 1 : Numerical solution of the heat equation (1D)," *Polytechnic University of Catalonia*, pp. 1–9, 2022.

[34] SOLEC, "SOLKOTE technical specifications," 2023. Available online at: https://solec.org/solkote/solkote-technical-specifications/ [accessed on 5 May 2023].

[35] Vaillant Group, "What is the ideal room temperature?," 2022. Available online at: https://www.vaillant.co.uk/homeowners/advice-and-knowledge/what-is-the-ideal-room-temperature-1769698.html [accessed on 31 May 2023].

[36] Glassdoor, "How much does a Junior Engineer make in barcelona, spain?," 2023. Available online at: https://www.glassdoor.com/Salaries/barcelona-junior-engineer-salary-SRCH_IL.0,9_IM1015_KO10,25.htm [accessed on 22 June 2023].

[37] ContractorUK, "What is the depreciation period and rate for business laptops or computers?," 2022. Available online at: https://www.contractoruk.com/limited_companies/what_depreciation_period_and_rate_business_laptops_or_computers.html [accessed on 22 June 2023].

[38] Selectra, "Regulated market electricity price today: kwh hourly price in spain," 2023. Available online at: https://selectra.es/energia/info/que-es/precio-kwh [accessed on 23 June 2023].

[39] Nowtricity, "Real time live emissions from energy production by country," 2022. Available online at: https://www.nowtricity.com/country/spain/ [accessed on 22 June 2023].